Nitrifying MBBR Performance Optimization in Temperate Climates Through Understanding Biofilm Morphology and Microbiome

Bradley Young

A thesis submitted to the Faculty of Graduate and Postdoctoral Studies in partial fulfillment of the requirements for the degree of Doctor of Philosophy in Environmental Engineering

Ottawa-Carleton Institute for Environmental Engineering

Department of Civil and Environmental Engineering

Faculty of Engineering

University of Ottawa

uOttawa

Abstract

Nitrification is currently the most common means of ammonia removal from wastewaters in temperate climates. In conventional suspended growth systems operating in northern climate regions, nitrification completely ceases at temperatures below 8°C. This is a considerable concern in passive treatment systems where wastewater temperatures can reach as low as 1°C for extended periods in the winter months. There is evidence biofilm technologies have the ability to nitrify at low temperatures, however, the literature is missing an understanding of low temperature nitrification and the subsequent impacts during seasonal changes. Additionally, there is an urgent need to gain a fundamental knowledge of the interplay between nitrifying performance optimization, biofilm morphology and the microbiome. This research aims to fill these needs using nitrifying moving bed biofilm reactors (MBBRs) at the lab and pilot scale.

This research concluded the most important factor determining MBBR carrier selection is a combination of surface area and pore space size. Although high surface area to volume carriers are attractive, the propensity to clog at high loading rates significantly decreases the removal rates. The viability of the biomass and ammonia oxidizing bacterial communities were not significantly changed, indicating the ammonia removal rates were reduced due to loss of surface area in the clogged carriers.

Operation at 1°C demonstrated significant rates of nitrification can be attained and stable for extended periods of operation. This study developed the first kinetic curve at 1°C with a maximum removal rate of 0.35 $gN/m^2 \cdot d$. The performance of the post carbon removal nitrifying MBBR systems were shown to be enhanced at 1°C by an increase in

the viable embedded biomass as well as thicker biofilm. This effectively increased the number of viable cells present during low temperature operation, which partially compensated for the significant decrease in rate of ammonia removal per nitrifying cell. At all studied loading rates at 1°C, the ammonia oxidizing bacteria were primarily in the family *Nitrosomonadaceae* (greater than 95 percent abundance of AOB population) and the nitrite oxidizing bacteria were primarily the genus *Nitrospira* (greater than 99 percent abundance of NOB population).

Operation at 20°C demonstrated high rates of removal in high loaded condition and robustness in extreme low loaded conditions. In both high loaded and extreme low loaded conditions the viability of the nitrifying biomass was sustained, with the family *Nitrosomonadaceae* as the primary ammonia oxidizing bacteria and the genus *Nitrospira* as the primary nitrite oxidizing bacteria. In extreme low loaded conditions and as well during start-up phases there are high prevalence of bacteria not directly related to the nitrification process. Their presence however indicates a dynamic process with changes in microbial composition within the biofilm matrix in response to varying conditions. Change in microbial composition likely helps stabilize and maintain the biofilm matrix enhancing process robustness in the temperate climates.

The new knowledge gained in this research optimizes the operation of nitrifying MBBR systems and elucidates the impacts of operational conditions on the biofilm and microbial community of nitrifying MBBR systems to further our understanding of nitrifying attached growth treatment technologies. The results of this study are anticipated to be used to design the first MBBR treatment system for year round ammonia removal in passive treatment systems located in northern climate regions.

Acknowledgements

I would like to thank my primary supervisor Dr. Robert Delatolla for his guidance, support and providing the freedom to explore ideas throughout my PhD project. I would also like to thank Dr. Robert Delatolla for his time, dedication and enthusiasm to every aspect of the project. I thank my co-supervisors Dr. Kevin Kennedy and Dr. Alain Stintzi for their guidance and support. I would especially like to thank Dr. Stintzi for providing the tools and expertise in next generation sequencing. This was paramount to the overall success of the PhD project.

I would like to thank all of my past and present coworkers for their support, technical assistance and friendship. In particular, I would like to thank Pat D'Aoust, Turki Abujamel, James Butcher and Jennifer Lee.

I am truly grateful for the collaborators of this project. Mr. Alain Gadbois, Mrs. Edith Laflamme, Mr. Christian Scott, Mr. Robert Lafond and Mr. Simon Vincent from Veolia Water Technologies. It with your support this project was commenced and I truly appreciate the opportunity provided.

This research would not have been possible without the financial contributions from Veolia Water Technologies and the Natural Science and Engineering Research Council of Canada (NSERC).

Finally, I would like to thank my family and close family members who even though are still convinced I "play with poop" were always 100% supportive and proud of my accomplishments.

Table of Contents

List of Abbreviations

AOB	Ammonia oxidizing bacteria
AOA	Ammonia oxidizing archaea
C/N	Carbon to nitrogen ratio
CAS	Conventional activated sludge
CBOD	Carbonaceous biochemical oxygen demand
CER	Cation exchange resin
CLSM	Confocal laser scanning microscopy
COD	Chemical oxygen demand
DO	Dissolved oxygen
DPA	Digital particle analysis
EPS	Extracellular polymeric substances
FA	Free phase ammonia
FISH	Fluorescent in situ hybridization
FLASH	Fast length adjustment of short reads
FNA	Free nitrous acid
HLC	High loading condition
HRT	Hydraulic retention time
IFAS	Integrated fixed film activated sludge
LC50	Lethal concentration for 50% mortality of rainbow trout after 96 hours
LDA	Linear discriminate analysis
LR	Loading rate
MBBR	Moving bed biofilm reactor

MTBL	Mass transfer boundary layer
NLC	Normal loading condition
NOB	Nitrite oxidizing bacteria
OTU	Operational taxonomical unit
PCoA	Principal coordinate analysis
PCR	Polymerase chain reaction
PIA	Polysaccharide intercellular adhesion
PN/PS	Protein to polysaccharide ratio
QIIME	Quantitative insights into microbial ecology
RR	Removal rate
SALR	Surface area loading rate
SARR	Surface area removal rate
SCOD	Soluble chemical oxygen demand
SRT	Solids retention time
SVI	Sludge volume index
TKN	Total Kjehldahl nitrogen
TP	Total phosphorus
TSS	Total suspended solids
USEPA	Unites states environmental protection agency
VSS	Volatile suspended solids
WRRF	Water resource recovery facility
WSER	Wastewater systems effluent regulations

List of Figures

List of Tables

Chapter 1: Introduction

1.1. Federal wastewater effluent regulations in Canada

The primary objective of water resource recovery facilities (WRRFs) is to remove contaminates from household sewage and surface runoff (combined sewer). The federal government of Canada has implemented the wastewater systems effluent regulations (WSER) as defined by the Fisheries Act (Canada Gazette, 2012). This regulation defines discharge limits for total suspended solids (TSS), five day carbonaceous biological oxygen demand ($CBOD_5$), total chlorine residual, effluent ammonia and defines that the water cannot be acutely toxic to rainbow trout. The WSER is applied to all treatment facilities that discharge more than 100 m^3/d, excluding facilities in the North West Territories, Nunavut or above the 54^{th} parallel in the provinces of Quebec and Newfoundland and Labrador.

With respect to ammonia, WSER states that wastewater discharge must contain less than 1.25 mg/L un-ionized ammonia as nitrogen (NH_3-N) at 15 ± 1 °C. The speciation of ionized (NH_4^+) ammonium and un-ionized (NH_3) ammonia in a solution (wastewater) is directly related to pH and temperature. The fraction of un-ionized ammonia is calculated according to the following Equations (1.1 and 1.2) where *pKa* is the acid dissociation constant and T is the solution temperature (°C).

$$pKa = 0.09 + \frac{2730}{273 + T} \qquad \text{Equation 1.1}$$

$$\%NH_3 = \frac{1}{1 + 10^{pKa - pH}} x100\% \qquad \text{Equation 1.2}$$

At equilibrium, the fraction of un-ionized ammonia has a positive correlation with increasing wastewater temperature and pH. Assuming a typical wastewater effluent pH of 7.2 (Metcalfe and Eddy, 2003) and standard temperature of 15°C, the total ammonia concentration would need to be approximately 355 mg/L to exceed 1.25 mg/L NH_3-N. As conventional ammonia concentrations in raw municipal wastewater in Canada is between 20 to 30 mg-N/L, the ammonia concentrations of municipal wastewater effluent from Canadian wastewater treatment facilities are highly unlikely to exceed 355 mg/L.

A secondary component of the WSER and the United States Environmental Protection Agency (USEPA) regulations is with respect to acute lethality. Both wastewater regulations dictate wastewater discharges cannot be acutely lethal, where acute lethality is defined as 50% mortality of rainbow trout after 96 h in 100% wastewater effluent (LC50) (Canada Gazette, 2012; USEPA, 2014). The effluent ammonia concentration of typical municipal wastewater treatment plants that has been demonstrated to fail the LC50 test is between 15-20 mg-N/L (Di Giulio and Hinton, 2008). As the average ammonia concentration of municipal wastewater is reported to be between 20 to 30 mg-N/L, the acute lethality of wastewater effluent will be the limiting factor for ammonia removal in Canada and the USA.

1.2. Nitrification

Biological treatment is the most common and currently the most cost-effective means of ammonia removal in wastewaters. The fundamental principal of biological treatment is to enrich the biomass of the wastewater treatment facilities with microorganisms that degrade deleterious compounds to nontoxic products (Metcalfe and Eddy, 2003). For conventional mainstream ammonia removal, the biomass would be enriched with

microorganisms performing nitrification. The process of nitrification operates in two-steps, first the biologically mediated oxidation of ammonia to nitrite (nitritation, Equation 1.3) followed by the biologically mediated oxidation of nitrite to nitrate (nitratation, Equation 1.4). Equation 1.5 presents the overall reaction for nitrification.

$$NH_4^+ + 1.5\,O_2 \rightarrow NO_2^- + H_20 + 2H^+ \qquad \text{Equation 1.3}$$

$$NO_2^- + 0.5\,O_2 \rightarrow NO_3^- \qquad \text{Equation 1.4}$$

$$NH_4^+ + 2O_2 \rightarrow NO_3^- + H_2O + 2H^+ \qquad \text{Equation 1.5}$$

As shown, the process of nitritation and nitratation consume oxygen. Stoichiometrically the required DO for nitritation and nitratation is 3.43 g-O_2/g-NH_4^+-N and 1.14 g-O_2/g-NO_2^--N, respectively. Thus the DO requirement for complete nitrification is 4.57 g-O_2/g-NH_4^+-N oxidized. The process of nitritation consumes alkalinity through the production of hydrogen ions. Similar to DO requirements, a stoichiometric balance yields a consumption of 7.14 g-$CaCO_3$/g-NH_4^+-N during the oxidation of ammonia to nitrite (Metcalfe and Eddy, 2003).

1.3. Taxonomy of nitrifying organisms

Nitrification redox reactions are performed by specific bacteria loosely termed nitrifiers. The bacteria predominantly responsible for the oxidation of ammonia are chemolithotrophic and classified as ammonia oxidizing bacteria (AOB). The most prominent AOBs in wastewater are *Nitrosomonas*, *Nitrosospira* and *Nitrosococcus* (Monteiro et al., 2014). *Nitrosomonas* is widely accepted as the dominant AOB in wastewater treatment (Rowan et al., 2003). Ammonia oxidizing archaea (AOA) have been identified in a wide range of marine, terrestrial and geothermal environments. The

most prominent AOAs are in the phylum *Crenarchaeota* and *Thaumarchaeota* (Konneke et al., 2014). Recent studies have postulated AOAs are outcompeted by AOBs in ammonia rich environments such as wastewater (Gao ete al., 2016). Lastly, there are various strains of heterotrophic nitrifying bacteria such as *Thiobasphaera* and *Alcaligenes*, however, their presence is most noted in high strength industrial wastewaters (Joo et al., 2005). Hence, in municipal wastewater the chemolithotrophic AOBs are likely to dominate.

Similarly, the bacteria responsible for the oxidation of nitrite are classified as nitrite oxidizing bacteria (NOB). The most prominent NOBs in wastewater are *Nitrobacter* and *Nitrospira*. Early studies postulated *Nitrobacter* as the primary NOB in wastewater, however, more recently *Nitrospira* has shown to dominate (Daims et al., 1999; Siripong and Rittmann, 2007; Wagner et al., 1996). Treatment of acidic wastewaters (pH between 5.7 to 6.0) has shown to enrich *Nitrotoga* as the dominant NOB (Hupeden et al., 2016). An additional NOB, *Nitrospina*, has been identified in warm diluted seawater (Spieck et al., 2014). Hence, in municipal wastewater treatment, *Nitrobacter* or *Nitrospira* are likely to dominate.

1.4. Nitrifying bacteria growth and energetics

Bacterial growth and energetics of the most prominent wastewater nitrifiers (*Nitrosomonadacea* and *Nitrospira*) and heterotrophs are fundamentally different. These nitrifiers produce energy from inorganic sources (ammonia and nitrite). Energy production from inorganic sources does not generate as much free energy as various organic carbons. In addition to the decreased energy production, nitrifiers also require high energy inputs to convert inorganic carbon sources for cellular use. This energy

production and conversion places nitrifiers at a competitive disadvantage with respect to growth rates and yield (Table 1.1).

Table 1.1 Oxygen half velocity constants (K_o), yields (Y) and maximum specific growth rates (μ_{max}) for prominent wastewater AOB, NOBs and general heterotrophs*

	K_o (g/m^3)	**Y (g-cells/g-substrate-utilized)**	**μ_{max} (1/d)**
Nitrosomonas	0.3 – 1.3	0.03 – 0.13	0.41 – 2.11
Nitrobacter	0.17 – 5.3	0.02 – 0.08	0.60 – 1.40
Nitrospira	0.07 – 0.19	0.11 – 0.19	0.50 – 1.99
Heterotroph	0.0007 – 0.1	0.37 – 0.79	7.2 – 17.0

*Data acquired from: Alleman, 1984; Beccari et al., 1979; Blackburne et al., 2007; Kindaichi et al., 2006; Manser et al., 2005; Metcalf and Eddy, 2003; Sharma and Ahlert, 1977

Comparing the most prominent municipal wastewater AOB (*Nitrosomonas*) and NOBs (*Nitrobacter*/*Nitrospira*) to broad-spectrum heterotrophic bacteria illustrates the competitive disadvantage of nitrifiers (Table 1.1). The higher oxygen half velocity constant (K_o) in nitrifiers signifies more oxygen is needed to oxidize ammonia and nitrite than organic carbon. Nitrifiers use a less efficient method of producing and using energy for their metabolic processes. This ultimately leads to lower yields (Table 1.1) signifying there is less biomass generated per gram of substrate consumed. Additionally, the replication time of nitrifying bacteria can range from 8 to 60 h, which is significantly longer than heterotrophs (approximately 30 min).

Temporally, nitrifiers in conventional suspended growth systems are low temperature sensitive. Specifically, at 5°C the minimum replication time for nitrifying bacteria is greater than 200 h (Kors et al., 1998). Empirical data in suspended growth systems shows nitrification becomes substantially impeded below 10°C and nearly non-existent below

5°C (Hurse and Connor, 1999; Oleszkiewicz and Berquist, 1988; Shammas, 1986). Van Dyke et al. (2003) investigated ten wastewater treatment facilities in the northern United States and determined on average nitrification rates significantly diminish after two to three weeks of operation at temperatures below 7°C. Hence, establishing nitrifying biomass at low temperatures is critical in the northern climate regions of Canada, Europe and the United States where it is not uncommon for wastewater temperatures to decrease below 8°C in the winter months.

To enhance low temperature nitrification several studies have investigated strategies to enrich nitrifiers in suspended growth systems. Increasing the solids retention time (SRT) compensates for the reduced nitrifier replication time, however, is accompanied with negative effects such as elevated sludge concentration, higher sludge loading to secondary clarifiers, reduced sludge settleability and higher oxygen demand (Krhutkovi et al., 2006). Maintaining short SRTs and bioaugmenting nitrifiers does provide significant improvements in nitrification rates below 10°C (Head and Oleszkiewicz, 2004; Leu and Stenstrom, 2010; Podmirseg et al., 2010; Stenstrom and Jansen, 2016). The most practical source of nitrifier seed is through side-stream treatment of sludge dewatering digester supernatant which has the ability to increase the nitrification rates by up to 41% at mainstream temperatures below 10°C (Stenstrom and Jansen, 2016). In wastewater treatment plants where side-streams are often not available, bioaugmentation requires significant dosages of an external source of nitrifiers to produce limited to no significant increase in nitrification rates (Abeysinghe et al., 2002; Rittmann and Whiteman, 1994).

The development of biofilm technologies, which have inherently long solids retention times, could partially compensate for the temperature sensitivity of nitrifiers and produce reliable long term low temperature nitrification. Biofilm technologies would be particularly effective in passive treatment systems, which rarely have side-streams, and are low temperature exacerbated due to large surface areas and long retention times. In fact, the effluent of the primary lagoons in Canada and the northern United States commonly reach 4°C while the polishing ponds become completely ice covered (effluent < 1°C).

1.5. Biofilm

A biofilm as defined by Costerton et al. (1999) is "a structured community of bacterial cells enclosed in a self-produced polymeric matrix and adherent to an inert or living surface." Biofilm formation is initiated as bacteria transition from a suspended (planktonic) state to an attached (sessile) state. The transition for microbial attachment and proliferation in a biofilm is a complex process that provides benefits due to diffusion limitations of the biofilm and genetic variation within the embedded microbial communities.

1.5.1. Mass transfer (diffusion limitations)

Mass transfer and diffusion principles govern the rate at which various solutes such as substrates, oxygen and toxins entering the biofilm matrix. Advective transport brings the solutes in close proximity to the biofilm surface where the flow of the bulk liquid is decreased along a viscous interface. This distance between the solutes and biofilm surface is the mass transfer boundary layer (MTBL) (Fig 1.1). The decreased flow in the

MTBL does not allow advective transport to continue thus requiring solutes to diffuse through the MTBL. Similarly due to the extracellular polymeric substances (EPS) and dense nature of the biofilm itself nutrients diffuse through the biofilm matrix. This diffusion is reported as a surface flux across the MTBL and through the biofilm (Equation 1.6 and 1.7) (Metcalfe and Eddy, 2003; WEF, 2010).

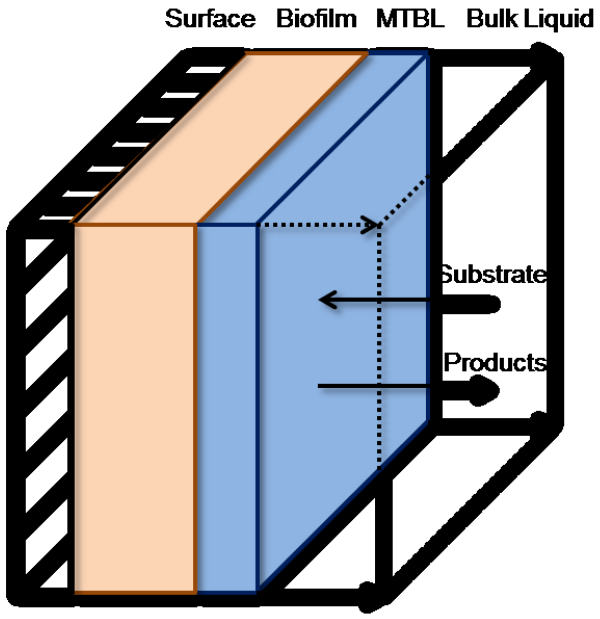

Figure 1.1 Transfer of substrates through the bulk liquid (clear), the mass transfer boundary layer (blue) biofilm (peach)

$$r_{sf} = -D_w\left(\frac{S_b - S_s}{L}\right) \qquad \text{Equation 1.6}$$

$$r_{bf} = -D_e\frac{dS}{dx} \qquad \text{Equation 1.7}$$

r_{sf} is the rate of mass transport to the biofilm (g/m^2·d), D_w is the diffusion coefficient in water (m^2/d), S_b is the concentration in the bulk liquid (g/m^3), S_s is the concentration at

the biofilm surface (g/m^3) and L is the effective thickness of the biofilm (m), r_{bf} is the rate of mass transport in the biofilm ($g/m^2 \cdot d$), D_e is the diffusion coefficient in the biofilm (m^2/d) and dS/dx is the substrate concentration gradient ($g/m^3 \cdot m$).

From Equations 1.6 and 1.7, it is evident that individual solutes will diffuse at different rates across the MTBL and into the biofilm. Minimizing the effective thickness of the MTBL significantly decreases the time of transport of a solute through the MTBL and subsequently the quantity diffusing into the biofilm. Minimizing the thickness of the MTBL is a function of flow with increasing velocities resulting in decreasing MTBL (Stewart, 2003; Taherzadeh et al., 2012).

The rate of diffusion into the biofilm is generally slower than the rate of bacterial metabolism (Bryers, 2000). This rate difference creates chemical environments that differ at depths. For example, as the DO diffuses into the biofilm it will be depleted by the top layer of aerobic bacteria. If the bulk liquid DO concentration is not high enough in a thick biofilm, the bacteria near the substratum could be living in an anoxic environment and must switch to anaerobic growth or cease growing. These substrate gradients theoretically promote a heterogeneous community with varying growth rates and ideal conditions stratified by substrate and oxygen requirements (Nadell et al., 2009).

1.5.2 Genotypic and gene expression

Biofilms embed a heterogeneous community with diverse genotypes and phenotypes. The genes in sessile bacteria have been demonstrated to be expressed differently compared to their planktonic state. In particular, it has been reported that over 57 proteins are differentially expressed in sessile *Pseudomonas* as compared to their planktonic state

(Hall-Stoodley and Stoodley, 2002). Often the expression of the genes coding for proteins involved in flagella assembly is downregulated while the genes encoding extracellular proteins are upregulated (Sutherland, 2001).

In a stressful environment, the heterogeneous community of many biofilms are able to rapidly adapt by sharing genetic components. In a phenomenon known as horizontal gene transfer, plasmids and fragments of cellular DNA are shared among clusters of bacteria in the biofilm matrix (Madsen et al., 2012). Sharing plasmids and fragments of DNA promotes mutation and the ability for susceptible bacteria to survive in an unfavorable environment (Thomas and Nielsen, 2005; Watnick and Kolter, 2000). Plasmids in particular allow bacteria to sample the gene pool in the biofilm for adaptive traits that may be advantageous in the local environment (Montanaro et al., 2011; Sorensen et al., 2005). Both planktonic and sessile bacteria are able to share genetic material, however, the clustering of bacteria in the biofilm matrix facilitates evolution and ecological diversity to increase reproductive fitness and survival in harsh environments (Flynn et al., 2016).

1.6. Nitrifying biofilms in wastewater treatment

As previously mentioned, nitrification is traditionally expressed as a two-step process. First AOBs oxidize ammonia to nitrite followed by NOBs oxidizing nitrite to nitrate. This two-step process causes biofilm embedded AOBs to consume ammonia in the wastewater and NOBs to consume the products from the AOBs (Fig 1.2).

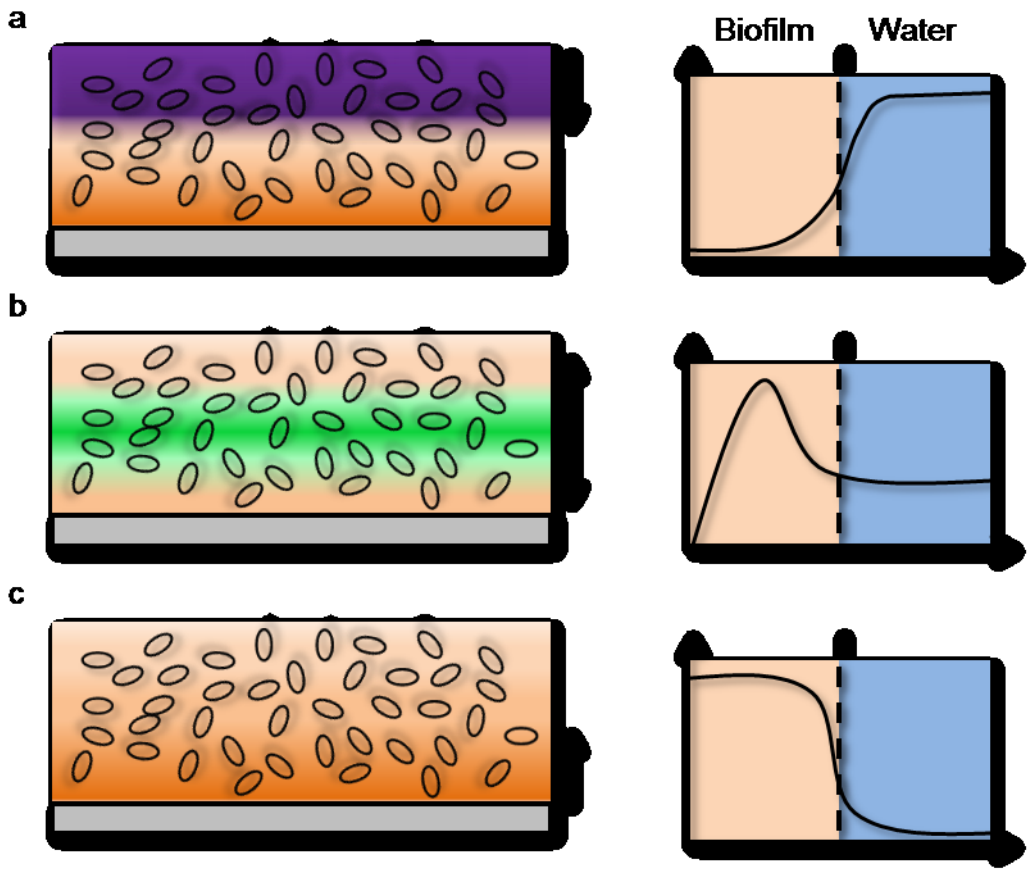

Figure 1.2 Diffusion of ammonia (purple), nitrite (green) and nitrate (orange) within a young non acclimatized biofilm matrix. a) the diffusion of ammonia from high concentration in the wastewater to low concentration at depth within the biofilm. b) the diffusion of nitrite into and out of the biofilm as the intermediate metabolite during the nitrification process. c) the diffusion of nitrate out of the biofilm from deep in the biofilm to the water (Adapted from Stewart and Franklin, 2008)

Based on diffusion principles, ammonia diffuses into the biofilm matrix where it is oxidized to nitrite. Nitrite is typically low in the environment causing it to diffuse in two directions, deeper into the biofilm and out of the biofilm. In an acclimatized nitrifying biofilm with sufficient oxygen and nutrients the nitrite should be completely oxidized to nitrate. Subsequently the final product, nitrate, diffuses out of the biofilm and into the wastewater (Fig 1.2). Daims et al. (2006) demonstrated that diffusion creates

microhabitats in nitrifying biofilms. The AOBs create nitrite gradients resulting in NOB clustering or stratifying throughout the biofilm matrix (Gieseke et al., 2005; Kindaichi et al., 2004; Lydmark et al., 2007; Okabe et al., 1999; Schramm et al., 1996). The stratification makes it possible for variable local environments and nitrifying populations throughout the biofilm matrix.

1.7. Moving bed biofilm reactor (MBBR) technology

There are several biofilm technologies designed for wastewater treatment. The moving bed biofilm reactor (MBBR) developed in the 1980s is an efficient standalone biofilm technology (Oleszkiewicz and Barnard, 2006). The MBBR's efficiency is increased through specially designed carriers. These carriers are designed to have a protected interior for biofilm growth and remain in constant movement in the reactor. The constant movement for MBBR carriers is generated by the aeration system of the reactor, which can support fill fractions of 20 to 75% relative to the total reactor volume (Fig 1.3). Thus the MBBR technology has a flexible design and can accommodate future increases in treatment capacity by increasing the fill fraction of the already installed reactor basin.

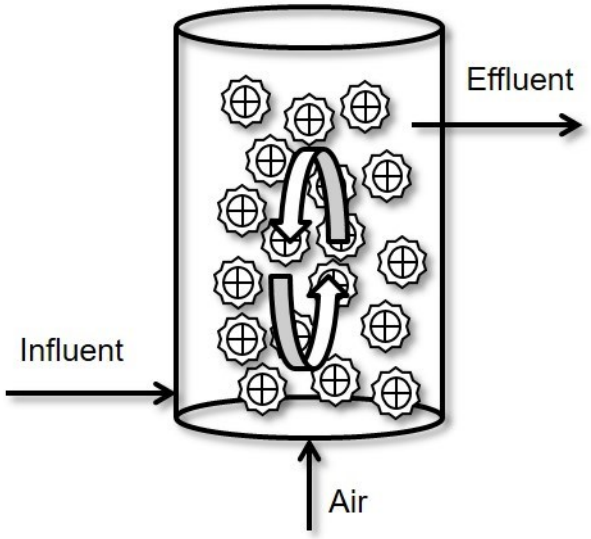

Figure 1.3 Schematic of a typical MBBR system completely mixed by aeration

The MBBR carriers, in an operating system, are constantly colliding and subject to hydrodynamic shear forces. These processes act as a self-cleaning mechanism for the carriers and hence enable a healthy biofilm attached to the carriers to be maintained. The self-cleaning mechanism eliminates the need for backwashing and exhibits a lower head loss than that associated with other biofilm technologies. There are many companies that manufacture and distribute MBBR carriers worldwide. The most widely used carrier brand for wastewater treatment is AnoxKaldnes (a Veolia subsidiary). The MBBR carriers currently in production are shown in Table 1.2. Few studies have been carried out on the effect of carrier type on nitrification performance. As such, optimization of carrier selection for post carbon removal nitrifying MBBR remains unknown.

Table 1.2 AnoxKaldnes Carrier Types*

Carrier Name	Bulk Specific Surface Area	Dimensions (Depth; Diameter)	Carrier Photograph
K1 or K1 Heavy	500 m^2/m^3	7 mm; 10 mm	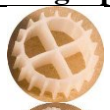
K3	500 m^2/m^3	12 mm; 25 mm	
Biofilm Chip M	1200 m^2/m^3	2 mm; 48 mm	
Biofilm Chip P	900 m^2/m^3	3 mm; 45 mm	
K5	800 m^2/m^3	4 mm; 25 mm	

*Data acquired from: WEF, 2011

Nitrifying bacteria in wastewater biofilms proliferate when the BOD_5/TKN (BOD/N) ratio is 0 to 1 (WEF, 2010). When the C/N ratio is higher than 1, a heterotrophic outer layer may outcompete the nitrifiers for oxygen and nutrients (discussed in section 1.2). Once the carbon is depleted the remaining oxygen will be available for the nitrification process. Hence, nitrifier growth proliferates in low carbon environments with the best nitrification rates and the most stable nitrifying biofilms achieved with a C/N ratio below 1 at the MTBL (Table 1.3).

Table 1.3 Influence of organic loading on nitrification rates in MBBR systems at 20°C*

Organic Loading ($gBOD_5/m^2 \cdot d$)	Nitrification Rate ($gNH_4\text{-}N/m^2 \cdot d$)
1-2	0.7-1.2
2-3	0.3-0.8
>5	0

*Data reproduced from: Hem et al., 1994

1.8. Application of low temperature nitrifying biofilm

The MBBR technology's overall simplicity and efficient operation is compatible to the lagoon model, thus the MBBR is a viable candidate for low temperature post carbon removal nitrification. The MBBR has been previously studied as an add-on technology for lagoon treatment facilities at the pilot-scale (Delatolla et al., 2010; Houweling et al., 2007; Ødegaard, 2006). These pilot MBBR systems were installed to treat the effluent from the first or middle lagoon in the treatment system. At this point of installation the temperatures were maintained above 4°C all year round, however, the C/N ratios were greater than 1. As previously discussed, at C/N ratios above 1 heterotrophic organisms dominate the outer layers of the biofilm which can cause substantial decrease in nitrification performance. Additionally, lagoons are effectively designed to remove CBOD throughout the entire treatment system. Thus placing the MBBR after the first or middle lagoon provides redundant treatment for CBOD. This combined effect makes the system less efficient and cost effective. It is important to note, the piloting studies with MBBR pilot systems installed after the first or middle lagoon were able to demonstrate limited nitrification in the MBBR at 4°C, which is not possible in suspended growth systems (Hurse and Connor, 1999; Shammas, 1986). At the pilot or full scale, however, there remains a lack of knowledge and research relating to the operation of a post carbon removal nitrifying MBBR treatment system after the last lagoon of a multi lagoon treatment facility and hence a nitrifying MBBR treatment system operating at 1°C during the winter months.

At the lab scale, Hoang et al. (2014a, b) demonstrated the feasibility of 1°C operation using synthetic wastewater. The lab demonstration showed 20% removal rates at 1°C

relative to 20°C operation and the cell viability was maintained at 1°C. These results suggest long term feasibility of post carbon removal MBBR nitrification at 1°C. Almomani et al., (2014) performed a similar lab study with real lagoon effluent and demonstrated the feasibility of 1°C tertiary MBBR operation with 1°C removal rates that were measured at 42% relative to 20°C operation. Both studies used conservative substrate and hydraulic loading rates, nonetheless these studies are effective in demonstrating the potential of the MBBR as a true post carbon removal nitrifying system. The feasibility studies, however, did not investigate the kinetic rates, impacts on the biofilm morphology or the microbial ecology.

1.9. Microbial ecology of nitrifying biofilms

The microbial ecology of nitrifying biofilms has previously been determined with denaturing gel gradient electrophoresis (DGGE) of the 16S rRNA gene amplicons or fluorescent in situ hybridization (FISH). Using these techniques, studies have identified *Nitrosomonas* and *Nitrobacter/Nitrospira* as the dominant AOB and NOBs in wastewater biofilms respectively (Delatolla et al., 2009b; Kindaichi et al., 2006; Lydmark et al., 2007; Nogueira et al., 2002; Okabe et al., 1999). More recent studies have shown *Nitrospira* to be the dominant NOB and correlated nitrite accumulation to a decreased relative abundance of *Nitrospira* (Hoang et al., 2014a; Shore et al., 2012). Using molecular methods, ratios of NOB/AOB in wastewater biofilms often range from 3 to 4 (Mozumder et al., 2014; Winkler et al., 2012). These results were confusing to researchers until metagenomic studies have demonstrated the potential for *Nitrospira* to perform complete ammonia oxidation to nitrate (comammox) in one step (Daims et al., 2015; Van Kessel et al., 2015). Gonzalez-Martinez et al. (2016) most recently postulated

commamox bacteria may be present in low nitrogen substrate and high dissolved oxygen environments.

Notwithstanding the significant advancements in fundamental knowledge of nitrifiers in biofilms, the entire microbiome remains largely unknown. By applying next generation sequencing and bioinformatics tools it is possible to elucidate fundamental principles regarding the bacteria present and their functional capabilities. Linking the kinetics rates, biofilm morphology, cell viability and microbial ecology may provide needed fundamental knowledge to understand how nitrifying biofilms behave year round in northern climate regions.

1.10. Rationale and objectives of the research

The objective of this research is to investigate post carbon removal nitrifying biofilms for their potential application in northern climate regions. This investigation includes ammonia removal kinetics while also using advanced methodological techniques to acquire fundamental information with respect to the biofilm thickness mass, density, cell viability and the nitrifying biofilm microbiome. The application of these techniques will be used to determine the feasibility of nitrifying biofilms year round in the northern climate region and provide novel fundamental scientific information with respect to nitrifying biofilms at various temperatures and loading rates.

The objectives of this study were investigated in four phases (i) investigate the effects of MBBR carrier type; (ii) investigate system start up with integrated fixed film activated sludge (IFAS) carriers; (iii) investigate the effects of rapid temperature decline through long term operation of 1°C; (iv) determine the maximum removal rates during the

summer months and ability for biomass to survive in low ammonia conditions during the summer months. Overall, these objectives advance current understanding, operation and design of post carbon removal MBBR nitrification.

1.11. Novel contributions

This work provides several novel contributions to the field of wastewater treatment. At the commencement of this project there were no mechanical, robust, biological technologies to achieve ammonia removal from lagoon effluents in northern climate regions. This work provides a comprehensive applicable solution to the growing concern of ammonia toxicity due to wastewater effluents in northern climate regions using MBBR technology. Specifically, this work developed the first kinetic design curve for 1°C nitrification and developed operational strategies to manage seasonal changes for nitrifying systems.

This study extends beyond wastewater quality measurements and provides novel information at the meso (biofilm) and micro (cellular) scale. Specifically, this study demonstrates the effects various temperatures and loading rates on biofilm thickness, mass and density. This data is viewed concurrently with cell viability to provide unique insights determining the environmental impacts of the biofilm morphology and subsequently reactor performance. This research provides the first complete understanding of the changes in biofilm morphology throughout the various temperatures and loading rates and was directly applied to provide empirical evidence for optimal biofilm carrier selection in post carbon removal nitrifying MBBRs.

This is one of the first studies to investigate the microbiome in post carbon removal nitrifying biofilms and the first to do so at 1°C, an important temperature for northern countries. The advent of metagenomics next generation sequencing in combination with bioinformatics tools provides quantitative insights of microbial communities. Applying this technique in combination with water quality and meso scale analysis provides the first fundamental knowledge of how nitrifying biofilms are capable of achieving high rates of removal at 1°C and maintain stability in extreme loading conditions. Additionally, this work provides empirical evidence of the recently discovered comammox bacteria in high oxygen and low loading conditions. In effect, this study develops new fundamental scientific and engineering knowledge with respect to nitrifying wastewater biofilms and can be used as the framework for future studies to further expand on the current art.

Chapter 2: Meso and micro-scale response of post carbon removal nitrifying MBBR biofilm across carrier type and loading

Bradley Young[a], Bahman Banihashemi[a], Daina Forrest[a], Kevin Kennedy[a], Alain Stintzi[b], Robert Delatolla[a*]

[a] Department of Civil Engineering, Faculty of Engineering, University of Ottawa, Ottawa, Canada

[b] Ottawa Institute of Systems Biology, Department of Biochemistry, Microbiology and Immunology, Faculty of Medicine, University of Ottawa, Ottawa, Canada

2.1. Statement of manuscript status and author contributions

The manuscript "Meso and micro-scale response of post carbon removal nitrifying MBBR biofilm across carrier type and loading" has been published in Water Research, 2016, 91, 235-243.

Young, B. Constructed 16S rDNA library for all samples. Young, B. performed and analyzed the bioinformatics processing on the sequencing data. Young, B. analyzed the cell viability data and assisted with the regression. Young. B. wrote and revised the manuscript.

Banihashemi, B. performed the cell viability regression. Banihashemi, B. reviewed the manuscript.

Forrest, D. operated and maintained the lab scale MBBR reactors. Forrest, D. performed VPSEM and CLSM for data analysis. Forrest, D. reviewed the manuscript.

Kennedy, K. was a project supervisor, helped conceive and design the project, provided direction and feedback on the experiments.

Stintzi, A. was a project supervisor, provided direction on 16S rDNA library construction and bioinformatics processing, provided direction and feedback on the results.

Delatolla, R. was the primary project supervisor, helped conceived and design the project, provided direction and feedback on the experiments. Delatolla, R. revised the manuscript.

2.2. Abstract

This study investigates the effects of three specific moving bed biofilm reactor (MBBR) carrier types and two surface area loading rates on biofilm thickness, morphology and bacterial community structure of post carbon removal nitrifying MBBR systems along with the effects of carrier type and loading on ammonia removal rates and effluent solids settleability. The meso and micro analyses show that the AOB kinetics vary based on loading condition, but irrespective of carrier type. The meso-scale response to increases in loading was shown to be an increase in biofilm thickness with higher surface area carriers being more inclined to develop and maintain thicker biofilms. The pore spaces of these higher surface area to volume carriers also demonstrated the potential to become clogged at higher loading conditions. Although the biofilm thickness increased during higher loading conditions, the relative percentages of both the embedded viable and non-viable cells at high and conventional loading conditions remained stable; indicating that the reduced ammonia removal kinetics observed during carrier clogging events was likely due to the observed reduction in the surface area of the attached biofilm. Microbial community analyses demonstrated that the dominant ammonia oxidizing bacteria for all carriers was *Nitrosomonas* while the dominant nitrite oxidizing bacteria was *Nitrospira*. The research showed that filamentous species were abundant under high loading conditions, which likely resulted in the observed reduction in effluent solids settleability at high loading conditions as opposed to conventional loading conditions. Although the settleability of the effluent solids was correlated to increases in abundances of filamentous organisms in the biofilm, analyzed using next generation sequencing, the ammonia removal rate was not shown to be directly correlated to specific

meso or micro-scale characteristics. Instead post carbon removal MBBR ammonia removal kinetics were shown to be related to the viable AOB cell coverage of the carriers; which was calculated by normalizing the surface area removal rate by the biofilm thickness, the bacterial percent abundance of ammonia oxidizing bacteria and the percentage of viable cells.

2.3. Introduction

The moving bed biofilm reactor (MBBR) was initially developed as a nitrogen removal system in the 1980's (Rusten et al., 1994) and quickly evolved to operate effectively as a chemical oxygen demand (COD) removal system (Ødegaard et al., 1994). The MBBR system houses biocarriers with attached biofilm, and as such the removal of the carbonaceous and nitrogenous constituents occurs through mass transfer into the biofilm and the subsequent metabolic processing of these constituents by bacterial cells. Thus, the performance of MBBR systems, measured at the macro-scale of influent and effluent concentrations, is ultimately dependent upon the meso-scale properties of the biofilm and the micro-scale bacterial cell community.

It is well known that diffusion into biofilm is dependent on flow velocities across the biofilm with increases in flow velocity resulting in larger localized concentration gradients in the biofilm and faster rates of diffusion through the biofilm (Stewart, 2003; Taherzadeh et al., 2012). Flow velocity changes can result from carrier orientation, carrier pore space configuration and the geometry of the biofilm surface (Herrling et al., 2015; Li et al., 2015). Thus the applied loading and MBBR carrier type used could influence the morphology and thickness of the biofilm matrix and subsequently affect the

rate of mass transfer of nutrients and substrates to the microbial community embedded in the biofilm.

Previous work on COD removal MBBR systems have concluded that system performance is not dependent on carrier type but instead is a function of surface area loading rate (Ødegaard et al., 2000). In this work however, Ødegaard et al. (2000) found inexplicable differences in effluent biomass settleability from the two different carrier types used in their study; indicating the possibility of a difference in biofilm morphology between different carriers and highlighting a potential variability in the bacterial communities. Martín-Pascual et al. (2012) has more recently shown that three MBBR systems with different carriers operated at various hydraulic retention times (HRTs) and filling ratios showed different COD removal efficiencies. Furthermore, additional studies have also shown increases in biofilm thickness as a response to increases in loading rates, which can be achieved through variations in HRT and fill fractions (Karizmeh et al., 2014; Wang et al., 2005). COD removal MBBR systems were shown to exhibit distinct morphologies at various loading conditions, with low density porous structures observed at low loading and filamentous-like morphologies observed at higher loading (Karizmeh et al., 2014). These distinct morphologies suggest a potential difference in the microbial communities within the biofilm.

To date there are limited studies examining the effects of carrier type and loading rate on nitrifying and nitrogen removal MBBR systems. In particular, no research exists in the literature on biofilm thickness, morphology and microbial population community shifts in response to carrier types and surface area loading rates in nitrifying MBBR systems. Population shifts have been observed in nitrifying trickling filters, with low ammonia

environments being dominated by *Nitrosospira*, while high ammonia concentrations were shown to harbour *Nitrosomonas* as the dominant AOB (Zhang et al., 2013). The study also found *Nitrobacter* to be the dominant NOB with high substrate availability and *Nitrospira* being dominant during low loading conditions.

Nitrifying MBBR treatment basins are conventionally located downstream and separate from carbon removal MBBR basins in municipal wastewater treatment trains to minimize the adverse effects of carbon removing heterotrophic populations overgrowing and smothering the nitrifying autotrophic populations (Lee et al., 2004; Nogueira et al., 2002). Further, nitrifying MBBR systems have become increasingly popular as lagoon upgrade systems with the implementation of a more stringent ammonia discharge regulation (Canada Gazette, 2012; WEF, 2011). These systems perform as cost effective, efficient, post carbon removal upgrade systems to current passive lagoon treatment systems that do not achieve ammonia removal. A true understanding of the meso and micro-scale effects of carrier type and loading on post carbon removal nitrifying MBBR systems is critical to further develop and optimize these cost-effective treatment systems. Therefore the aim of this study is to establish the effect of carrier type and ammonia loading rate at the meso and micro-scale within post carbon removal nitrifying MBBRs. In particular, this study focuses on biofilm thickness and morphology, cell viability and bacterial community analysis in response to carrier type and variations in ammonia loading as well as their correlation to ammonia removal rates and effluent settleability.

2.4. Material and methods

2.4.1. Reactor configuration and synthetic wastewater

Four lab scale reactors with three different carrier types were operated under identical conditions at two distinct loading conditions, a high loading condition (HLC) of a surface area loading rate (SALR) of 1.89 g-N/m^2·d and a conventional or normal loading condition (NLC) of an SALR of 0.9 g-N/m^2·d. The total operation time of the four reactors (including start-up, HLC, transition phase to NLC, and NLC) was approximately 2160 HRT cycles (9 months). In particular, the start-up phase was approximately 1200 HRT cycles (5 months); the steady state HLC phase occurred over a periods of 300 HRT cycles (approximately 38 d); the transition phase to NLC conditions occurred over a period of 225 HRT cycles (approximately 28 d); and the steady state NLC phase occurred over a period of 435 HRT cycles (approximately 54 d) where steady state was defined as less than 10% variation in nitrification kinetics and effluent concentration. The reactors were operated at a conventional HRT of 3 h (WEF, 2011), pH of 8.0 ± 0.1, a dissolved oxygen concentration (DO) of 9.0 ± 0.9 mg/l and were fed with synthetic wastewater. A synthetic wastewater was used throughout the experimental phase to provide stable loading rates with limited variations. Synthetic wastewater (modified version of Delatolla et al., 2009a) with an influent ammonia concentration of 50 mg-N/L was used to feed the reactors throughout the HLC experimental phase to provide stable loading rates with limited variations: $(NH_4)_2SO_4$: 235.82 mg/L, $NaHCO_3$: 650 mg/L, $MgSO_4.7H_2O$: 325 mg/L, $CaCl_2.2H_2O$: 29.34 mg/L, KH_2PO_4: 79.09 mg/L, $FeSO_4.7H_2O$: 4.98 mg/L. Carbon source: $C_6H_{12}O_6$: 3.8 mg/L, sodium acetate: 2.0 mg/L, Peptone: 3.8 mg/L. Trace nutrients

included $MnCl_2.4H_2O$: 200 µg/L, $NaMoO_4.2H_2O$: 49.62 µg/L, $CuSO_4.5H_2O$: 205.1 µg/L, $CoCl_2.6H_2O$: 2 µg/L, $ZnSO_4.7H_2O$: 59.82 µg/L.

The glucose, acetate and peptone were supplied to mimic the readily degradable carbonaceous content of wastewater at a concentration of 10 mg BOD_5/L under HLC. Nitrifying MBBR systems are conventionally designed, with respect to BOD_5 concentration, to achieve BOD_5 < TKN and $sBOD_5$ < 12 mg/L in order to minimize the adverse effects of heterotrophic overgrowth on autotrophic nitrifiers in the same treatment basin (WEF, 2011). Hence, nitrifying MBBR basins are conventionally designed separate to carbon removal MBBR units, with nitrifying MBBR basins being located downstream of carbon removal MBBR units or carbon removal lagoon treatment units. Nitrification is often inhibited year round in northern country lagoon treatment systems due to the effect of winter operation and furthermore the ammonia concentrations have been shown to increase in the lagoon due to the process of ammonification that occurs in the settled sludge bed in the lagoons. The NLC concentrations and loadings of the carbonaceous and nitrogenous substances to the nitrifying MBBR reactors in this study was based on conventional municipal treatment systems in multi-basin MBBR treatment systems and post lagoon treatment conditions that does not achieve ammonification. The HLC concentrations and loadings of the carbonaceous and nitrogenous substances were based on post carbon removal lagoon treatment where ammonification occurs in the settled sludge bed of the lagoon and has increased the ammonia concentration in the lagoon effluent.

After the reactors were analyzed at steady state HLC, the ammonia, alkalinity and BOD_5 were gradually decreased to proportionally half of the concentrations at HLC to maintain the same nitrogen to alkalinity and nitrogen to carbon ratios at NLC operation.

Reactors 1 and 2 were 2 L cylindrical reactors operating with 50% fill of K3 AnoxKaldnes biofilm carriers. The K3 carrier is 25 mm in diameter and 12 mm in depth with an available surface area of 500 m^2/m^3 (WEF, 2011). Reactors 3 and 4 were 1.2 L cylindrical reactors operating with 30% fill of the AnoxKaldnes P carrier and 20% of the AnoxKaldnes M carrier, respectively. The P carrier is 2 mm in depth with a diameter of 48 mm and available surface area of 900 m^2/m^3, while the M carrier is 2 mm in depth with a diameter of 48 mm and a surface area for biofilm attachment of 1200 m^2/m^3 (WEF, 2011). Reactors 3 and 4 were sized differently from reactors 1 and 2 to promote better rotation of the P and M carriers in the reactors. Specifically, the modified diameter to height ratio of reactors 3 and 4 enabled better rotation of the P and M carriers, while potentially minimizing the wall effects on the carriers (Leyva-Díaz et al., 2013). The air inflow rate of the reactors containing the K3, M and P carriers was approximately 4, 3, and 3 L/min, respectively. The rate of aeration in each reactor was designed to maintain constant rotation of the carriers in the reactors while supplying sufficient oxygen for the necessary biological processes. Based on the aeration requirement for carrier movement in the reactors, the DO concentrations were maintained at 9.0 ± 0.9 mg/l throughout the entire study. As the effluent ammonia concentrations and hence the reactor bulk phase ammonia concentrations were below 5 mg-N/L throughout the study, the kinetics of the reactors were likely ammonia mass transfer rate limited and not oxygen mass transfer rate

limited (WEF 2011); hence minimizing the effects of elevated DO concentrations on the kinetics of the study.

2.4.2. Constituent analysis

Effluent concentrations of ammonia, nitrite and nitrate were measured in accordance with standard methods (APHA, 1998); methods 4500- NH_3, 4500-NO_3^- B, and 4500-NO_2^-. DO and pH measurements were acquired using a symphony Multi Parameter Meter with attached DO and pH probes (VWR, Canada, Ontario). Temperature within the reactors was measured daily using a glass thermometer and maintained at 22±1˚C by the thermostat controlled environment within the laboratory. Total suspended solids (TSS) and volatile suspended solids (VSS) were measured according to Standard Methods (APHA, 1998); 2540 D- Total Suspended Solids (total suspended solids dried at 103-105˚C), 2540 E- Volatile Suspended Solids (volatile solids ignited at 550˚C). All wastewater constituent samples were collected in triplicate and were filtered through a 0.45 μm filter before testing to reduce the effect of suspended solids on measured values.

2.4.3. Settleability of effluent solids

Due to the fact that the nitrifying MBBR process produced a low concentration of effluent TSS, the sludge volume index (SVI) of the samples could not be measured accurately for this study. Hence, the settleability of the solids produced by the reactors was investigated using a digital particle analyzer (Brightwell Technologies Inc., Canada, Ontario). Digital particle analysis (DPA) enabled the distribution of particles between 2.25 μm and 400 μm to be measured. Using DPA to quantify the particle distribution of the solids prior to and following 30 min of settling enabled the settleability of the solids

to be quantified in this study. Five effluent samples were collected from each reactor and the DPA measurements of each sample was analysed in triplicate.

2.4.4. Microbial analysis

I. Biofilm morphology and mass

Biofilm morphology and thickness were observed through the use of a Vega II-XMU variable pressure scanning electron microscope (VPSEM) (Tescan USA Inc., USA, Pennsylvania). During each phase of the study a carrier was randomly selected from each reactor and without sample preparation analysed in the VPSEM chamber at 40 Pa. The VPSEM was optimized to 40 Pa pressure for maximum exposure of 5 min to prevent morphological changes due to dehydration. Images were acquired at 20 points across the carrier with magnifications ranging from ×20 to ×5000. Though VPSEM may produce shrinkage of the biofilm with long exposure (exposures times were restricted in this study to minimize biofilm shrinkage), it eliminates the need for destructive sample preparation which is a necessity of traditional SEM (Delatolla et al., 2009b; Flemming et al., 2000).

Three carriers were harvested from the reactors to measure the mass of biofilm on the carriers. The carriers were centrifuged in 85 ml centrifuge tubes for 30 min at 9000 rpm in a Sorvall centrifuge (Thermo Fisher Scientific, Massachusetts, USA). Subsequently, the samples were vortexed using a vortex-genie (Fisher Scientific, New York, USA) for 15 min at a maximum speed of 10. The TS and VS were measured on the resultant extracted biofilm according to Standard Methods (APHA, 1998): 2540 B – TS and 2540 E – VS.

II. Cell viability

One carrier was randomly selected from each reactor for analysis during both HLC and NLC. The carrier was cut to expose the inner surfaces and stained with Propium Iodide and Syto 9 of the film Tracer™ LIVE/DEAD® biofilm viability kit (Life Technologies, Ontario, Canada) along with calcofluor to illuminate the extracellular polymeric material of the biofilm in blue. Confocal light scanning microscopy (CLSM) has become a conventional method for the enumeration of micro-organisms on surfaces and the characterization of biofilms. CLSM allows for the non-destructive optical sectioning of the biofilm. An LSM 510/Axio imager M.1 confocal microscope (Carl Zeiss Canada Ltd, Ontario, Canada) equipped with argon and helium-neon lasers was used to image the biofilm samples in this study. A total of 20 images per reactor or 4 stacks of 5 images acquired within an approximate total depth of 30 μm were captured for each sample and were analysed using NI Vision Assistant 7.1 (LabView 8.0- National Instruments Canada, Vaudreuil-Dorion, Canada). The biofilm area and the area of the fluorescent red and green illuminated cells were quantified (Delatolla et al., 2009b).

III. DNA extraction and amplification

For each set of microbial community data five replicate carriers were randomly selected from each reactor. For each carrier, 0.25 g of biofilm was abraded from the media into a 1.5 mL sterilized Eppendorf tube. DNA was extracted from the biofilm using FastDNA® spin kit (MP Biomedicals, Santa Ana, CA) and the DNA was stored at -80°C until it was used for library construction. DNA amplification utilized a two-step polymerase chain reaction (PCR) targeting the V6 hyper-variable region of the 16s rRNA gene was achieved using Phusion® High-Fidelity PCR Master Mix (Thermo Fisher

Scientific Inc., Waltham, MA). The primers used for the first and second PCR reaction were selected from a barcoding approach previously described by Abujamel et al. (2013). The PCR amplicons were inspected by electrophoresis on a 2% agarose gel and purified with a Montage PCR96 cleanup kit (EMD Milipore, Billerica, MA). The purified amplicons were quantified using Quant-iT^{TM} dsDNA HS Assay Kit (Life Technologies, Burlington, Canada) and pooled with 200 ng of DNA from each sample to be sequenced using an Illumina Hiseq2500 at the center for applied genomics (TCAG, Toronto, Canada).

IV. DNA sequencing analysis

The entire DNA sequencing analysis was disseminated using Bio Linux operating platform. The paired-end reads were assembled using the fast length adjustment of short reads (FLASH) software (Majoc and Salzberg, 2011) and quality filtered using the Fastq_quality_filter command from the Fastx toolkit with the minimum quality score of 20 over 97% of the sequences. Reads that passed the quality filter were demultiplexed and the barcodes were trimmed using Novobarcode (Goecks et al., 2010). The quantitative insights into microbial ecology (QIIME) software, version 1.8, (Majoc and Salzberg, 2011) was used to compute operational taxonomical unit (OTU) clustering with a closed reference of 97% sequence similarity. QIIME compared the OTUs with UCLUST against the Greengenes database 13.8; the singletons were removed and the relative abundance of the bacterial taxa present in the biofilm was determined (Caporoso et al., 2010). The biofilm samples were highly diverse with greater than 800 OTUs per sample. To ensure adequate coverage for subsequent analysis and minimize false positives due to low read numbers, samples with less than 15,000 reads were removed

from the sample set (with a total of 5 samples being analyzed for each carrier at HLC and NLC). The samples with greater than 15,000 reads were analyzed for differential abundance of bacterial taxa using metagenomeSEQ (Paulson et al., 2013).

V. Microbial activity

In this study kinetic rates were normalized with respect to the biofilm thickness, cell viability, and AOB relative abundance. The ammonia removal rate was expressed per biofilm volume by dividing the SARR by the biofilm thickness in an aim to evaluate the biofilm volume ammonia removal rate (BVRR) across carrier type and loading conditions (Hoang et al., 2014a)

$$\text{BVRR} = \frac{\text{SARR}}{B_T} \qquad \text{Equation 2.1}$$

Where BVRR is biofilm volume ammonia removal rate (g-N/m^3·d), SARR is surface area removal rate (g-N/m^2·d) and B_T is biofilm thickness (m).

The ammonia removal rate was also expressed per viable cell volume by dividing the SARR by the viable cell coverage of the biofilm in order to evaluate the viable cell ammonia removal rate (VCRR) across carrier type and loading conditions (Hoang et al., 2014a). Previous work has shown a rapid decrease in oxygen and substrates from the surface of the biofilm to the carrier support, which could cause a decrease in cellular kinetics (Li et al., 2015). To account for potential loss in cellular kinetics, the viable cell coverage of the biofilm was interpolated through the entire measured biofilm thickness based on the CLSM viable cell data analysed for the upper 30 μm thick biofilm section of the samples. Interpolation used a least squares fitting method to interpolate the live cell coverage for the entire thickness of the biofilm for each carrier.

$$\text{VCRR} = \frac{\text{SARR}}{B_T \times L_C} \qquad \text{Equation 2.2}$$

Where VCRR is viable cell ammonia removal rate (g-N/m^3·d) and L_C is percent live cell coverage (%).

Furthermore, the ammonia removal rate is also expressed per viable AOB cell volume by dividing the SARR by the viable AOB cell coverage (VAOBRR) across carrier type and loading conditions. This analysis uses the interpolated viable cell coverage above and assumes the viable cell coverage is uniform across the bacterial population.

$$\text{VAOBRR} = \frac{\text{SARR}}{B_T \times L_C \times \%AOB} \qquad \text{Equation 2.3}$$

Where VAOBRR is viable AOB ammonia removal rate (g-N/m^3·d) and %AOB is the relative abundance of AOB.

VI. Statistical analysis

All constituent statistical analyses were based on 5 samples taken in triplicate (15 measurements); biofilm thicknesses were based on 20 measurements acquired from 5 images; cell viability analyses were based on 20 acquired images and sequencing percent abundances were based on 5 replicate samples. Statistical significance of measured constituents, biofilm thickness, cell viability and percent abundance values across carrier types and between the two loading phases were tested by the t-test with a *p*-value of 0.05 for statistical significance using GraphPad Prism 6. All constituent, biofilm thickness, cell viability and percent abundance samples were acquired at steady state defined by less than 5% variation in effluent nitrogenous compounds.

For the bacterial community shift analysis, statistical significance within the weighted uni-frac beta diversity was tested using nonparametric statistical method (ADONIS) from the program QIIME (Caporoso et al., 2010). Statistical significance within the taxa was tested using a zero inflated Gaussian model incorporated into the metagenomeSEQ package.

2.5. Results and discussion

2.5.1. Nitrifying kinetics

High removal efficiencies of ammonia were observed at both HLC and NLC with average system removal efficiencies of 93.6 ± 3.0% at HLC and 97.6 ± 1.0% at NLC and with surface area removal rate (SARR) values of 1.82 ± 0.01 g-N/m^2·d and 0.89 ± 0.01 g-N/m^2·d, respectively (Fig. S1). The effluent ammonia concentrations of all reactors were below 2 mg-N/L, with the exception of the M carrier at HLC that was 4.70 ± 2.45 mg-N/L (Table S1). All reactors showed limited nitrite accumulation, with effluent nitrite concentrations remaining less than 1 mg-N/L in all reactors at HLC and NLC (Table S1). No significant difference in substrate removal rates was observed for different carrier types at HLC or NLC with the exception of the M carrier at HLC (Fig. S1). Other studies also showed more stability in ammonia removal rates for K3 carriers at various loading conditions (Gilbert et al., 2015; Zhang et al., 2013). The lower SARR values of the M carrier compared to other carriers at HLC is attributed to the clogging of the carrier's pore spaces due to excessive biofilm growth; leading to reduced biofilm surface area for substrate penetration. The clogging of the M carriers not only showed lower SARR values but also demonstrated small fluctuations in the effluent ammonia concentrations as compared to the other carriers that remained unclogged at higher loading. Hence, the

type of carrier used in MBBR systems showed little effect on nitrifying kinetics for all unclogged carrier conditions. However, at high loading condition the highest surface area to volume ratio carrier showed a tendency to clog and subsequently lower its removal efficiency and the stability of the effluent ammonia concentrations.

2.5.2. Settleability of effluent solids

The average percentage of effluent particles removed by 30 min of settling at HLC for all carriers was 45 ± 19%. The result of effluent particles removal for each carrier shows that the P carrier (59 ± 21%) and the K3 carrier (56 ± 25%) produce effluent with significantly better settling characteristics than the M carrier (11 ± 5%). The effluent of the M carrier reactor at HLC showed the poorest solids settlement, which coincides to a clogging of the carriers and the subsequent slower kinetics compared to the other carriers.

At NLC the average percent settlement of effluent particles was 70 ± 6%, the M and P carrier demonstrated similar settling (79 ± 3% and 79 ± 4%) and the K3 carrier (62 ± 9%) showed the least settlement. Hence, the study shows that higher nitrogen loading conditions cause a reduction in particle settleability. This is in agreement with previous studies on carbon loaded MBBR systems that showed poor biomass settleability at higher carbon loads (Ivanovic et al., 2006; Ivanovic and Leiknes, 2012).

2.5.3. Biofilm morphology and mass

The morphology and mass results (Fig. 2.1) show thicker biofilms with greater biofilm mass per reactor at HLC than NLC. This observation is expected as higher loadings promote deeper substrate penetration into the biofilm as well as a thicker biofilm (Gerardi, 2002). The morphology and mass results also offer a comparison of the biofilm

growth across different carrier types and demonstrate no significant differences in biofilm thickness or biofilm mass per reactor between the K3 and P carriers at HLC. However the biofilm thickness of the M carrier (carrier with the highest surface area to volume ratio) at HLC differs significantly compared to both the K3 and P carriers. The significantly thicker biofilm of the M carrier at HLC corresponds to the clogging of the M carrier. Under HLC the clogged M carrier demonstrated significantly higher biofilm mass per reactor measurements compared to K3, significantly lower SARR values and lower effluent solids settleability compared to the K3 and P carriers in addition to demonstrating small fluctuations in the effluent ammonia concentrations. These fluctuations were likely a result of limitation of substrate penetration into the biofilm. For example, it has been shown on average the maximum penetration depth of oxygen in an aerobic reactor is 100-150 μm (Tijhuis et al., 1994). The depth of penetration in this study was likely to be at the higher boundary due to oxygen saturation in the bulk liquid, however, the clogged M carrier significantly exceeded the maximum penetration depth of oxygen. This would have created anoxic zones at depth in the biofilm and likely caused the operational instability.

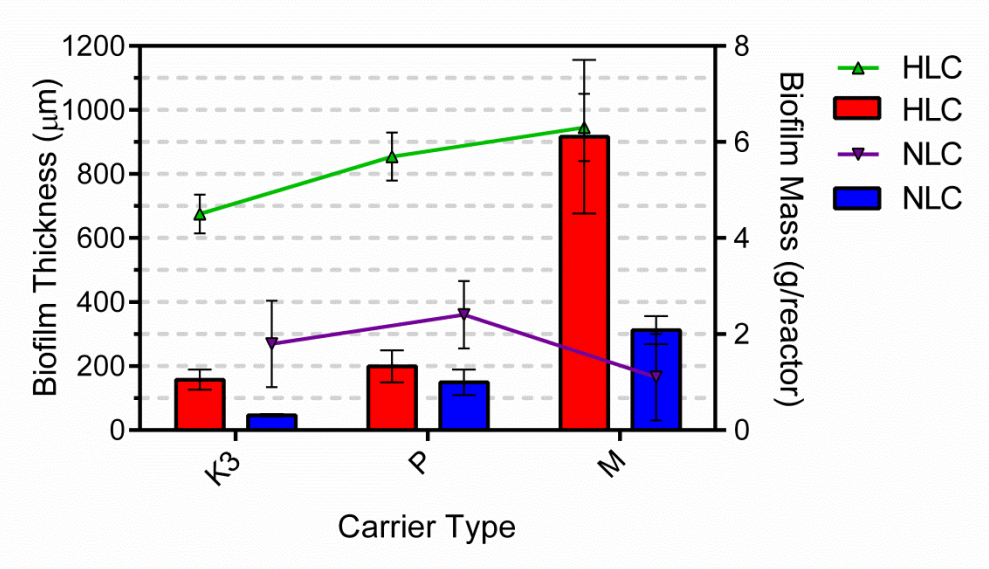

Figure 2.1 Average and 95% confidence interval (n=20) values of measured biofilm thickness (bars) and biofilm mass (symbols) per reactor across carrier type and loading condition (data sets acquired after three weeks of steady state operation)

Under NLC the M and P carriers (carriers with higher surface to volume ratios compared to the K3 carriers) show a significantly greater biofilm thickness than the K3 carrier where M had the highest biofilm thickness, with the biofilm mass per reactor not demonstrating a significant change across carriers; during this phase however the SARR value of the M and P carriers was similar to the SARR of the K3 carrier. Therefore for nitrifying MBBRs biofilm thickness and biofilm mass per reactor are not direct indicators of system performance; however under high loading conditions excessive growth promotes clogging which can significantly reduce the nitrifying kinetics. Furthermore, the biofilm thickness, biofilm mass per carrier and the solids settlement results for the studied carriers at NLC, suggest that excessive biofilm growth produces solids with a greater propensity to settle within 30 minutes.

Researchers studying MBBR carbon loaded systems were able to observe distinct differences in the biofilm morphology between different loading conditions; clear shifts from thick to fibrous films and clear changes in density (Karizmeh et al., 2014). Fibrous structural elements were not observed in the nitrifying biofilm grown of this study (Fig. 2.2). The acquired VPSEM images do however highlight differences in the protozoa, nematodes and water mite communities across carrier type and across loading conditions. At HLC an abundance of water mites on the K3 carrier was observed (Fig. 2.2a), as well as their absence on the P and M carriers (Fig. 2.2b and 2.2c). In addition there were numerous ciliates present at the surface of the P and M carriers biofilm at HLC, which were absent from the K3 carrier. Stalked ciliates were seen to be the predominant feature on the P carrier (Fig. 2.2b) while free-ciliates and nematodes tend to be more dominant on the M carrier (Fig. 2.2c). These results suggest that the meso-scale environments developed on each carrier type differ and that the micro-scale results may also differ; as a result each carrier type may promote the proliferation of different abundances of microorganisms. At NLC the VPSEM images of all carriers show the absence of the protozoa, nematodes and water mites observed at HLC and at NLC distinctly thinner biofilms are observed as compared to HLC. Further, Fig. 2.2c demonstrates that the clogging of the M carriers was not uniform across the pore spaces. It is evident that not all pore spaces are completely clogged by biofilm, but some pores spaces maintained their integrity and others were partially clogged which indicates that the effective surface area of the biofilm attached to the M carrier at HLC is reduced as excess biofilm grows in the carriers pore spaces (Fig 2.2c).

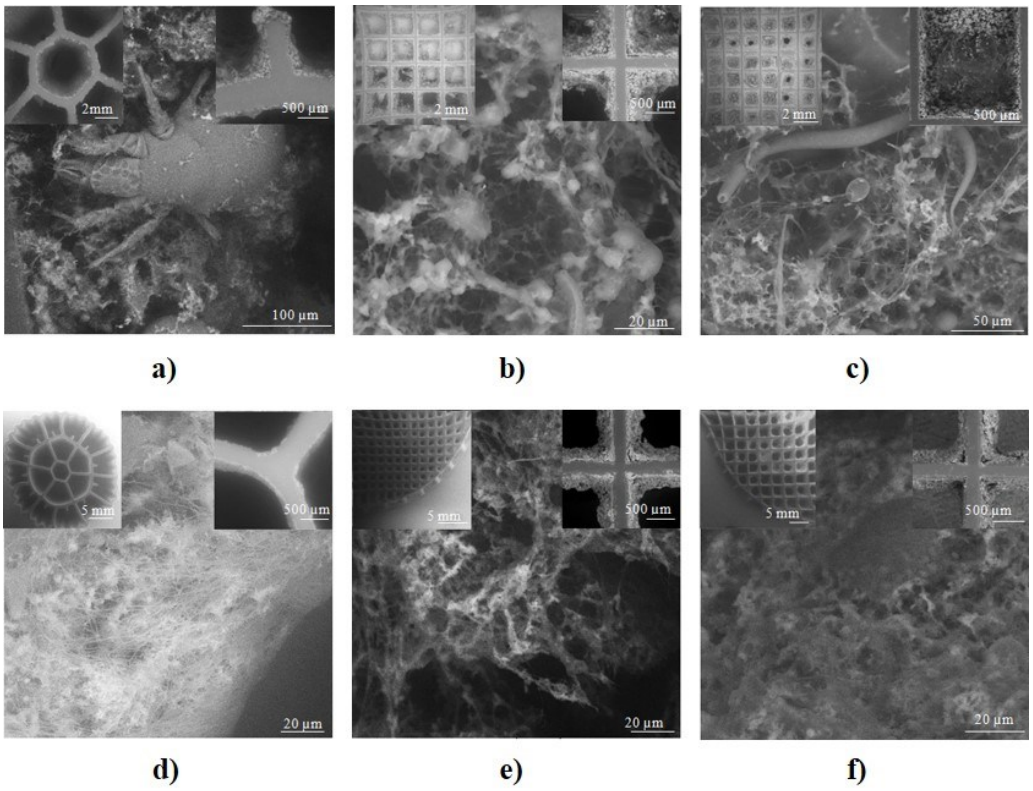

Figure 2.2 VPSEM images acquired after three weeks of steady state operation; a) K3 carrier-HLC, b) P carrier-HLC, c) M carrier-HLC, d) K3 carrier-NLC, e) P carrier-NLC, f) M carrier-NLC

2.5.4. Cell viability

The viability test illuminates viable cells in green and non-viable cells in red and was used in this study in combination with confocal microscopy to capture images of cell viability at five distinct depths in the biofilm of the harvested samples (Fig. S2). The percent of viable and non-viable cells were quantified in the upper 30 µm thick biofilm section of the samples (Fig. 2.3). Viability analysis was limited to a depth of 30 µm to ensure that when analyzing carrier samples with thinner biofilm (with an approximate minimum thickness of 30 µm) the same depths and number of images acquired for each

sample analyzed was consistent throughout the study. Further, the upper 30 µm of the biofilm is believed to be the most active section of the biofilm.

No significant difference was observed between HLC and NLC with respect to the percent of viable cells, percent of non-viable cells or percent of total cells per area of biofilm for each of the carriers (Fig. 2.3). No difference in percentage of total cells was observed at HLC as compared to NLC despite the fact that significantly thicker biofilms were shown at HLC as compared to NLC.

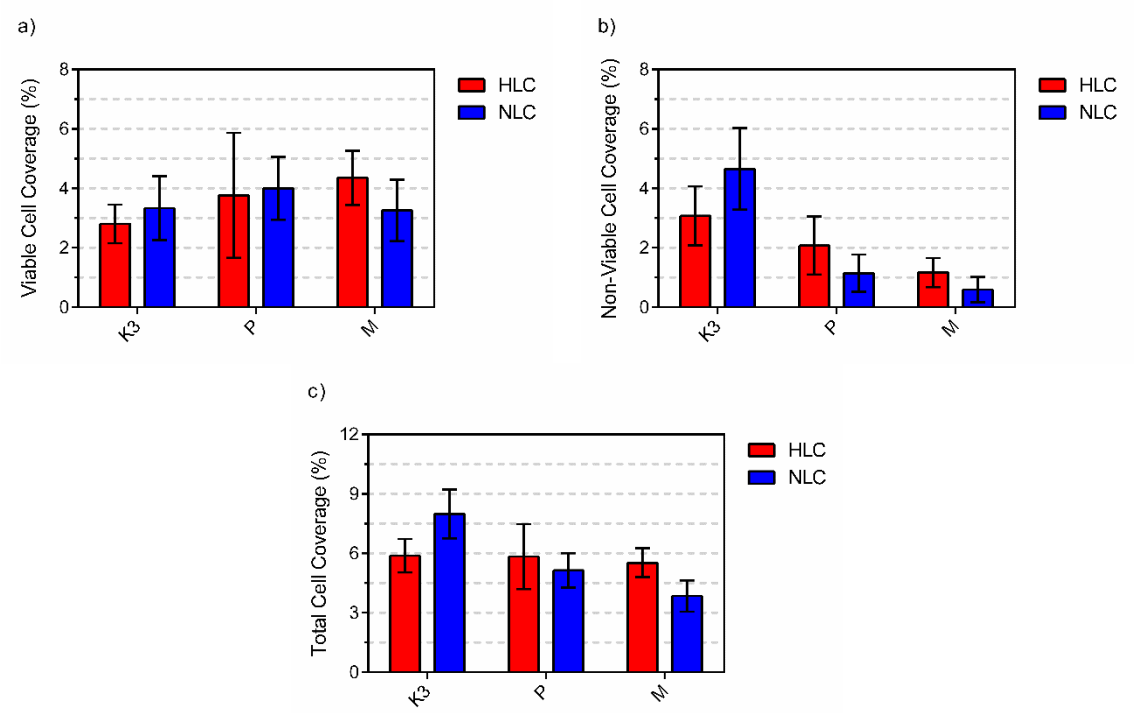

Figure 2.3 Percent cell coverage and standard deviation (n=5) of biofilm area at HLC and NLC (CLSM images acquired after three weeks of steady state operation); a) viable cell coverage, b) non-viable cell coverage, c) total (viable and non-viable cell coverage)

The research was also aimed at determining effects of carrier type on the viability of the biomass. The various carriers investigated in this study demonstrated similar percent coverage of viable cells per biofilm area irrespective of carrier type at HLC and NLC (Fig. 2.3). The M and P carriers, however, did demonstrate a significantly lower percent

coverage of non-viable cells as compared to K3 carriers at NLC. This significant difference in non-viable cell coverage can be due to the fact that the M carriers were consistently clogged during operation at HLC. Subsequently, during the transition from HLC to NLC a large change in biofilm thickness occurred in the M carrier, where the thickness of the biofilm was reduced by approximately one-third (Fig. 2.1). This sloughing of the biofilm thickness may have exposed deeper areas of biofilm that was less active due to restrictive mass transferring of nutrients and substrates during the excessive overgrowth observed in the clogged M carriers (Li et al., 2015; Tijhuis et al., 1994). Hence, growth of newly formed biofilm may have been initiated after sloughing at NLC until the system reached steady state conditions. Therefore, at NLC it is likely that the upper biofilm of the M carriers was newly generated biofilm (younger biofilm) that subsequently contained less non-viable cells compared to K3 carriers that did not go through a sloughing event and maintained a mature upper biofilm with an overall higher coverage of non-viable cells.

Although the biofilm thickness measurements of the P carrier do not demonstrate a large change in biofilm thickness between HLC and NLC, the P carriers are believed to have experienced excessive biofilm growth at the end of the HLC experimental phase. This excessive growth was not captured by the VPSEM imaging of the study and thus does not appear in Fig. 2.3. The excessive growth period, which occurred just prior to the transition to NLC, is believed to have caused a similar sloughing condition to the clogged M carriers and may be responsible for the observed lower coverage of non-viable cells as compared to the K3 carriers. The clogging at HLC observed in this study occurred in the carriers with the smallest pore spaces, where the M carrier (1200 m^2/m^3) clogged

immediately, the P carrier (900 m^2/m^3) clogged at the end of the HLC and the K3 carrier (500 m^2/m^3) did not experience any clogging events in this study.

2.5.5. Bacterial community composition

Fig. S3 shows the phylogenetic tree identifying the core microbial phyla present within the biofilm samples analyzed in this study with the relative abundance of the genus of the various carriers at HLC and NLC. A dominance of *Proteobacteria* is observed in the samples, which is expected as synthetic wastewater with a low organic load was fed to all the reactors. Low organic loadings at both HLC and NLC were used to simulate nitrification conditions following conventional secondary treatment.

The OTUs were analyzed for overall variation using the uni-frac distance (Fig. 2.4). As mentioned above, 5 replications were run per sample and runs producing less than 15,000 reads were removed from the data set. The uni-frac beta diversity is a principal coordinate analysis which identifies the OTUs most responsible for differentiation in the communities. This analysis was performed unweighted, presence/absence of OTUs, and weighted which takes the OTU relative abundance into account. ADONIS test using uni-frac distance did not find significant separation with respect to HLC and NLC or carrier type. However, the weighted uni-frac beta diversity with respect to HLC and NLC does demonstrate clear separation in communities (Fig. 2.4a). Using an analysis of variance for distance matrices (ADONIS), it is found that there is a significant shift in populations comparing HLC and NLC conditions (13% explained variation, $p = 0.006$). Although this analysis does not identify the OTUs responsible for community separation, it does indicate the microbial ecology is affected by loading conditions. However Fig. 2.4b shows no clear separation between carrier types at equivalent loading conditions;

indicating loading condition is the largest driver of microbial community population shifts. Additionally, the primary cause of separation between HLC and NLC in Fig. 2.4b is likely due to the observed shift in abundance of the species within the communities at the two operating conditions.

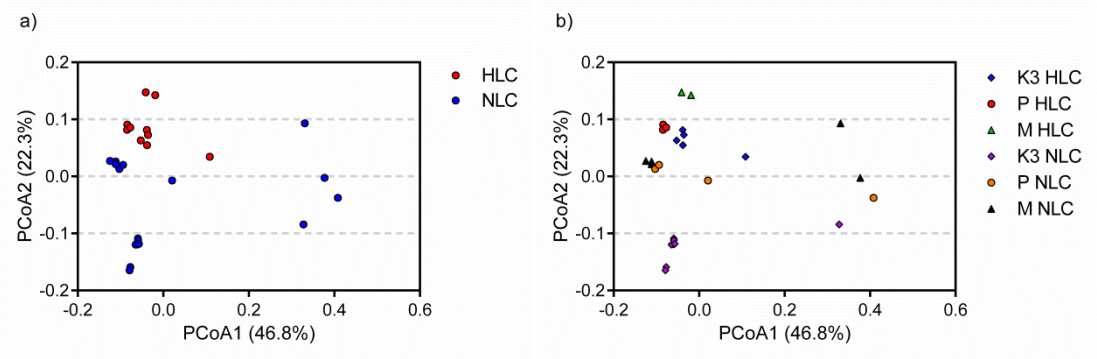

Figure 2.4 Weighted Uni-Frac principal coordinate analysis measured after three weeks of steady state operation for a) HLC and NLC grouped, b) all sample groups

At both HLC and NLC, the family *Nitrosomonadacea* showed the highest relative abundance of ammonia oxidizing bacteria (AOB). Within the family *Nitrosomonadacea*, the genera *Nitrosomonas* and *Nitrosospira* were shown to be the most abundant ammonia oxidizers in this study. The genus *Nitrosococcus* was not detected in the samples even with *Nitrosococcus* being a suspected wastewater AOB in nitrifying systems (Daims et al., 1999; Gieseke et al., 2001; Park et al., 2008). At HLC and NLC, the family *Nitrospiraceae* showed the highest relative abundance of nitrite oxidizing bacteria (NOB). Within the family *Nitrospiraceae,* the genus *Nitrospira* was shown to be responsible for nitrite oxidation in this study. The genus *Nitrobacter*, a suspected wastewater NOB, was not detected in the samples.

Grouping the known AOB taxa shows that there is a significant decrease in AOB relative abundance from HLC to NLC (Fig. 2.5a). The average AOB relative abundance

at HLC and NLC is 4.1 ± 0.9% and 7.2 ± 1.6% respectively, a ratio of 1:1.7. Although this appears counter intuitive, the biofilm thickness ratio at HLC to NLC is 2.6:1. As the NLC and HLC both demonstrate greater than 96% ammonia removal, HLC likely creates an environment suitable for other species of bacteria to be enriched in the biofilm matrix. This enrichment could partly cause the reduction in percent AOB cells and the significant increase in biofilm thickness. The NOB remained constant at both HLC and NLC with relative abundances of 21.1 ± 7.0% and 23.9 ± 4.6% respectively.

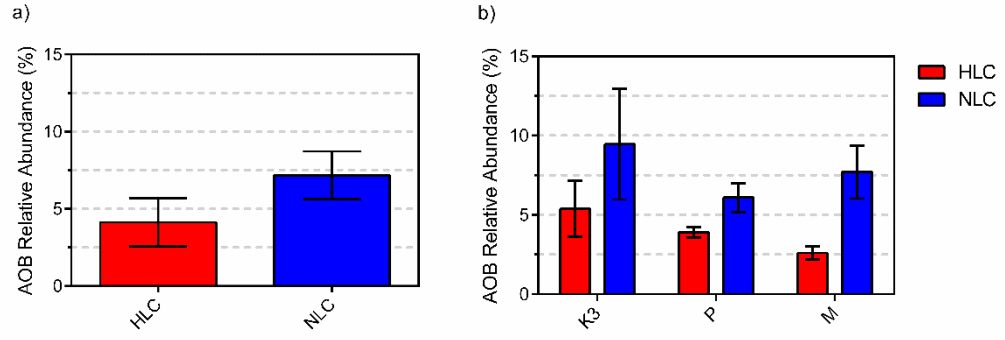

Figure 2.5 Relative abundance and standard deviation (n=5) of 16S rRNA gene amplicon reads measured after three weeks of steady state operation of a) AOB at HLC and NLC for all carriers and b) AOB embedded in the biofilm of each carrier type at HLC and NLC

The AOB relative abundance was also analyzed to determine the effects of carrier type on the population of AOB (Fig. 2.5b). The various carriers investigated in this study demonstrated similar relative abundance of AOB between the K3 carrier and the P carrier at HLC (Fig. 2.5b). The M carrier, being clogged at HLC, did demonstrate a significantly lower relative abundance of AOB as compared to the K3 and P carriers at HLC. The carriers demonstrated similar relative abundance of AOB across all studied carrier types at NLC. The NOBs in this study also were shown to not significantly change across carrier types.

To determine the differentially abundant species at HLC, the OTU table was analysed with metagenomeSEQ. This analysis allows for the determination of differentially abundant taxa with loading conditions as the main variable and carrier type as a covariate. For this analysis a positive $\log_2$ change indicates 76 unique taxa, which were abundant at statically different percent abundances at HLC as compared to NLC. The taxa belonged to three phyla, *Bacteroidetes*, *Firmicutes* and *Proteobacteria*, which are common in wastewater treatment plants and are diverse in their metabolic functionality.

At NLC the harvested samples are shown to be enriched with *Firmicutes*. Within this phylum, the most prominent differentially abundant genus is *Comamonas* with 24.04 $\log_2$ change. *Comamonas* is a ubiquitous organism that is common in wastewater treatment plants and was likely outcompeted by the enriched bacteria in the HLC.

At HLC the samples are shown to be enriched with *Bacteroidetes* and *Proteobacteria*. Within these two phyla, the most prominent differentially abundant genera are *Zoogloea* and *Haliscomenobacter* with $\log_2$ fold changes of 4.86 and 7.28 respectively. *Zoogloea* and *Haliscomenobacter* are well known filamentous bulking organisms in conventional activated sludge treatment facilities (Aonofriesei and Petrosanu, 2007; Xue et al., 2012). Enrichment in filamentous bacteria, as low as 1% relative abundance, has been shown to lead to a decrease in sludge settlement (Kaewpipat and Grady, 2002; Martins et al., 2004). At HLC, *Zoogloea* and *Haliscomenobacter* represented 2.2% and 4.3% relative abundance as compared to 0.08% and 0.03% at NLC, respectively. This increase in filamentous bacteria is likely the cause of the poor settlement observed at HLC.

The microbial communities were also compared with respect to carrier type. As expected, the effect of differing carrier type produced fewer differentially abundant taxa

than the effect of high versus conventional loading. The K3 carrier incorporated 8 differentially abundant taxa belonging to the *Proteobacteria* phylum as compared to the P and M carriers. The P carrier incorporated 6 differentially abundant taxa belonging to the *Planctomycetes* and *Proteobacteria* and phyla. Lastly, the M carrier incorporated 5 differentially abundant taxa belonging to the *Bacteroidetes*, *Firmicutes* and *Proteobacteria* phyla. All of the taxa identified were ubiquitous organisms and represented less than 0.2% relative abundance in the population. Thus the identification of the population shifts is an increase/reduction of few bacteria in the biofilm matrix.

2.5.6. Evaluation of cellular activity and bacterial population

The kinetics were normalized based on the biofilm morphology, cell viability and AOB relative abundance. At HLC the BVRR of the K3 and P carriers do not differ significantly, while the M carrier BVRR is significantly lower than both the K3 and P carriers (Table 2.1); indicating that the thicker biofilm on the M carrier at HLC is less efficient with respect to ammonia removal kinetics relative to total attached biofilm. At NLC there are significant differences between the BVRR values of the K3 carriers as compared to both the P and M carriers. Statistical difference are also observed between the BVRR values of the P and M carriers where the carrier with the highest surface area per volume, M, demonstrates the lowest BVRR (Table 2.1).

At HLC the VCRR of the K3 carriers are significantly higher than both the P and M carriers. The VCRR of the P carrier is significantly greater than the M carrier. Hence, the cells embedded in the K3 carriers, the carriers with the lowest surface area per volume, demonstrate a higher cellular activity than the carriers with the highest surface area per volume. At NLC, however, there were no statistical differences observed between the

VCRR values of the carriers. The significant change in VCRR and BVRR of the M carrier could be influenced by the bulk liquid flow to the biofilm attached to the carriers and the subsequent mass transport through the biofilm. Although not studied for the specific carriers used in this study, the flow and mass transport through carrier pore spaces has been shown to be influenced by biofilm thickness and the filling of the pore spaces by biofilm (Herrling et al., 2015). The biofilm thickness of the M carrier in this study reduced the pore spaces of the M carrier, thus potentially decreasing the efficiency of flow through the carrier pore space and reducing the transport kinetics from the bulk liquid phase into the biofilm.

At HLC and NLC, no significant VAOBRR differences were observed across all carrier types investigated in this study (Table 2.1). This finding indicates that the viable AOBs present in the biofilm likely have similar kinetics irrespective of biofilm morphology, thickness or carrier type and irrespective of clogging conditions. Hence, these findings indicate that the clogged carriers do not decrease the AOB kinetics within the biofilm; instead clogging reduces the mass transfer rate likely through a reduction of the effective surface area of the attached biofilm. Further, this research shows that the viable AOBs present in the biofilm at HLC have faster kinetics as compared to the viable AOBs present at NLC, which is expected as larger quantities of ammonia are expected to be transferred to respective depths in the attached biofilm at higher loading conditions.

Table 2.1 Average and 95% confidence interval values of the biofilm volume ammonia removal rate (BVRR), the viable cell ammonia removal rate (VCRR) and the viable AOB ammonia removal rate (VAOBRR) at HLC and NLC measured across steady state

Condition	Carrier type	BVRR × 10^3 ($gN/m^3 \cdot d$)	VCRR× 10^3 ($gN/m^3 \cdot d \cdot$%viable cells)	VAOBRR× 10^3 ($gN/m^3 \cdot d \cdot$%viable AOB cells)
HLC	K3	10.6 ± 2.1	17.2 ± 2.0	264 ± 41
	P	8.5 ± 2.6	10.9 ± 1.8	281 ± 55
	M	1.9 ± 0.5	7.6 ± 1.6	280 ± 59
NLC	K3	19.6 ± 2.2	7.5 ± 1.7	81 ± 25
	P	5.8 ± 0.5	3.9 ± 0.7	85 ± 26
	M	2.8 ± 0.1	4.8 ± 0.4	63 ± 18

2.6. Conclusion

Post carbon removal nitrifying MBBR biofilm was studied over a period of 9 months at the meso and micro-scale with respect to three different carrier types and two ammonia loading rates. The study shows the highest surface area to volume carriers demonstrate the highest propensity for clogging. The clogged pore spaces resulted in significantly lower ammonia removal rates and also the poorest solids settlement at HLC when compared to the other carriers. The research also shows that filamentous species were abundant under high loading conditions across all carriers, which likely resulted in the observed reduction in effluent solids settleability at high loading conditions as opposed to conventional loading conditions. The relative percentage of both live and dead cells at high and conventional loading were observed to remain stable for all carriers; where *Nitrosomonas* was found to be the dominant AOB and *Nitrospira* was the dominant NOB. The viable AOBs present in the biofilm at high loading appear to have faster kinetics as compared to the viable AOBs present at conventional loading. Moreover, the

results suggest that clogging events reduce the effective surface area of the carriers but it does not appear to inhibit the cellular activity of the AOBs present in the biofilm. Finally, the study showed similar cellular activity rates of the AOB population irrespective of carrier type at both high and conventional loading conditions. Therefore, the research suggests that reactor performance cannot be predicted solely by the biofilm thickness, the biofilm mass per reactor, the bacterial percent abundance of ammonia oxidizing bacteria and the percentage of viable cells; instead post carbon removal MBBR ammonia removal kinetics is related to the viable AOB cell coverage of the carriers, which was calculated by normalizing the surface area removal rate by the biofilm thickness, the bacterial percent abundance of ammonia oxidizing bacteria and the percentage of viable cells.

2.7. Acknowledgements

The authors are grateful for the financial support from the Natural Science and Engineering Research Council of Canada. The authors thank Edith Laflamme of Veolia Water Technologies Canada for her technical support.

Chapter 3: Nitrification, biofilm response and microbial abundance shifts of seeded MBBR carriers during start-up of post carbon removal nitrifying MBBR

Bradley Young[a], Robert Delatolla[a*], Turki Abujamel[b,c], Kevin Kennedy[a], Edith Laflamme[d], Alain Stintzi[b]

[a] Department of Civil Engineering, Faculty of Engineering, University of Ottawa, Ottawa, Canada

[b] Ottawa Institute of Systems Biology, Department of Biochemistry, Microbiology and Immunology, Faculty of Medicine, University of Ottawa, Ottawa, Canada

[c] Department of Medical Technology, Faculty of Applied Medical Sciences, King Abdulaziz University, Jeddah, Saudi Arabia

[d] Veolia Water Technologies Canada. Montreal, Quebec, Canada

3.1. Statement of manuscript status and author contributions

The manuscript "Nitrification, biofilm response and microbial abundance shifts of seeded MBBR carriers during start-up of post carbon removal nitrifying MBBR" has been published in Bioprocess and Biosystems Engineering, DOI 10.1007/s00449-017-1739-5.

Young, B. Conceived and designed the project, operated and maintained the pilot MBBR, performed all lab work and analysis. Young. B. wrote and revised the manuscript.

Delatolla, R. was the primary project supervisor, conceived and designed the project, provided direction and feedback on the experiments. Delatolla, R. wrote and revised the manuscript.

Abujamel, T. assisted in 16S rDNA library construction and bioinformatic analysis. Abujamel, T. wrote and revised the manuscript.

Kennedy, K. was a project supervisor, helped conceive and design the project, provided direction and feedback on the experiments.

Laflamme, E. was an industrial collaborator and project supervisor. Laflamme, E. helped conceive and design the project, provided direction and feedback on the experiments.

Stintzi, A. was a project supervisor, provided direction on 16S rDNA library construction and bioinformatics processing, provided direction and feedback on the results. Stintzi, A. wrote and revised the manuscript.

3.2. Abstract

The high occurrence of ammonia as a deleterious substance in aquatic environments has created a worldwide demand for upgrade technologies capable of ammonia removal from wastewaters. The moving bed biofilm reactor (MBBR), due to its compact and efficient operation, has demonstrated success as a potential upgrade technology for post carbon removal nitrification treatment. Operating the MBBR as a post carbon removal system requires long start-up times in comparison to carbon removal systems due to slow growing autotrophic organisms. This study investigates the use of carriers seeded in a carbon rich treatment system prior to inoculation in a nitrifying MBBR system to promote the rapid development of nitrifying biofilm in an MBBR system. In particular, this work explores the biofilm morphological shift along with shifts in the bacterial communities of pre-seeded carriers during the start-up phase of a pilot scale post carbon removal MBBR system. Results show that nitrification was initiated by the carbon removal carriers after 22 hours of operation in a post carbon removal nitrifying MBBR. The biofilm underwent initial sloughing periods observed with variable pressure scanning electron microscope (VPSEM) imaging and mass of biofilm measurements. High throughput 16S-rDNA sequencing indicates that the sloughing period was a result of heterotrophic organism detachment and the recovery and stabilization period included a growth of *Nitrosomonas* and *Nitrospira* as the dominant ammonia oxidizing bacteria (AOB) and nitrite oxidizing bacteria (NOB) in the biofilm. Peripheral microorganisms such as *Myxococcales*, a rapid EPS producer, appear to have contributed to the recovery and stabilization of the biofilm.

3.3. Introduction

The high occurrence of ammonia as a deleterious substance in the aquatic environment has created a worldwide demand for cost-effective and compact technologies to upgrade current wastewater treatment systems for ammonia removal (Canada Gazette, 2012). The most efficient and conventional approach for ammonia removal is nitrification (Metcalf and Eddy, 2003), which can be performed in a suspended growth or biofilm treatment system. Biofilm processes allow for nitrification with decreased sludge production and have demonstrated an ability to withstand acute toxicity (Flemming and Wingender, 2010; Maas et al., 2008). Specifically, the moving bed biofilm reactor (MBBR) has shown potential as a nitrifying upgrade option at temperate climates and recently at cold climates in the northern United States, Canada and Europe (Delatolla et al., 2012; Di Trapani et al., 2013; Hoang et al., 2014a).

The MBBR process uses carriers, which remain in suspension and are circulated through the entire reactor volume by mixing or aeration. These carriers provide a surface for biofilm attachment and proliferation. One of the challenges with regard to nitrifying MBBR systems is the start-up period and in particular the time required to generate stable nitrifying biofilms. Both groups of bacteria responsible for the process of nitrification, ammonia oxidizing bacteria (AOB) and nitrite oxidizing bacteria (NOB), are autotrophic and are very slow growing with limited abilities to produce extracellular polymeric substance (EPS) (Hibiya et al., 2000; Tsuneda et al., 2001). Practical experiences in the start-up of post carbon removal nitrifying MBBR systems demonstrate start-up times in North America of six to eight weeks.

Efforts have been made to decrease the time period required for permanent attachment of nitrifying biomass and development of nitrifying biofilm. Methods investigated have included cellular entrapment as well as immobilization on surface-modified membranes, both demonstrating varying degrees of success (Hibiya et al., 2000; Sumino et al., 1992; Wijffels et al., 1994). The complicated and time consuming nature of these attachment methods have rendered them impractical for current full-scale applications. Tsuneda et al. (2001) seeded cement ball particles with heterotrophic, high rate EPS producing bacteria to promote nitrifying biomass attachment and nitrifying biofilm development. This study was unfortunately unable to verify the success of the technique.

A recent hybrid technology for secondary treatment is the integrated fixed film activated sludge (IFAS) process which incorporates MBBR carriers in a conventional activated sludge (CAS) aeration tank. MBBR carriers are inserted into the aeration tank of a CAS to create the hybrid suspended and attached growth IFAS treatment system. Municipal, secondary treatment IFAS systems have become increasingly installed in North America and Europe as zero footprint upgrade technologies for CAS. These IFAS systems are typically operated at carbon to nitrogen (C/N) ratios of 4 to 6 (Sriwiriyarat et al., 2008). Under conventional, secondary IFAS treatment conditions that are not specifically designed for nitrification, a heterotrophic biofilm is generated on the added carriers that often include AOB and NOB populations embedded in the biofilm; with the nitrifying populations representing less than 1% relative abundance of the total bacterial population (Kwon et al., 2010). As such, seeded carriers from secondary IFAS treatment systems (the most common application of IFAS in North America and hence the most

readily available source of seeded carriers) may be suitable sources of inoculated carriers to promote the rapid start-up of a post carbon removal nitrifying MBBR system. However, the kinetic benefits of using seeded carbon-removal IFAS carriers to inoculate nitrifying MBBR systems remains unknown and further it is unclear how the biofilm and nitrifying biomass of the IFAS carriers will respond to a sudden shift from an organic carbon rich environment to a post carbon removal, ammonia rich environment.

The overall objective of this study is to investigate post carbon removal nitrification MBBR start-up at the macro, meso and micro-scale using carriers seeded from a secondary, carbon-removal IFAS treatment system. The specific objectives are to determine the start-up time and kinetic efficiency over the start-up period; to quantify the biofilm response as it relates to biofilm thickness, biofilm mass, biofilm density and production of total suspended solids (TSS); to characterize the bacterial communities in the IFAS biofilm and the microbial community shift during the MBBR start-up phase using next generation high-throughput Illumina sequencing.

3.4. Material and methods

3.4.1. Biofilm samples

The carriers used to seed the MBBR system in this study were harvested from a secondary, carbon removal IFAS treatment plant located in Hawkesbury, Ontario, Canada. The carriers harvested from the IFAS system is AnoxKaldnes K5 with a surface area/volume of 800 m^2/m^3. The IFAS system was operated at carbon and nitrogen loads of 3200 $gCOD/m^3 \cdot d$ and 220 $gN/m^3 \cdot d$ respectively. The average influent temperature, soluble chemical oxygen demand (SCOD) and ammonia (NH_4-N/NH_3-N) concentrations were 9.0 ± 0.1°C, 230 ± 2 mg/L and 23.9 ± 0.6 mg/L, respectively. Using conventional

biochemical oxygen demand to SCOD ratio of 0.5 (Metcalf and Eddy, 2003), the biofilm in the IFAS system was acclimatized to a C/N ratio of 4.8. The hydraulic retention time (HRT) of the treatment unit was 2.7 h and the removal efficiencies for SCOD and ammonia were 57% and 27%, respectively. The IFAS system was in operation for over two years; hence, the biofilm on the harvested carriers were considered fully acclimatized to the IFAS system. Upon harvesting of the carriers, the carriers were immediately transported to the MBBR pilot system, located 45 min away in Masson Angers, Quebec, Canada.

3.4.2. MBBR pilot system

The pilot MBBR system consisted of two parallel aerobic MBBR treatment reactors, denoted MBBR1 and MBBR2. The pilot was installed as a means of post carbon removal treatment for ammonia removal at the Masson Angers lagoon treatment facility. The effluent from the lagoon (and hence the influent to the pilot) SCOD and ammonia concentrations were stable at 30 mg/L and 22 mg-N/L, respectively. The temperature, pH and dissolved oxygen (DO) in both reactors were constant at 7.6 ± 0.7°C, 7.0 ± 0.1 and 8.8 ± 0.1 mg/L respectively.

The pilot reactors were operated at low loading rates (LRs) throughout the start-up. MBBR systems are typically loaded at approximately half of the design LR during start-up to promote biofilm development. Operating at half of typical nitrifying design LRs also decreases the shock effect to the seeded carriers, which may promote complete failure of the biofilm matrix (Telgmann et al., 2004). As conventional LRs for post carbon removal nitrifying MBBR systems are approximately 240 to 360 $gN/m^3 \cdot d$, the start-up LRs for the two treatment reactors in this study were set to 144 and 86 $gN/m^3 \cdot d$

with each reactor having an HRT of 5.6 hours (Table S2). The LRs were altered based on carrier volume with MBBR2 having 1.6 times more carriers than MBBR1.

3.4.3. Constituent analysis

Nitrification kinetic rates were measured twice per week in triplicate throughout the experimental period. Ammonia (NH_4/NH_3-N), nitrite (NO_2-N) and nitrate (NO_3-N) concentrations along with TSS and volatile suspended solids (VSS) were measured using standard methods (APHA, 1998). SCOD concentrations were measured using HACH method 8000. Biofilm mass was measured using the protocol adopted from Delatolla et al. (2008).

3.4.4. VPSEM image acquisition and analysis

Variable pressure scanning electron microscope (VPSEM) imaging was used to measure in-situ biofilm thickness. VPSEM imaging does not require sample preparation and hence minimizes sample destruction prior to analysis (Delatolla et al., 2009b). The samples were analyzed a maximum of 4 hours after being harvested and images were acquired at a pressure of 40 Pa using a Vega II-XMU SEM (Tescan USA Inc., Cranberry, PA). Five images of four replicate carriers (20 total images) were analyzed for thickness at ×60 magnification. The images were taken at random locations across the carrier surface. Biofilm thicknesses were quantified using Atlas image processing software (Tescan USA Inc., Cranberry, PA). VPSEM images in supplemental material (Fig. S4).

3.4.5. DNA sequencing analysis

Approximately 25 mg of wet biofilm was abraded from five carriers from each MBBR reactor into a 1.5 mL sterile Eppendorf tube. DNA was extracted from the biofilm

using FastDNA® spin kit (MP Biomedicals, Santa Ana, CA) and the extracted DNA was stored at -80°C until used for sequencing library construction.

Profiling the bacterial community was performed utilizing two-step polymerase chain reaction (PCR) strategy targeting the V6 hyper-variable region of the 16S rDNA gene as described previously (Young et al., 2016a). The first step involved amplification of the V6 region and simultaneously adding 4-6 nucleotides barcodes and the Illumina sequencing adapters at 3' ends of amplicons. At this step, unique combination of forward and reverse barcoded primers was used for each sample. The second PCR step involved adding the Illumina flow cell adapter at the 3' ends of the first step PCR amplicons using PCRFWD1/PCRRVS1 primers pair. Template DNA and PCR component concentrations and amplification conditions for the first and second PCR were done as described elsewhere (Young et al., 2016a). Following the second PCR amplification, amplicons were inspected on 2% agarose gel and purified with a Montage PCR96 cleanup kit (EMD Milipore, Billerica, MA). The purified amplicons were quantified using Quant-iT™ dsDNA HS Assay Kit (Life Technologies, Burlington, Canada) according to instructions, and equimolar amount of DNA amplicons from each sample were pooled together. The pooled sample was subjected to deep sequencing on a Illumina Hiseq2500 platform at The Center for Applied Genomics (TCAG, Toronto, Canada), which generates paired-end reads of 2x100 bases in length for downstream analysis.

The entire sequence analysis was disseminated using Bio Linux operating platform run on Dell Precision T7610 workstation. The 2x100 base paired-end reads were assembled using the Fast Length Adjustment of SHort reads (FLASH) software (Magoč and Salzberg, 2011) then quality filtered using the fastq_quality_filter command from the

Fastx toolkit with a minimum quality score of 20 over 90% of the sequences. Reads that passed the quality filter were demultiplexed and barcodes trimmed using Novobarcode (Goecks et al., 2010). The Quantitative Insights Into Microbial Ecology (QIIME) software, version 1.8 (Caporaso et al., 2010), was used to compute operational taxonomical unit (OTU) clustering with closed reference strategy at 97% sequence similarity. QIIME aligned the OTUs against the Greengenes database 13.8 utilizing UCLUST algorithm. Singleton OTUs were removed and the OTU table was normalized by dividing the biofilm mass in each sample group. The normalized OTU table was used to calculate the relative abundance of the bacterial taxa present in the biofilm and compute alpha and beta diversity. The differences in bacterial relative abundance were identified using Linear Discriminate Analysis (LDA) using Galaxy software (Blankenberg et al., 2010; Giardine et al., 2005; Goecks et al., 2010). Finally, fold changes were calculated by dividing the relative abundance of the significant taxa in the MBBR at day 28 by their corresponding relative abundance in the IFAS.

3.4.6. Statistical analysis

Statistical significance for the constituent and biofilm thickness data was tested using the t-test with p-values less than 0.05 considered significant. Statistical significance for the microbial community shifts were tested using a Kruskal-Wallis (KW) sum-ranked test followed by Dunn's post-hoc and linear discriminant analysis (LDA) (Segata et al., 2011). Bacterial taxa with LDA log-score of 2 and higher were selected. Correlation between ammonia concentration and AOB relative abundance was conducted by calculating Spearman’s rank correlation coefficient (R) for each time point. Lastly, the trend in increasing AOB relative abundance was calculated with a linear regression curve.

3.5. Results and discussion

3.5.1. Ammonia removal kinetics

Following the harvesting of carriers from the carbon removal IFAS system with limited nitrification, the carriers were placed into the pilot post carbon removal nitrifying MBBR reactors, MBBR1 and MBBR2. After 22 h of operation in the pilot-scale post carbon removal MBBR system, ammonia removal rates of 105.6 and 72.0 $gN/m^3 \cdot d$ were achieved for MBBR1 and MBBR2, respectively, which corresponds to ammonia removal efficiencies of 73.3% and 83.7% (Fig. S5). The removal rate (RR) values of the MBBR reactors increased by an average value of 1.4 $gN/m^3 \cdot d$ per day until the 21st day of operation. Between the 18th and 21st day of operation, based on mass transfer limitations using diffusivity constants of 0.578 cm^2/d and 0.569 cm^2/d for DO and ammonia respectively (WEF, 2010), the system transitioned from DO mass transfer limited to ammonia mass transfer limited. During the eight days of ammonia mass transfer limited condition the average increases in RR of MBBR1 and MBBR2 were negligible where both reactors were at steady state and achieved removal efficiencies of 96% or greater (with effluent ammonia concentrations less than 1.0 mg-N/L in both reactors).

Ammonia, nitrite and nitrate were measured throughout the experimental phase to confirm nitrogen mass balances in both reactors (Fig. S6). The maximum mass balance discrepancy between the influent and effluent nitrogen concentrations observed during the study was 15% (with less oxidized nitrogen being measured). An average mass balance error of 8.2 ± 6.6% was calculated over the experimental phase (Fig S6). Hence, the results demonstrate that nitrogen mass balances are relatively stable during start-up, acclimatization periods of operation in MBBR systems when seeded with carbon-removal

IFAS carriers. As the operation of the post carbon removal MBBR reactors proceeded, the influent nitrogen was observed to be consistently higher than the oxidized nitrogen. The loss of nitrogen observed in this study is believed to be attributed to bacterial synthesis of nitrogen and laboratory error.

3.5.2. Solids and biofilm mass, thickness

Throughout the entire study the influent TSS concentration entering the pilot system remained stable at an average value of 7.3 ± 1.4 mg/L. Elevated effluent TSS values in both reactors were observed after the first 22 hours of operation, which is indicative of an early sloughing event from the harvested carriers (Fig. 3.1). After 22 hours of operation the TSS concentrations were 227.0 ± 27.3 mg/L and 164 ± 31.7 mg/L for MBBR1 and MBBR2, respectively. MBBR1 maintained a stable elevated TSS concentration of 32.7 ± 6.9 mg/L after the 22 hour sloughing event until the 16^{th} day of operation. On the 16^{th} day of operation a second major sloughing event was recorded with a spike in TSS concentration to 85.3 ± 10.0 mg/L. Following the second sloughing event (day 16) the TSS concentration of MBBR1 became increasingly stable with an average of 16.8 ± 4.2 mg/L.

The effluent TSS concentrations of MBBR2 demonstrated more fluctuations in concentration than MBBR1 with three distinct sloughing events during the first 16 d of operation. The first observed sloughing event occurred after 22 h of operation (TSS of 164 ± 31.7 mg/L), the second sloughing event occurred on the 7^{th} day of operation with a spike in TSS concentration to 204.7 ± 64.7 mg/L. The third sloughing event occurred on the 16^{th} day of operation with a TSS concentration of 122.0 ± 40.7 mg/L. Following the

third sloughing event (day 16) the TSS concentration of MBBR2 decreased daily to a final average of 21.0 ± 13.1 mg/L.

The additional sloughing event observed in MBBR2 as compared to MBBR1 along with the overall higher TSS concentrations in MBBR2 resulted in the average TSS concentration to be 1.6 times greater in MBBR2 as compared to MBBR1. The average TSS concentration for the 28 day start-up period was 51.0 mg/L for MBBR1 and 81.7 mg/L for MBBR2. This increase in produced effluent TSS by the sloughing of the seeded carriers that was observed in MBBR2 as compared to MBBR1 was expected due to the fact that the total mass of biofilm initially added into MBBR2 was 1.6 times higher than MBBR1. In particular, 1.6 times more carriers and hence more biofilm mass was added to MBBR2 than MBBR1 during the carrier filling process, which is precisely the average increase in effluent TSS values between the two reactors. It should be reiterated that once the biofilm and biomass became acclimatized in both reactors, the stabilized measured effluent TSS concentrations of both reactors were very similar with no statistical difference between the measured concentrations (p=0.47).

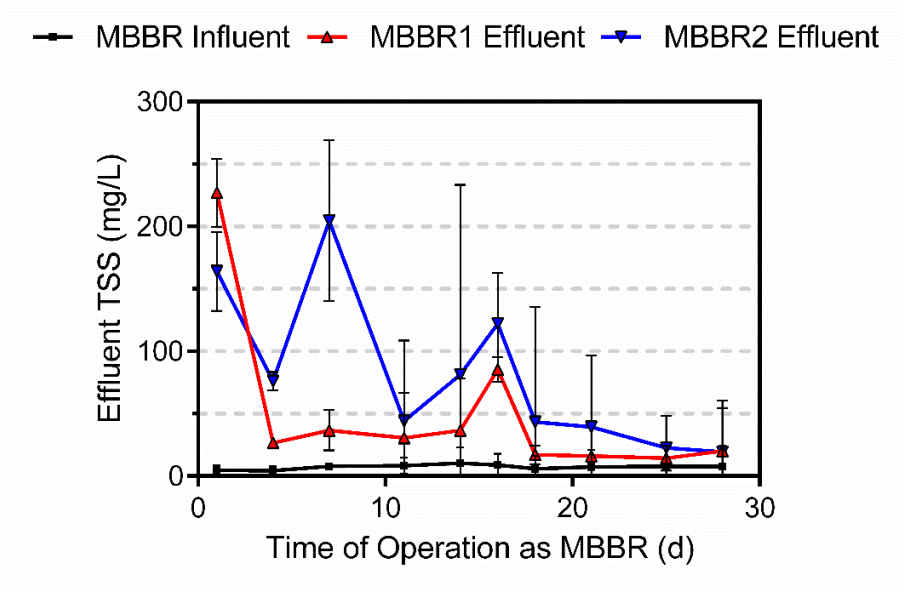

Figure 3.1 Effluent TSS concentrations and standard deviation (n=3) indicating biofilm sloughing events and stabilization of the attached biofilm

The biofilms transition throughout the start-up period with respect to thickness, mass and density was characterized for both MBBR reactors (Fig. 3.2). The biofilm thickness and mass measurements showed similar trends to the effluent TSS measurements for both reactors. In particular, MBBR1 and MBBR2 both showed decreases in biofilm thickness and mass during the first 19 d of operation while the biofilm was sloughing off the carriers and acclimatizing to post carbon removal treatment conditions. The dry density of biofilm in both reactors decreased during the first 12 d of operation; which was characterized by large sloughing events and a strong increase in ammonia removal efficiency. Although the dry density decreased during the initial start-up period, the dry density of the biofilms in both reactors remained within the range of densities expected for wastewater biofilms (30 to 60 kg/m^3) (Laspidou and Rittmann, 2004). The biofilm density of both reactors, following 12 d of operation, then showed a significant increase at 19 days of operation which corresponds to the period of stable effluent TSS

concentrations, stable ammonia removal rates and the transition from a DO mass transfer limited biofilm to an ammonia mass transfer limited biofilm. Further, the dry density of the biofilm in both reactors, after 19 days of operation, returned to similar densities measured for the IFAS harvested carriers.

Both reactors showed a regrowth of the biofilm after 19 days of operation. The measured biofilm characteristics along with the effluent TSS measurements of this study indicate that the kinetics and the biofilm both stabilized after a period of approximately 19 days of operation. As such, the use of carriers from a carbon removal IFAS system to seed a post carbon removal MBBR treatment system with low carbon concentrations and high ammonia concentration did not exhibit failure due to severe shock effects on the biofilm and the system demonstrated a short acclimatization period.

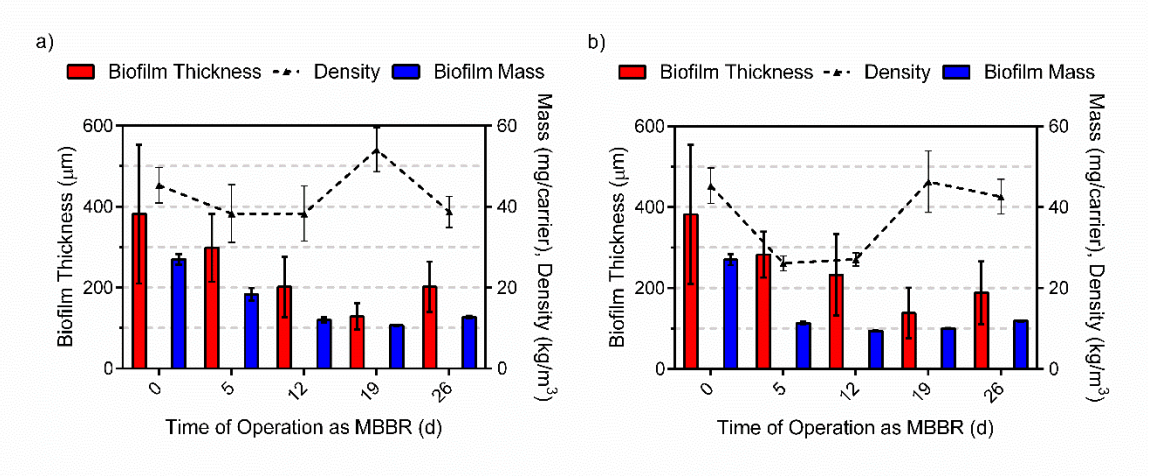

Figure 3.2 Biofilm sloughing and stabilization with standard deviation (biofilm thickness n=20, biofilm mass n=5), a) MBBR1 and b) MBBR2

3.5.3. Bacterial community shift

High-throughput Illumina sequencing generated a total of 29,752,892 sequences with an average of 367,320 ± 209,130 high quality reads per sample. Normalizing the high

quality reads to biofilm mass yielded an average of 30,100 ± 21,320 high quality reads per sample per milligram of biofilm. Using the normalized reads, the Chao1 alpha diversity was not statistically significant between the IFAS biofilm (day 0) and each day operated as a post carbon removal MBBR system (Fig. S7). This indicates that the IFAS (day 0) and MBBR share the same richness.

Principal coordinate analysis (PCoA) was performed based on the unweighted UniFrac distances from the biofilm microbiota at each time point (Fig. 3.3). Clustering occurred on the first two coordinate axes, PC1 and PC2, which account for 19.6% and 12.1% of the total variation respectively. In addition, an analysis of similarity (ANOSIM) of each time period was applied where R=1 indicating maximum dissimilarity. ANOSIM of the entire sample group showed the biofilm microbes clustered based on the time of operation as a post carbon removal MBBR (R=0.43, p=0.001). Concomitantly, comparing the IFAS biofilm (time 0) to the 28 d operation as a post carbon removal MBBR shows maximum dissimilarity (R=1, p=0.001) confirming the biofilm underwent a transition in the microbial structure with respect to time of operation as a post carbon removal MBBR. The taxonomical shift at the phylum level and most abundant genus is presented in Fig. 3.4 and supplemental Table S3.

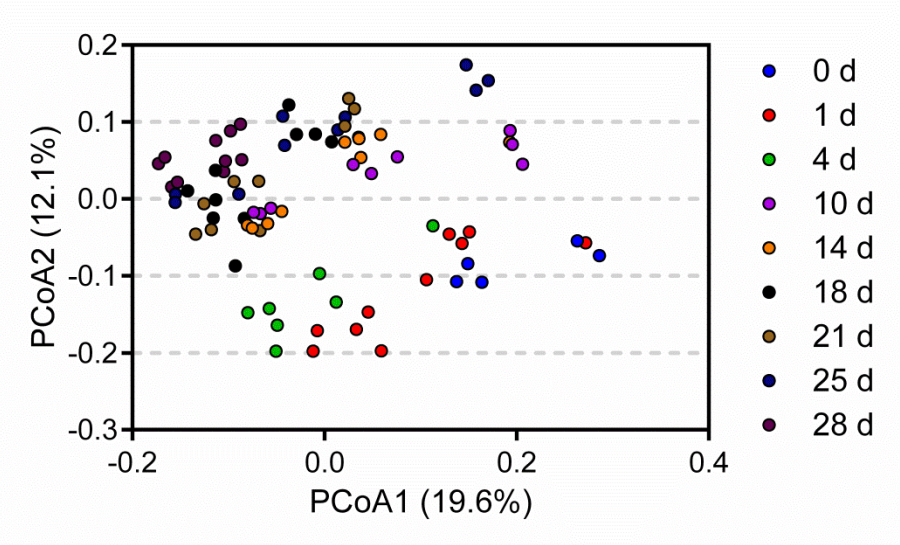

Figure 3.3 Beta diversity presented by 2D principle coordinate analysis (PCoA) plot of unweighted UniFrac distances revealed microbial diversity with respect to the time of operation as a post carbon removal MBBR

3.5.4. Biofilm taxonomy

The IFAS biofilm was analyzed for microbial populations following harvesting from the IFAS full-scale treatment facility. The microbial community in the IFAS biofilm consisted of 36 phyla with 8 phyla representing 1% relative abundance or greater (Fig. 3.4). The most prominent phylum in the sampled IFAS biofilm was *Proteobacteria* with 50.1 ± 23.2% relative abundance. Within the *Proteobacteria* phylum, there were 366 unique genera detected; with *Novosphingobium* (4.9 ± 2.7%), *Zoogloea* (4.5 ± 3.4%), *Thiomonas* (3.9 ± 2.9%) and *Dechloromonas* (1.9 ± 1.4%) being recorded as the most abundant. These bacteria are heterotrophic organisms that are often associated with aromatic compound degradation (Bryan et al., 2009; Dugan et al., 2006; Kertesz and Kawaski, 2010). The second most abundant phylum in the sampled IFAS biofilm was *Bacteroidetes* with 38.9 ± 19.2% relative abundance. Within the *Bacteroidetes* phylum, there were 83 unique genera detected with *Flavobacterium* (7.5 ± 3.5%) and *Fluviicola*

(2.2 ± 1.1%) as the most abundant genera. These genera of bacteria are also heterotrophic and are often observed in symbiotic roles with *Proteobacteria* and decompose high-molecular-mass organic matter (Cottrell and Kirchman, 2000). The AOB population of the IFAS biofilm represented 2.0 ± 1.5% of the total identified bacterial cells embedded in the biofilm. The dominant genus of the AOB group was *Nitrosomonas* with *Nitrosoccocus, Nitrosospira, and Nitrosovibrio* also being detected at small percent abundances. NOBs were also detected in the IFAS biofilm. Their relative abundance was less than $7x10^{-3}$%. The only genus detected in the NOB group was *Nitrospira*.

During operation of the MBBR pilot plant, the post carbon removal MBBR biofilm samples were analyzed for microbial populations twice per week (9 total samples) during the 28 day start-up period. Throughout the entire start-up period, the same 36 phyla observed in the IFAS biofilm were detected in the MBBR biofilm. Along with the same observed phyla, the same 8 phyla that demonstrated a relative abundance of at least 1% in the IFAS biofilm were again observed at relative abundances equal to or greater than 1% in the MBBR biofilm (Fig. 3.4). After operating for 4 days in the post carbon removal MBBR system, the bacterial community increased its average relative abundance of the *Proteobacteria* phylum (containing AOBs) from 50.1 ± 23.2% to 65.3 ± 2.2% (p=0.50). The increase in *Proteobacteria* corresponded with a decrease in *Bacteroidetes*. The *Bacteriodete* phylum decreased from a relative abundance of 38.9 ± 19.2% to a relative abundance of 26.9 ± 1.2% (p=0.98) (Fig. 3.4). In the last seven days of post carbon removal MBBR operation culminating with day 28, the microbial community did not significantly change with respect to the percent abundance of the *Proteobacteria* (p=0.51) or *Bacteroidete* (p=0.80) phyla; however, there was a significant increase in

Acidobacteria. The *Acidobacteria* phylum represented 0.8 ± 0.2% relative abundance for each sampling period during the first 21 days of post carbon removal MBBR operation, which increased to 1.4 ± 0.2% (p=0.02) relative abundance after 28 days of post carbon removal MBBR operation (Fig. 3.4). *Acidobacteria* is a relatively newly classified phylum that shares similar genetic composition to *Proteobacteria*. The organisms of this phylum has proven difficult to culture and as such their overall function and specifically their function in wastewater biofilms is currently not well understood (Lee et al., 2008). Species in the *Acidobacteria* phylum that have been cultured have been shown to be important to the biogeochemical cycle through their use of decomposing organic matter as a substrate (Kulichevskaya et al., 2010; Lee et al., 2008).

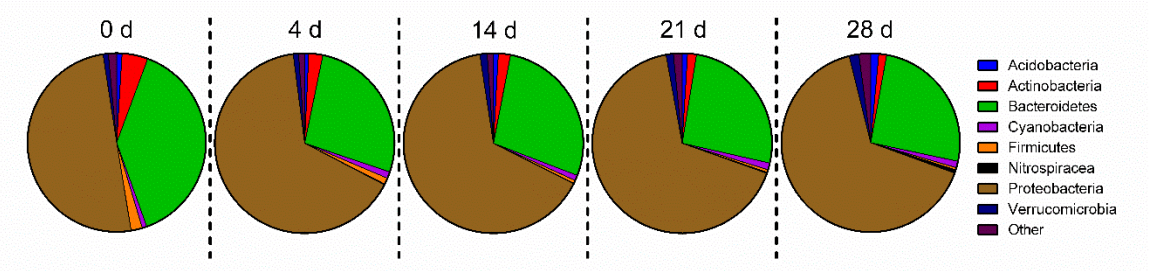

Figure 3.4 Relative abundance at the phylum level in the IFAS (day 0) and MBBR biofilm after 4, 14, 21 and 28 days of operation

The most abundant heterotrophic genera observed in the IFAS biofilm decreased significantly after 21 days of post carbon removal MBBR operation (Table S3). The dominant heterotrophic genera observed in the IFAS biofilm samples, *Novosphingobium, Zoogloea, Thiomonas* and *Dechloromonas, Flavobacterium* and *Fluviicola,* were still among the most prevalent genera in the post carbon removal MBBR biofilm after 4 days of operation (Table S3). Conversely the prominent heterotrophic organisms present in the

IFAS system, were depleted after the 28 day period. A sustained lack of carbon in the influent likely stressed the heterotrophic organisms to detach or lyse and be decomposed.

Differentially abundant taxa comparing the IFAS (day 0) biofilm and day 28 of post carbon removal MBBR operation identified *Nitrosomonas, Myxococcales, Bryobacter* and *Nitrospira* among the enriched bacteria in the MBBR system (Fig. 3.5). *Nitrospira,* a prominent NOB in wastewater and the dominant NOB in the biofilm of this study exhibited the highest enrichment with a fold change of 79.3. This large fold change is due to the near 0 relative abundance for the IFAS biofilm (day 0) and growth of *Nitrospira* in the MBBR biofilm. The post carbon removal nitrifying MBBR biofilm was shown to become enriched with *Nitrospira* without nitrite accumulation (Figs. 3.5 and S6). This lack of nitrite accumulation demonstrates the adaptability and robustness of biofilm subjected to rapid change.

Nitrosomonas, a prominent AOB in wastewater and the dominant AOB in the biofilm of this study, demonstrated an enrichment with a fold change of 2.46. *Myxococcales* demonstrated the second highest enrichment with a fold change of 2.95. *Myxococcales* is a rapid EPS forming bacteria which might have aided in stabilizing the nitrifying biofilm. Wastewater AOBs and particularly *Nitrosomonas* are poor EPS producing organisms. It is likely that this rapid EPS forming bacteria are partly responsible for the stabilization of the biofilm thickness and mass observed after the 19th day of operation (Fig. 3.2). Lastly, *Bryobacter,* a decomposing *Acidobacteria* represented significant enrichment with a fold change of 2.86. As previously mentioned, after 28 days of post carbon removal MBBR operation, the biofilm had a significant increase in *Acidobacteria* (Fig. 3.4). *Bryobacter*, a decomposing organism was the prominent genus in the *Acidobacteria* phylum.

Bryobacter has been demonstrated to use polysaccharides, galacturonic and glucuronic acids as substrates that are formed during decomposition of organic matter (Kulichevskaya et al., 2010). It is possible that the *Bryobacter* consumed the lysed heterotrophic bacteria that remained in the biofilm after MBBR start-up. The natural propagation of such organisms has been proposed to aid in preventing a failure of the biofilm matrix under acclimatized conditions (Telgmann et al., 2004).

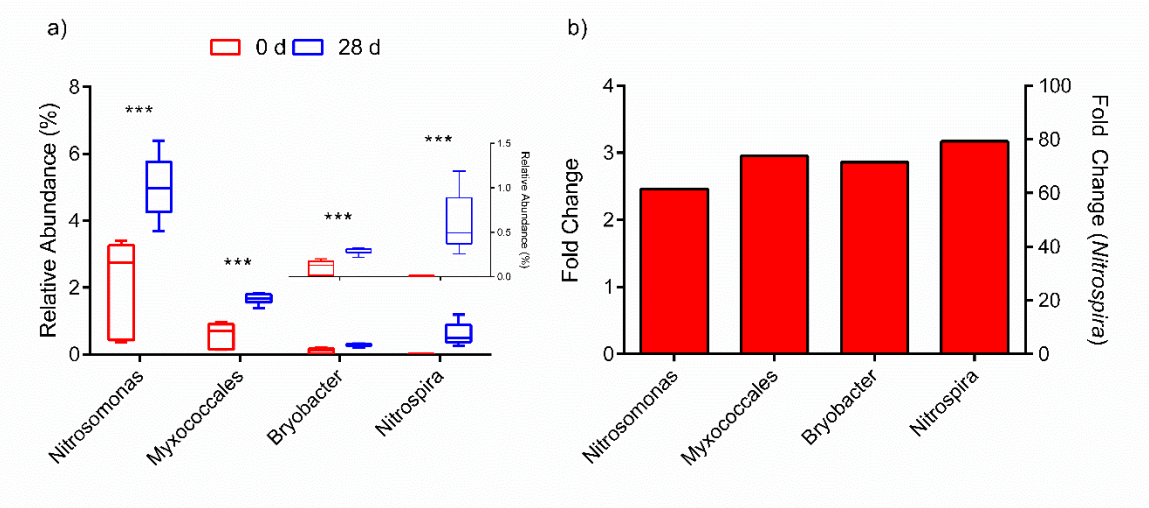

Figure 3.5 Bacterial genera, a) statistically differential abundance from day 0 to day 28 of post carbon removal MBBR operation (***p<0.001) with embedded graphic showing smaller scale for *Bryobacter* and *Nitrospira* genera and b) fold changes relative to the IFAS system with right-hand y-axis showing fold change for *Nitrospira* genera

The AOB and NOB population percent abundances during the start-up of the MBBR pilot were compared to the kinetics of nitrification throughout the start-up phase of the system in this research (Fig. 3.6). The IFAS system was operating at a C:N ratio of 3:1. Ideal conditions for autotrophic growth range from C:N ratios of 0.5:1 to 1:1 (WEF, 2010), and as such the IFAS system demonstrated an oxidation of 27 ± 7% of the influent ammonia to nitrate. At the time of harvesting, the SRT of the suspended cells of the IFAS facility ranged between 4 to 6 days and temperature was 9.0 ± 0.1°C. Hence,

the moderate ammonia conversion rate observed at the facility was expected. It is most probable that the AOB and NOB populations of the biofilm, although low in percent abundances, were responsible for the limited nitrification and served as inoculum for the post carbon removal MBBR start-up.

The AOB population showed a linear increase (R^2=0.97) in relative abundance up to 8.1 ± 1.0% during the first 19 days of post carbon removal MBBR operation until the biofilm transitioned from DO or kinetic rate limited to ammonia mass transfer rate limited. In the DO or kinetic rate limited time period the decrease in ammonia concentration is correlated to the increasing AOB relative abundance (Spearman R=-0.90, *p*=0.04). At this transitory point from a DO to an ammonia rate limited biofilm, the AOBs reached their final measured relative abundance at a percent abundance of 5.8 ± 0.7% of the total organisms. *Nitrosomonas* represented the majority of the AOB population with *Nitrosoccocus, Nitrosospira, and Nitrosovibrio* being detected at percent abundances less than 0.2%. The percent abundance of the NOB population was significantly lower than the AOB population, with an average relative abundance of 0.1 ± 0.1% after 19 days of operation. The relative abundance of the NOB population increased to 0.6 ± 0.3% after the full 28 day start-up period. There wasn't an observable correlation between ammonia concentration and NOB relative abundance (Spearman R=-0.62, *p*=0.12). *Nitrospira* was the dominant NOB with *Nitrobacter* representing less than $1x10^{-4}$% of the microbial community.

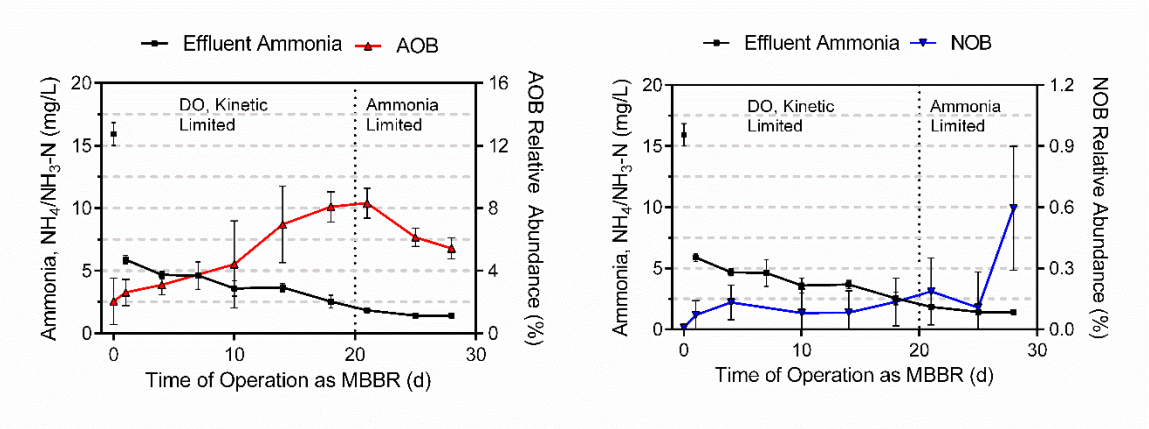

Figure 3.6 Relative abundance and standard deviation (n=5) of AOB and NOBs using 16S rRNA gene amplicon reads with respect to ammonia effluent

The increase in AOB and NOB relative abundance through the 21 day acclimatization period was likely affected by the detachment of the biofilm during the acclimatization to high ammonia, low carbon conditions. In particular, the initial increase in relative abundance of AOBs and NOBs in the post carbon removal MBBR biofilms was likely due to the preferential detachment of heterotrophic organisms that dominated the outer layers of the IFAS biofilm (0 d). Based on previous studies, the heterotrophic communities are most prevalent in the outer layers of wastewater biofilm as they out-compete the slower growing autotrophic, nitrifying, organisms (Lee et al., 2004). The detachment observed by elevated effluent TSS concentrations (Fig. 3.1) and a reduction in biofilm thickness and mass (Fig. 3.2) did not appear to destabilize the underlying nitrifying biomass as is evident by the maintained ammonia removal kinetics (Fig. S5). After 19 days of operation, the biofilm successfully stabilized with respect to kinetic rates, biofilm morphology (thickness, mass, density) and the AOB relative abundance within the biofilm. The NOB relative abundance increased after the 19 days of operation

and may have continued to increase in the biofilm due to their slow growth as compared with AOBs.

3.6. Conclusion

This study effectively demonstrates seeded carriers from a carbon removal IFAS system, which exhibited limited nitrification, rapidly acclimatized to MBBR post carbon removal nitrifying treatment. After 22 hours of operation, the post carbon removal nitrifying MBBR removed 73.3% and 83.7% of the influent ammonia and reached steady state after 18 days of operation. This steady state operation corresponded to 96% of the influent ammonia (effluent concentrations less than 1 mg-N/L). The 18^{th} day of operation also corresponded to stabilization of the biofilm and microbial community. It was observed the biofilm undergoes an initial sloughing period with rapid EPS producing bacteria, such as *Myxococcales*, stabilizing the biofilm matrix. The stabilized biofilm reached equilibrium relative abundance of AOBs and NOBs indicating the post carbon removal nitrifying MBBR has adapted to a true nitrifying system. As secondary IFAS treatment systems are the most common application of the IFAS technology, carriers from these systems may be more readily available for harvesting to seed MBBR nitrifying systems. Although seeding a full scale MBBR plant would present challenges with respect to the harvesting of a substantial volume of carriers, this study indicates the potential of using seeded carriers from an IFAS system to partially seed a new MBBR plant.

3.7. Acknowledgements

The authors are grateful for the financial support from the Natural Science and Engineering Research Council of Canada and Veolia Water Technologies. The authors thank Daina Forrest, Walid Mottawea and James Butcher of the University of Ottawa for their technical support. The authors acknowledge the Saudi Arabian Cultural Bureau in Canada for scholarship contribution from King Abdulaziz University.

Chapter 4: Pilot-scale tertiary MBBR nitrification at 1°C: characterization of ammonia removal rate, solids settleability and biofilm characteristics

Bradley Young[a], Robert Delatolla[a*], Baisha Ren[a], Kevin Kennedy[a], Edith Laflamme[b], Alain Stintzi[c]

[a] Department of Civil Engineering, Faculty of Engineering, University of Ottawa, Ottawa, Canada

[b] Veolia Water Technologies Canada. Montreal, Quebec, Canada

[c] Ottawa Institute of Systems Biology, Department of Biochemistry, Microbiology and Immunology, Faculty of Medicine, University of Ottawa, Ottawa, Canada

4.1. Statement of manuscript status and author contributions

The manuscript "Pilot-scale tertiary MBBR nitrification at 1°C: characterization of ammonia removal rate, solids settleability and biofilm characteristics" has been published in Environmental Technology, 2016, 37(16), 2124-2132.

Young, B. Conceived and designed the project, operated and maintained the pilot MBBR, performed constituent analysis, VPSEM and digital particle analysis. Young, B. wrote and revised the manuscript.

Delatolla, R. was the primary project supervisor, conceived and designed the project, provided direction and feedback on the experiments. Delatolla, R. wrote and revised the manuscript.

Ren, B. performed biofilm EPS extraction and analysis.

Kennedy, K. was a project supervisor, helped conceive and design the project, provided direction and feedback on the experiments.

Laflamme, E. was an industrial collaborator and project supervisor. Laflamme, E. helped conceive and design the project, provided direction and feedback on the experiments.

Stintzi, A. was a project supervisor, provided feedback on the experiments.

4.2. Abstract

Pilot scale moving bed biofilm reactor (MBBR) is used to investigate the kinetics and biofilm response of municipal, tertiary nitrification at 1°C. The research demonstrates that significant rates of tertiary MBBR nitrification are attainable and stable for extended periods of operation at 1°C, with a maximum removal rate of 230 $gN/m^3 \cdot d$ at 1°C. At conventional nitrogen loading rates, low ammonia effluent concentrations below 5 mg-N/L were achieved at 1°C. The biofilm thickness and dry weight mass ($mass_{dw}$) were shown to be stable; with thickness values showing a correlation to the protein/polysaccharide ratio of the biofilm extracellular polymeric substances (EPS). Lastly, tertiary MBBR nitrification is shown to increase the effluent suspended solids concentrations by approximately 3 mg TSS/L, with 19 to 60% of effluent solids being removed after 30 minutes of settling. The settleability of the effluent solids was shown to be correlated to the nitrogen loading of the MBBR system.

4.3. Introduction

Point source polluters, such as wastewater treatment plants, are adding large quantities of nutrients to surface waters (Murdoch et al., 2000). Increasing the nutrient concentrations in surface waters can cause eutrophication and various other undesirable ecological impacts. Specifically, unionized ammonia is toxic to fish and other aquatic organisms. In an attempt to mitigate pollution from wastewaters, various countries are developing more stringent wastewater effluent regulations (Canada Gazette, 2012; EEC, 1991; USEPA, 2014). Current treatment technologies have shown to be effective in removing carbonaceous biochemical oxygen demand (CBOD) and total suspended solids (TSS), however, these technologies are often limited with respect to nitrification once

temperatures decrease below 10°C (Hurse and Connor, 1999; Randall and Buth, 1984; Shammas, 1986).

Passive treatment systems, such as multi-pond lagoons, are common in northern climates where land is readily available. These systems are able to nitrify in the summer months due to their long solids retention time (SRT). In the winter months wastewater temperatures can reach as low as 1°C for extended periods of operation (Canada Gazette, 2012). At this temperature passive treatment systems are incapable of nitrification and as such there has been an increased interest in add-on nitrifying biofilm technologies. Biofilms have shown the potential to decrease the temperature sensitivity of the embedded nitrifiers (Wijffels et al., 1994).

Recently, the moving bed biofilm reactor (MBBR) has demonstrated the potential for cold temperature nitrification (Almomani et al., 2014; Delatolla et al., 2010; Hoang et al., 2014a; Hoang et al., 2014b; Houweling et al., 2007; Ødegaard, 2006). The MBBR system houses bio-carriers, which remain in constant movement in the MBBR reactor during operation. The movement of the carrier eliminates the need for backwashing of the system. The combined efficiency and simple operation of the MBBR makes it ideal as a potential upgrade technology for passive treatment systems (Oleszkiewicz and Barnard, 2006).

The first studies with respect to MBBR nitrification in cold wastewaters were performed on MBBR upgrade systems installed at multi-pond lagoon treatment facilities. These studies investigated upgrade MBBR nitrification systems installed after the first or middle pond of a multi-lagoon treatment system to minimize the temperature decrease of the wastewater through the treatment process prior to entering the nitrifying MBBR

system (Delatolla et al., 2010; Houweling et al., 2007; Ødegaard, 2006). The wastewater temperatures after the first or middle pond of multi-lagoon facilities in northern climates were observed to reach temperatures as low as 4°C as opposed to 1°C; hence providing higher minimum temperatures to achieve nitrification in the MBBR systems. Although the minimum temperature of wastewater from the first or middle ponds of passive treatment facilities are higher, the five day carbonaceous biochemical oxygen demand ($CBOD_5$) to total Kjeldahl nitrogen (TKN) ratio, which effects the competition between faster growing heterotrophic and slower growing nitrifiers, is also higher at the first and middle lagoons. The optimal conditions for MBBR nitrification requires a soluble biochemical oxygen demand ($sBOD_5$) less than 12 mg/L and $CBOD_5$/TKN ratio less than 1 (Figueroa and Silverstein, 1992; Lee et al., 2004; WEF, 2010). The effluent exiting from the first or middle lagoon often has a $CBOD_5$/TKN greater than 1. Hence, the preferred location for a nitrifying MBBR upgrade system from a $CBOD_5$/TKN perspective is after the last lagoon in the system. More recent studies (Almomani et al., 2014; Hoang et al., 2014a; Hoang et al., 2014b) investigated the feasibility of tertiary MBBR nitrification after the last lagoon in the treatment system where the temperature decreases to as low as 1°C. These studies established that tertiary MBBR nitrification is feasible at 1°C; however, there currently remains a gap in knowledge with respect to maximum kinetic rates, optimal loading and the biofilm and effluent solids response during long exposure to 1°C.

The overall objective of this study was to investigate the maximum kinetics along with the biofilm and effluent solids response of tertiary MBBR nitrification systems operating at 1°C at the pilot scale. The specific objectives were to investigate loading rate

effects on tertiary MBBR nitrification at 1°C; to investigate the biofilm morphology and protein/polysaccharide ratio at various loading rates at 1°C; and to investigate the effluent solids concentration, particle size distribution and settleability at various loading rates at 1°C.

4.4. Material and methods

4.4.1. MBBR pilot plant

A tertiary nitrifying pilot plant consisting of four 223 L MBBR reactors was installed at the Masson Angers, Quebec, Canada lagoon municipal wastewater treatment facility. The MBBR pilot plant housed two parallel treatment trains, each treatment train consisting of two MBBR reactors operated in series. The MBBR pilot plant was installed as a tertiary nitrifying system, and as such the final effluent from the lagoon treatment facility was fed to the pilot. The lagoon effluent offers the lowest $CBOD_5$/TKN ratio (advantageous to nitrification kinetics) in the treatment process; however, the lagoon effluent also has the lowest temperature during winter conditions (disadvantageous to nitrification kinetics). Table 4.1 shows the lagoon effluent characteristics, and hence the characteristics of the influent wastewater entering the MBBR pilot during the winter months of operation that pertains to this study. The influent wastewater had a $CBOD_5$/TKN ratio of 0.8, which is in the optimal range of 0 to 1 for nitrification (Figueroa and Silverstein, 1992; Lee et al., 2004; WEF, 2010). Similarly, the influent wastewater's alkalinity, pH and total phosphorus (TP) were all within the suitable range for nitrification (Metcalf and Eddy, 2003).

Table 4.1 Influent wastewater characteristics of MBBR pilot at 1°C operation

Constituent	Value
Temperature	1.0 ± 0.2°C
Ammonia (NH_4^+/NH_3-N)	22.7 ± 0.4 mg/L
Nitrite (NO_2^--N)	0.1 ± 0.0 mg/L
Nitrate (NO_3^--N)	0.8 ± 0.3 mg/L
TKN	22.3 ± 1.4 mg/L
TSS	11.3 ± 1.0 mg/L
$CBOD_5$	17.3 ± 0.9
COD	88.8 ± 19.9 mg/L
SCOD	55.0 ± 3.1 mg/L
Alkalinity ($CaCO_3$)	153 ± 1.9 mg/L
pH	7.2 ± 0.1
TP	1.5 ± 0.1 mg/L

The biofilm carriers housed in the MBBR pilot plant were the AnoxKaldnes K5 carriers (Veolia Water). The K5 carriers are cylindrical with a diameter of 25 mm, height of 4 mm and a surface area to volume ratio of 800 m^2/m^3. Throughout the study, the hydraulic flow was modulated with automated flow valves and the aeration rate was supplied using a regenerative blower (FUJI, USA, NJ) to provide adequate carrier mixing and dissolved oxygen (DO) concentrations in the MBBR reactors. The carriers were seeded using an integrated fixed film activated sludge (IFAS) reactor and were operated as a tertiary nitrifying MBBR for nine months prior to 1°C operation. During the summer months of May to August, the tertiary MBBR remained at a temperature of 20.7 ± 0.5°C.

The biofilm maintained an average thickness and $mass_{dw}$ of 71.6 ± 14.6 μm and 9.2 ± 0.9 mg/carrier, respectively, during the summer operation.

The temperature of the wastewater in the pilot plant decreased from 20.7 ± 0.5°C in the summer months to 1.0 ± 0.2°C during winter operation. In the fall months of September to December, a period of four consecutive months, the temperature decreased from approximately 20°C to 3.2°C. Subsequently, during the first three weeks of January, the wastewater maintained a steady temperature of 2.6 ± 0.5°C. From January 20th to March 27th, a period of two months, the tertiary nitrifying MBBR maintained a steady, temperature of 1.0 ± 0.2°C. It is during this two month operation at 1.0 ± 0.2°C that the data for this study were acquired.

During 1°C operation, the MBBR reactors were operated at a constant HRT of 2.2 h across five normalized loading rates (LRs) of 60, 250, 440, 600 and 690 $gN/m^3 \cdot d$. The loading rates of the MBBR reactors were varied while maintaining constant HRTs by operating the reactors in series and by adjusting the volume of carriers in the MBBR reactors. As mentioned above, the MBBR pilot plant was operated in two parallel treatment trains, each treatment train consisting of two reactors in series. Hence, the effluent ammonia concentration of the first reactors in series was the influent ammonia concentration of the second reactors in series; resulting in the lower loading rates for the second reactors in series. Further the ability to increase/decrease loading rates in MBBR systems through the addition/removal of carriers in a fixed reactor volume was used to adjust the loading rates of the reactors while maintaining the same HRTs. The LRs in this study range from conservative to overloaded loadings relative to a conventional normalized LR of approximately 250 $gN/m^3 \cdot d$ (WEF, 2010). Each LR was maintained in

the respective reactor for a minimum of four weeks at 1°C to validate steady state operation. A minimum of 15 samples were analyzed to quantify kinetic rates at steady state operation. Each reactor maintained a constant average DO of 7.3 ± 0.4 mg/L, pH of 6.99 ± 0.04 and effluent soluble chemical oxygen demand (SCOD) of 34.4 ± 2.7 mg/L.

4.4.2. Wastewater constituents and mass transfer

Ammonia (NH_4^+/NH_3), nitrite (NO_2^-), nitrate (NO_3^-), TKN, TSS, $CBOD_5$, alkalinity and TP were measured using standard methods (APHA, 1998). SCOD concentrations were measured using HACH method 8000. Nitrification rates were normalized to the surface area of the carriers. Equation 1 was used to determine if DO or ammonia concentrations were mass transfer rate limiting in the MBBR reactors; where DO is mass transfer rate limiting if Equation 1 holds true (WEF, 2010).

$$S_{ba} < \frac{D_{wd} \cdot v_a \cdot MW_a}{D_{wa} \cdot v_d \cdot MW_d} \cdot S_{bd} \qquad \text{Equation 4.1}$$

Where, S_{ba} is the bulk liquid concentration of DO, D_{wd} is the diffusivity constant of ammonia in water, v_a is the molar stoichiometric reaction coefficient of oxygen, MW_a is the molecular weight of oxygen, D_{wa} is the diffusivity constant of oxygen in water, v_d is the molar stoichiometric reaction coefficient of ammonia, MW_d is the molecular weight of ammonia and S_{bd} is the bulk liquid concentration of ammonia.

4.4.3. Biofilm thickness and mass$_{dw}$

Variable pressure scanning electron microscope (VPSEM) imaging was used to measure in-situ biofilm thickness. VPSEM imaging does not require sample preparation and hence minimizes sample destruction prior to analysis (Delatolla et al., 2009b). The

samples were analyzed a maximum of 4 hours after being harvested and images were acquired at a pressure of 40 Pa using a Vega II-XMU SEM (Tescan USA Inc., Cranberry, PA). Five images of four replicate carriers (20 total images) were analyzed for thickness at ×60 magnification resulting in 90 thickness measurements per carrier. The images were taken at random locations across the carrier surface to avoid location bias. Biofilm thicknesses were quantified using Atlas image processing software (Tescan USA Inc., Cranberry, PA).

The dry weight biofilm mass ($mass_{dw}$) was measured using the protocol adopted from Delatolla et al. (2008). The biofilm carriers were harvested from the MBBR reactors and dried at 105°C overnight. The dried carriers were allowed to cool in a desiccator for twenty minutes and their weight was recorded (W1). The dried carriers were then thoroughly cleaned with warm water and a stiff bristled brush. The clean carriers were dried at 105°C overnight, allowed to cool in a desiccator for twenty minutes and their weight was recorded (W2). The biofilm $mass_{dw}$ is then the difference between W1 and W2.

4.4.4. Biofilm extracellular polymeric substances (EPS)

EPS was extracted using the cation exchange resin (CER) method (Frolund et al., 1995). Biofilm were physically abraded from the carriers and added to 40 mL of extraction buffer (2mM Na_3PO_4, 4 mM NaH_2PO_4, 9 mM NaCl and 1 mM KCl). CER (Dowex Marathon C, 20-50 nm mesh, sodium form, Fluka91973) was washed in 150 mL of extraction buffer at a pH of 7 for 1 hour and then added to the harvested biofilm at a dose of 75 g/gVS. Following 1 hour of mixing at 4°C, the mixture was allowed to settle with the supernatant being centrifuged at 12,000 x g for 0.5 h at 4°C. The centrifuged

supernatant constitutes the extracted EPS, which was subsequently analyzed for protein and polysaccharide content.

The protein of the the extracted EPS was measured using the Folin-Phenol method adopted from Frølund et al. (1995). 1 mL of EPS solution was harvested separately from 6 random carriers sampled at each LR; with each sample being measured in triplicate. The polysaccharide content of the EPS was quantified using the Dubois et al. (1956) method. 2 mL of EPS solution was harvested from 6 randomly selected carriers at each loading rate; with each sample being analyzed in triplicate.

4.4.5. Digital particle analysis

The wastewater solids distribution was determined using a Brightwell Technologies Dynamic Particle Analyzer (DPA). The DPA was equipped with a BP-4100-FC-400-U (Brightwell Technologies, Canada, ON) low magnification flow cell attached to 0.8 mm ID tubing. Using this set up, the DPA is able to observe and quantify particles in the range of 2.25 to 400 μm in diameter.

The samples were first filtered through a 400 μm mesh to protect the flow cell from clogging. This filtered mass was dried and measured for subsequent analysis. The filtrate was pumped through the flow cell at a rate of 0.35 mL/min. The sample was monitored by an internal camera imaging in a continuous light field within the DPA. The camera images were subjected to an algorithm to quantify a count number, concentration and circularity coefficient of the particles. The particle size distribution of the sample was analyzed within the range of 2.25 to 400 μm. The samples were analyzed after being gently mixed to suspend all particles and subsequently after 30 minutes of settling in an imhoff 1000 mL cone. Particle size distributions were averaged across 6 runs per sample.

4.4.6. Statistical analysis

Statistical analysis for the ammonia removal efficiencies was tested using the t-test with a *p*-value less than 0.05 considered significant. Regression analysis for the removal rates is based on a non-linear second order polynomial. Statistical analysis for the biofilm thickness, $mass_{dw}$ and TSS were tested using a one-way ANOVA with a *p*-value less than 0.05 being considered significant. Correlation analyses used was Spearman's correlation with a *p*-value less than 0.05 indicating significance.

4.5. Results and discussion

4.5.1. Ammonia removal kinetics

The nitrification kinetics of the pilot MBBR operation at 1°C is presented as the removal rate (RR) per m^3 of reactor volume (Fig. 4.1a). The conservative (LR = 60 $gN/m^3 \cdot d$) and conventional (LR = 250 $gN/m^3 \cdot d$) loaded reactors demonstrated high removal efficiencies of 89.5 ± 4.1 and 75.4 ± 7.4%, respectively, and low effluent ammonia concentrations of 2.1± 0.1 and 5.8 ± 1.2 mg-N/L, respectively (Table 4.2). Ammonia concentrations of 12.6 mg-N/L and above have previously shown to demonstrate acute lethality (CCME, 2010), where acute lethality is defined by 50% rainbow trout mortality after 96 hour exposure to 100% wastewater effluent (LC_{50} = 12.6 mg -N/L). Hence, acute lethality testing demonstrated that the effluent wastewater from the nitrifying MBBR pilot operating at 1°C was not toxic at LRs of 60 and 250 $gN/m^3 \cdot d$.

Transitioning from a conventionally loaded operation (LR = 250 $gN/m^3 \cdot d$) to an overloaded operation of LR = 440 $gN/m^3 \cdot d$ at 1°C corresponds to a significant loss in ammonia removal efficiency (Table 4.2) and a plateau of the ammonia removal rate (Fig.

4.1a); indicating that the maximum ammonia removal rate for the tertiary nitrifying MBBR system of this study operating at 1°C is attained. This loss in ammonia removal efficiency expectedly results in an increase in effluent ammonia concentrations (Table 4.2). The effluent ammonia concentrations of the overloaded reactor operating at LR = 440 $gN/m^3 \cdot d$ was shown to be at the ammonia threshold concentration of toxicity (LC_{50} = 12.6 mg -N/L) (CCME, 2010). Similarly, the overloaded reactor operating at LR = 600 $gN/m^3 \cdot d$ shows a loss in ammonia removal efficiency (Table 4.2) and was again operated near the threshold of acute lethality.

The highest loaded reactor of LR = 690 $gN/m^3 \cdot d$ demonstrated a statistically significant decrease in the ammonia removal rate compared to the same system loaded at 440 and 600 $gN/m^3 \cdot d$; which is indicative of potential inhibition to the process of nitrification (Abeling and Seyfried, 1992; Furukawa et al., 2009). As the influent wastewater characteristics shown in Table 4.1 did not vary compared to the lower loading conditions investigated in this study and the background constituent concentrations that were not measured in this study (such as trace metal concentrations) did not likely vary in the wastewater between the different loading conditions, it is likely that kinetic inhibition was caused by free ammonia (FA) concentrations at the highest loading condition. The bulk liquid phase FA and free nitrous acid (FNA) at a pH of 6.99 and temperature of 1°C for the highest loaded reactor of LR = 690 $gN/m^3 \cdot d$ are 0.022 and 1.2×10^{-4} mg-N/L, respectively (Anthonisen et al., 1976). Although these FA and FNA concentrations are below conventional toxicity thresholds for nitrification inhibition, it is important to note that fundamental studies of nitrification inhibition did not include empirical data at 1°C

(Anthonisen et al., 1976). Hence, nitrification inhibition is likely exacerbated at 1°C and hence is observed in this study at a FA concentration of approximately 0.022 mg-N/L.

LRs 60, 250, 440 and 600 $gN/m^3 \cdot d$ along with their respective RRs follow a first order reaction that transitions to a mixed order reaction between LRs of 250 and 440 $gN/m^3 \cdot d$ and a zero order reaction between LRs 440 and 600 $gN/m^3 \cdot d$. The decreased performance of the highest loaded reactor (LR = 690 $gN/m^3 \cdot d$) does not reach the maximum RR, possible due to inhibition, and as such is omitted from the maximum RR analysis. The maximum normalized RR at 1°C is 230 $gN/m^3 \cdot d$; indicated by a horizontal dashed line in Fig 4.1a. The maximum RR of 230 $gN/m^3 \cdot d$ at 1°C is approximately 25% of the maximum RR, 1020 $gN/m^3 \cdot d$, that was measured in the same reactors under similar operating conditions at 20°C during the summer operation.

Operation of the tertiary MBBR reactors at 1°C at all LRs investigated in this study exhibited nitrogen mass balance errors of less than 10% (Fig. 4.1b). Further, almost complete conversion from ammonia to nitrate was demonstrated at all loading conditions, with a maximum nitrite accumulation of 0.11 ± 0.08 mg of NO_2^--N/L being observed at LR = 600 $gN/m^3 \cdot d$. Nitrite accumulation signifies incomplete nitrification and is often an indication of nitrite oxidizing bacteria inhibition. The lack of nitrite accumulation and the measured significant rates of ammonia removal at various LRs at 1°C suggests tertiary MBBR nitrification is a solution for ammonia removal during long exposure periods to cold temperatures. Additionally, the research shows that conservatively loaded systems (LR = 60 $gN/m^3 \cdot d$) and conventionally loaded systems (LR = 250 $gN/m^3 \cdot d$) produce low ammonia effluent concentrations with an ammonia concentration that meets acute lethality testing using rainbow trout.

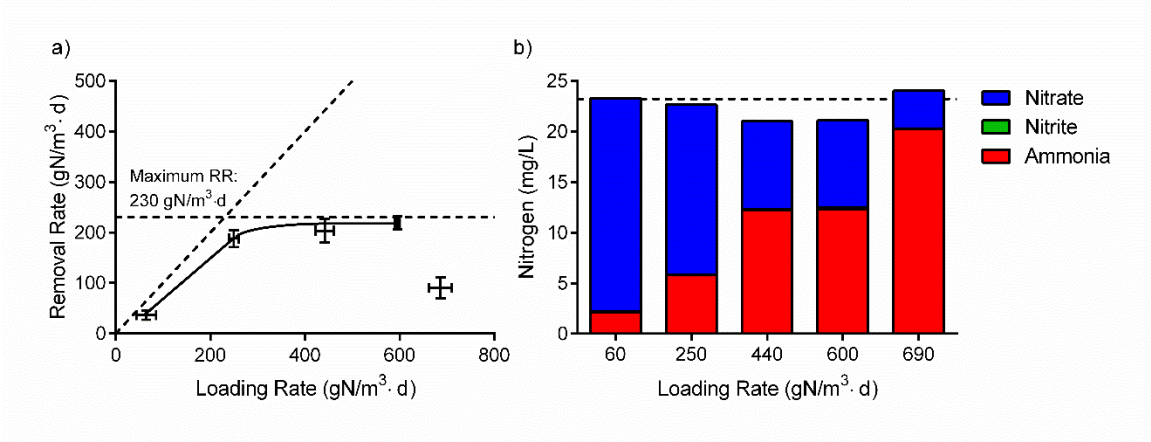

Figure 4.1 Ammonia removal in tertiary nitrifying MBBR pilot at 1°C, a) RRs normalized per m^3 of reactor volume; b) nitrogen mass fractionation showing effluent ammonia concentrations and conversion from ammonia to nitrate at each LR. The horizontal dashed line represents the total nitrogen into the MBBR.

Table 4.2 Effluent ammonia, $mass_{dw}$ and TSS production across LRs.

LR ($gN/m^3 \cdot d$)	Effluent ammonia (mgN/L)	$Mass_{dw}$ (mg/carrier)	TSS production (mgTSS/L)
60	2.1 ± 0.7	30.9 ± 2.6	0.8 ± 2.8
250	5.8 ± 1.2	30.1 ± 3.6	2.1 ± 2.6
440	12.3 ± 0.4	29.9 ± 3.4	6.0 ± 3.8
600	12.4 ± 1.2	27.6 ± 4.2	1.7 ± 3.1
690	20.3 ± 0.2	32.7 ± 3.1	6.4 ± 4.5

4.5.2. Biofilm response

The biofilm response for the tertiary nitrifying MBBR steady state operation at 1°C is presented with respect to biofilm $mass_{dw}$, thickness and protein/polysaccharide (PN/PS) ratio of biofilm EPS at each LR. Based on mass transfer flux models (Gönenç and Harremöes, 1985; WEF, 2010) the estimated ammonia concentration for which nitrifying MBBR systems transition from DO mass transfer rate limited to ammonia rate limited at

20°C is 2.8 mgNH_4^+/NH_3-N/L. At 1°C and at the operational conditions and ammonia removal rates of this study (Fig 4.1a), the ammonia concentration at which the nitrifying MBBR system transitions from DO mass transfer rate limited to ammonia rate limited is 5.4 mgNH_4^+/NH_3-N/L. Using this estimated transition ammonia concentration, the biofilm samples in the conservatively loaded reactor (LR = 60 gN/m^3·d) is DO mass transfer limited, the conventionally loaded reactor (LR = 250 gN/m^3·d) is at the transitory point and the overloaded reactors (LR = 440, 600, 690 gN/m^3·d) are ammonia mass transfer limited.

The biofilm $mass_{dw}$ and thickness are significantly higher during operation at 1°C than 20°C. The biofilm $mass_{dw}$ increased from 9.2 ± 0.9 to 30.2 ± 1.8 mg/carrier and the biofilm thickness increased from 71.6 ± 14.6 to 297 ± 110 µm. The increase in biofilm $mass_{dw}$ and thickness with decreased temperature is likely a combined effect of a decrease in cellular activity and increase in DO penetration into the biofilm due to higher DO concentrations that increased from 4.0 ± 0.9 at 20°C to 7.3 ± 0.4 mg/L at 1°C. The increased oxygen penetration allows for a deeper active nitrifying layer and hence a thicker biofilm (Delatolla et al., 2010; Hoang et al., 2014a). The increase in biofilm thickness and $mass_{dw}$ is possibly indicative of a higher concentration of embedded bacteria, which would be indicative of tertiary MBBR nitrification being stable at 1°C.

The biofilm $mass_{dw}$ does not change significantly at 1°C across loading rates (Table 4.2, p=0.13) and maintains an average $mass_{dw}$ of 30.2 ± 1.8 mg/carrier across all loading rates investigated in this work; indicating that the biofilm $mass_{dw}$ is not dependent on loading rates or ammonia or DO mass transfer limiting condition. The biofilm thickness, however, significantly changes across loading rates (p<0.0001) (Fig. 4.2). The

conservative (LR = 60 gN/m^3·d) and conventional (LR = 250 gN/m^3·d) operating conditions show thick biofilm, which may not be optimal for solute transport within the biofilm matrix (Stewart, 2003). The overloaded operating conditions (LR = 440 and 600 gN/m^3·d), operating near the maximum ammonia RR of 230 gN/m^3·d, have thinner biofilms. This is possibly the optimal thickness for tertiary nitrification at 1°C. Lastly, the highest loaded operating condition (LR = 690 gN/m^3·d) shows an increase in thickness. At this condition, there is potential inhibition leading to the less optimal thickness and lower than maximum RR.

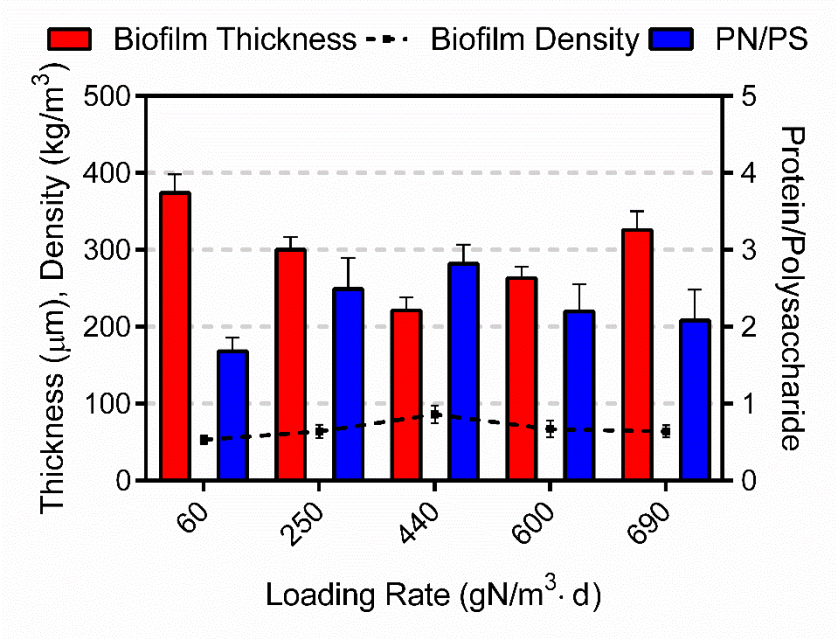

Figure 4.2 Biofilm thickness with standard deviation (n=90), density with standard deviation (n=5) and protein to polysaccharide ratios with standard deviation (n=3) at 1°C across loading rates

The dry densities of the reactors at 1°C range from 53 to 86 mg/cm^3 with the thickest biofilms being the least dense. This range of densities is within the typical range of biofilm density of 25 to 90 mg/cm^3 at comparable DO and biofilm thicknesses (Ahimou

et al., 2007; Laspidou and Rittmann, 2004). Previous studies in nitrifying biofilms postulate a decrease in biofilm density in thick biofilms is attributed to filamentous biofilm morphology (Jang et al., 2003; Karizmeh et al., 2014). This filamentous morphology was observed at 1°C in the thickest biofilm (LR = 60 $gN/m^3 \cdot d$) (Fig. 4.3a), with the thinnest biofilm (LR = 440 $gN/m^3 \cdot d$) not showing filamentous morphology (Fig. 4.3b).

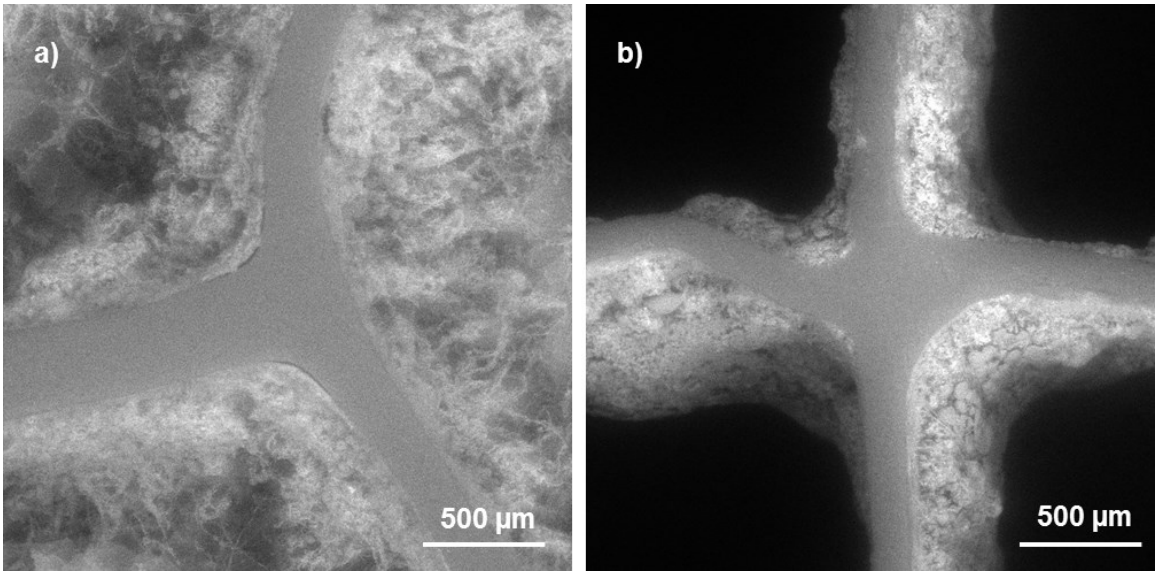

Figure 4.3 Biofilm morphology, a) thickest biofilm, LR 60 $gN/m^3 \cdot d$, showing filamentous morphology b) thinnest biofilm, LR 440 $gN/m^3 \cdot d$, showing more compact dense biofilm morphology

The PN/PS ratio of the biofilm is presented across all loading rates investigated at 1°C (Fig. 4.2). The conservatively loaded reactor (LR = 60 $gN/m^3 \cdot d$) has the lowest PN/PS ratio (Fig. 4.2). The PN/PS ratio increases during operation at the conventionally loaded conditions (LR = 250 $gN/m^3 \cdot d$), where it remains stable during overloaded operation (LR = 440 and 600 $gN/m^3 \cdot d$). Using Pearson's correlation, the PN/PS ratio to the biofilm thickness show a significant relationship with a correlation coefficient R=-0.89 and $p<0.05$. This relationship signifies the biofilm has a higher composition of

polysaccharides in the thicker biofilm. Polysaccharides increase the cohesiveness of the biofilm thereby reducing detachment due to shear forces (Jang et al., 2003). The increased cohesiveness explains the stability of the thicker biofilm (LR = 60, 250, 690 $gN/m^3 \cdot d$). Additionally, the optimal loaded reactors (LR = 440, 600 $gN/m^3 \cdot d$) with biofilm thicknesses of 222 ± 17 and 264 ± 15 μm achieve the maximum RR of 230 $gN/m^3 \cdot d$ at 1°C and show the highest PN/PS ratio. Higher protein concentrations may be indicative of higher enzyme concentrations that might allow for effective degradation within the biofilm matrix. Thus, the EPS PN/PS ratio of approximately 3 in the optimally loaded reactors are likely indicative of the biofilm having a higher degradation activity (Flemming et al., 2007).

4.5.3. Solids response

The solids in this study were analyzed with respect to TSS produced in the tertiary nitrifying MBBR system and changes in particle size distribution as a result of the tertiary nitrification. The TSS produced is calculated as the difference between the effluent TSS of the MBBR reactor and the influent TSS to the MBBR reactor (Table 4.2).

The TSS produced at the various loading rates is not significantly different and does not correlate to the LRs. The overall average value of the TSS produced across all LRs at 1°C is 3.4 ± 3.9 mgTSS/L. This TSS production corresponds to an average TSS detachment rate for a tertiary nitrifying MBBR at 1°C of 36.5 ± 42 $gTSS/m^3 \cdot d$. The TSS production can also be used to calculate the TSS yield of the tertiary nitrifying MBBR at 1°C. To calculate the average TSS yield the highest loaded reactor (LR = 690 $gN/m^3 \cdot d$) was removed to avoid the possible effects of inhibition and stress on the system. The average TSS yield of an operational tertiary nitrifying MBBR at 1°C is 0.31 ± 0.24

gTSS/gN removed. A low TSS production across all loading rates indicates a stable biofilm that is not actively sloughing. In addition the observed low detachment rate at 1°C at all loading rates supports the observed trend of increasing biofilm thickness at cold temperature operation. Although the TSS production due to the pilot nitrifying MBBR system at 1°C is modest, an upgrade MBBR system may require an additional settling step if the effluent solids concentration leaving the upstream treatment facility is approaching regulation prior to installation of the tertiary nitrifying MBBR unit. DPA was performed on unsettled MBBR influent, unsettled MBBR effluent along with MBBR influent and effluent settled for 30 minutes each LR at 1°C to determine the particle size distribution and settleability (Fig. 4.4). The MBBR influent (final effluent of the lagoon treatment facility) has a near uniform unsettled particle size distribution. After thirty minutes of settling, the majority of the particles greater than 150 μm in the MBBR influent settled with 55.9 ± 7.9% of the total solids settling after 30 minutes (Fig. 4.4a, 4.5).

The unsettled particle size distribution across the loading rates does not demonstrate an apparent trend, with similar particle size distributions being observed between the MBBR influent and effluent (Fig. 4.4a-f). Removing the highest loading rate (LR = 690 $gN/m^3 \cdot d$) due to likely inhibition effects, the settled particle size distributions indicate a decrease in settleability of the detached biofilm at lower loading conditions (LR = 60 and 250 $gN/m^3 \cdot d$) to more optimal loading conditions (LR = 440 and 600 $gN/m^3 \cdot d$) (Fig. 4.5). Additionally, the highest loading rate of 690 $gN/m^3 \cdot d$ shows an increase in settleability of detached biofilm. Hence, the most optimally loaded operation from an ammonia removal perspective demonstrates the poorest effluent solids settleability. Decreased settleability

with increased loading rates in MBBRs has been shown in COD treatment systems (Karizmeh et al., 2014; Ødegaard et al., 2000), however, has it has not been demonstrated in tertiary nitrifying systems. Practically, the addition of effluent solids due to the tertiary nitrifying MBBR after 30 minutes of settling in the conventionally loaded reactor (LR = 250 gN/m^3·d) is less than 1.5 mgTSS/L and it is unlikely wastewater treatment plants will require advanced settling.

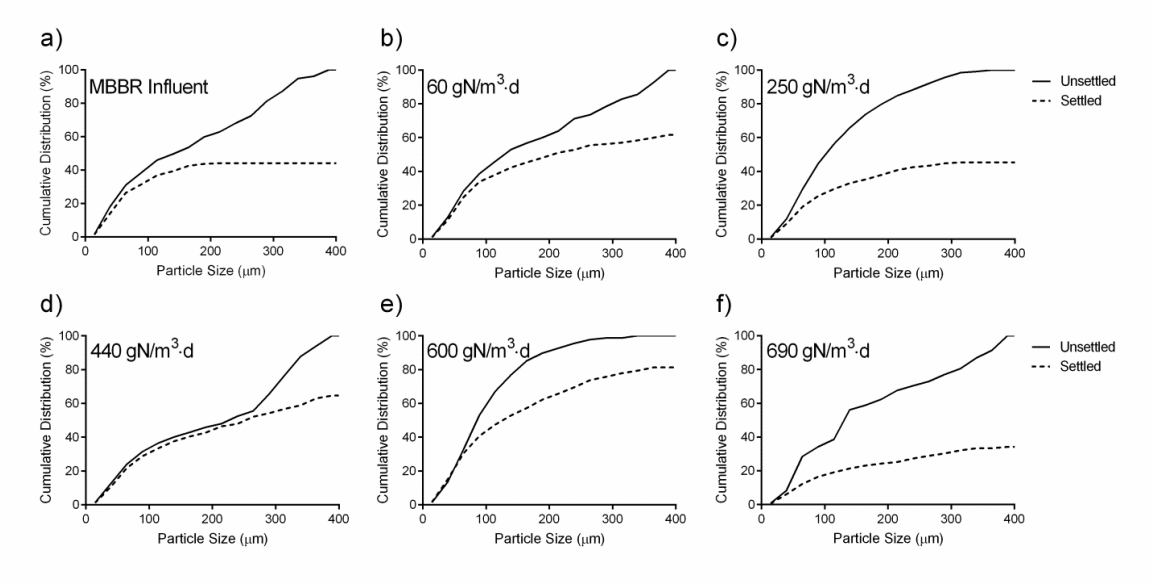

Figure 4.4 Cumulative distribution of the unsettled particle size distribution and normalized particle size fraction after 30 minutes of settling; a) MBBR influent; b) 60 gN/m^3·d; c) 250 gN/m^3·d; d) 440 gN/m^3·d; e) 600 gN/m^3·d; f) 690 gN/m^3·d

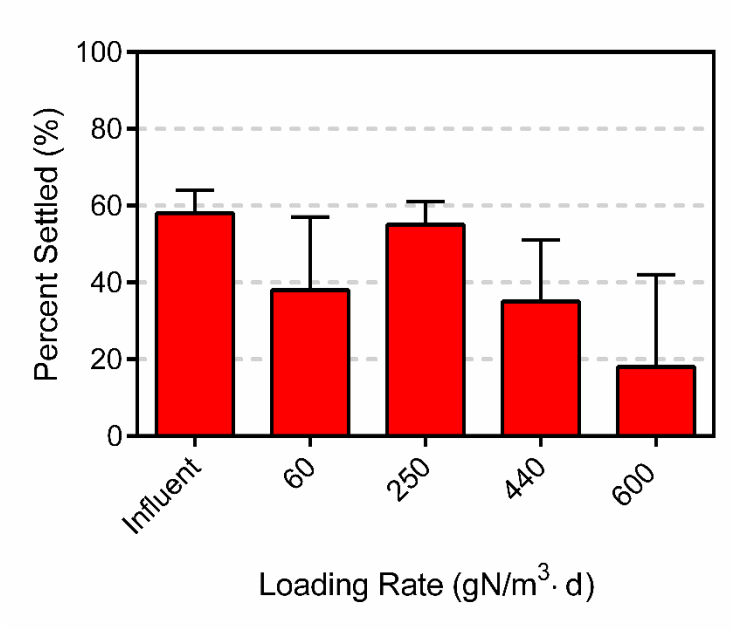

Figure 4.5 Fraction of solids settled after 30 minutes with standard deviation (n=5)

4.6. Conclusion

Tertiary MBBR nitrification at 1°C shows a maximum ammonia removal rate of approximately 230 $gN/m^3 \cdot d$, effluent ammonia concentrations below 2.2 mg-N/L and effluent that is not acutely lethal to rainbow trout. The results demonstrate the importance of proper LR to achieve desired RRs and effluent ammonia quality. This study also demonstrates that biofilm thickness is correlated to protein to polysaccharide ratio and stable from a $mass_{dw}$ and detachment perspective; with the EPS PN/PS ratio approaching an approximately value of 3 at optimally loaded conditions. Lastly, solids settleability is shown to decrease with increasing loading rates.

Chapter 5: Low temperature MBBR nitrification: microbiome analysis

Bradley Young[a], Robert Delatolla[a*], Kevin Kennedy[a], Edith Laflamme[b], Alain Stintzi[c]

[a] Department of Civil Engineering, Faculty of Engineering, University of Ottawa, Ottawa, Canada

[b] Veolia Water Technologies Canada. Montreal, Quebec, Canada

[c] Ottawa Institute of Systems Biology, Department of Biochemistry, Microbiology and Immunology, Faculty of Medicine, University of Ottawa, Ottawa, Canada

5.1. Statement of manuscript status and author contributions

The manuscript “Low temperature MBBR nitrification: microbiome analysis” has been published in Water Research, 2017, 111, 224-223.

Young, B. Conceived and designed the project, operated and maintained the pilot MBBR, performed all constituent, microscopy, library creation and bioinformatics processing. Young, B. wrote and revised the manuscript.

Delatolla, R. was the primary project supervisor, conceived and designed the project, provided direction and feedback on the experiments. Delatolla, R. wrote and revised the manuscript.

Kennedy, K. was a project supervisor, helped conceive and design the project, provided direction and feedback on the experiments.

Laflamme, E. was an industrial collaborator and project supervisor. Laflamme, E. helped conceive and design the project, provided direction and feedback on the experiments.

Stintzi, A. was a project supervisor, provided feedback on the experiments. Stintzi, A. wrote and revised the manuscript.

5.2. Abstract

This study aims to investigate post carbon removal moving bed biofilm reactor (MBBR) nitrification through the transition from 20°C to 1°C and during long term operation at 1°C. Four pilot nitrifying MBBR reactors were operated at various ammonia loading rates to elucidate the temperature effects on ammonia removal rates, cell viability and bacterial communities. The transition from 20°C to 1°C and during long term operation at 1°C were modeled using Arrhenius temperature correction coefficients. Specifically, the steady state removal rates at 1°C on average were 22.8% of the maximum ammonia removal rate at 20°C, which corresponds to an Arrhenius temperature correction of 1.086 during steady operation at 1°C. The microbial communities of the nitrifying MBBR biofilm were shown to be significantly more diverse at 20°C as compared to 1°C operation. Although less diverse at 1°C, 2,000 OTUs of bacteria were identified in the nitrifying biofilm during operation at this low temperature. The family *Nitrosomonadaceae* were shown to be the dominant ammonia oxidizing bacteria (AOB) and the genus *Nitrospira* was shown to be the dominant nitrite oxidizing bacteria (NOB) in all the pilot MBBR reactors at all temperatures. The performance of the post carbon removal nitrifying MBBR systems were shown to be enhanced at 1°C by an increase in the viable embedded biomass as well as thicker biofilm. This effectively increases the number of viable cells present during low temperature operation, which partially compensates for the significant decrease in rate of ammonia removal per nitrifying cell. Operation at the highest loading conditions tested in this study at 1°C was shown to reduce the ammonia removal rate compared to lower

loading conditions at 1°C. The lower performance at higher loading conditions at 1°C demonstrated an enrichment in the stress response metagenomics pathways of the system.

5.3. Introduction

The regulatory framework throughout the world is becoming more stringent with respect to effluent ammonia discharge from municipal wastewater treatment plants. These regulations are challenging in northern climate regions due to significant temperature effects in conventional biological treatment systems (EEC, 1991; Canada Gazette, 2012; USEPA, 2014). This temperature effect is exacerbated in northern passive biological systems where the temperature of the final effluent decreases to 1°C and lower for extended operation.

Nitrification (biological oxidation of ammonia to nitrate through nitrite) is an economical and sustainable means of ammonia removal as it eliminates the need for chemical addition. This biological process, however, is conventionally sensitive to low temperatures with nitrification ceasing below 8°C (Hurse et al., 1999; Randall et al., 1984; Shammas et al., 1986). In an effort to nitrify below 8°C there has been an increased interest in biofilm technologies as add-on units for municipal wastewater treatment plants. One of the premier biofilm technologies is the moving bed biofilm reactor (MBBR), which was specifically designed to enhance the nitrification process (Rusten et al., 1994; Ødegaard, 2006). The MBBR technology promotes biofilm attachment and growth on engineered carriers that are maintained in constant suspension. The attached biofilms are maintained and protected from abrasion with other carriers in the interior spaces of the MBBR carriers.

To achieve nitrification below 8°C, the MBBR technology has been implemented at various locations in passive treatment systems. Implementing the MBBR technology after the first lagoon in multi-lagoon systems has demonstrated the potential for long term operation of low temperature MBBR nitrification at 4°C. However, it should be noted that implementation of a nitrifying MBBR unit after the first lagoon also demonstrated that nitrification rates were significantly impeded by heterotrophic overgrowth (Houweling et al., 2007; Delatolla et al., 2010). More recently, lab and field scale nitrifying MBBR systems have been studied after the last lagoon of multi-lagoon systems. Installation after the last lagoon, with operation at conservative hydraulic and substrate loading rates, has shown that nitrifying MBBR units are able to achieve significant nitrification kinetics at 1°C (Almomani et al., 2014; Hoang et al., 2014). However, recent pilot work has indicated that long term operation at high ammonia loading rates and elevated bulk phase total ammonia concentrations can reduce the kinetic performance of low temperature nitrification (Young et al., 2016b).

The relationship between nitrifying kinetics and temperature has been adequately modeled in previous studies between temperatures of 10 to 28°C using an Arrhenius temperature correction coefficient (θ); with θ values being reported between 1.086 – 1.109 and an average θ value of 1.09 being suggested for MBBR systems (Rusten et al., 1995; Salvetti et al., 2006). Further, Delatolla et al., (2010) modeled nitrifying kinetics during the transition from 8°C to 4°C by plotting the Arrhenius coefficient as a function of time according to Equations 5.1 and 5.2.

$$\theta = 3.81 \times 10^{-2} \cdot \ln(t) + 9.83 \times 10^{-1} \qquad \text{Equation 5.1}$$

$$K_2 = K_1\theta^{T_2-T_1}$$ Equation 5.2

Where θ is the Arrhenius correction coefficient, t is the elapsed time at low temperatures (d), K is the removal rate ($gN/m^2 \cdot d$) and T is temperature (°C).

Nitrifying biofilms attached to MBBR carriers have demonstrated highly diverse microbial populations (Otawa et al., 2006). In the context of nitrification, the functional bacteria are chemoautotrophic and these organisms are traditionally referred to as ammonia and nitrite oxidizing bacteria (AOB and NOB). Recently, through the application of molecular techniques, it has been shown that several different AOB and NOB populations exist in nitrifying biofilms (Gieseke et al., 2003; Terada et al., 2010; Almstrand et al., 2013). At wastewater temperatures between 15-30°C the AOBs are primarily of the *Nitrosomonas* and *Nitrosospira* genera, and the NOBs are primarily of the *Nitrospira* and *Nitrobacter* genera (Shore et al., 2012; Almstrand et al., 2013; Ramierez-Vargas et al., 2015; Bassin et al., 2015). Previous studies observed temporal changes in the AOB communities below 8°C (Hallin et al., 2005; Layton et al., 2005; Siripong and Rittman, 2007). It has currently been hypothesized that the symbiotic relationship between several genera of AOBs and NOBs is thought to maintain stable nitrification performance at variable climates and during operational change (Siripong and Rittmann, 2007; Wittebolle et al., 2008).

In addition to the potential of diverse groups of AOBs and NOBs contributing to the stabilization of nitrification during environmental transitions, recent research has postulated that the peripheral bacterial community of biofilms may also contribute to the stabilization of nitrification. The bacterial community in nitrifying biofilms has been observed to be highly diverse with heterotrophic bacteria contributing a significant role in

sustained nitrification (Bae et al., 2015). The heterotrophic bacteria are believed to be responsible for the assimilation of soluble microbial products that prevent the buildup of metabolites and waste materials of AOBs and NOBs to significant levels in the biofilm as well as being responsible for promoting the formation and development of the biofilm itself (Kindaichi et al., 2004; Bae et al., 2015).

The determination of the relative composition of AOBs, NOBs and the peripheral organisms in environmental samples and biofilms has traditionally been challenging. However, the advent of next generation sequencing techniques has advanced our ability to analyze microbial community structures at high resolution and improve our understanding of many microbial systems (Caporaso et al., 2010). Additionally, various bioinformatic tools have been developed to categorize bacterial functions within the community (Langille et al., 2013). To date, however, the application of these tools has not been largely reported for biofilm wastewater treatment, with their application to this area of study having the potential to enhance the development of a comprehensive understanding of nitrifying biofilms, specifically when applied to nonconventional treatment conditions such as 1°C .

The aim of this work is to investigate the effects of ammonia loading rates on ammonia removal rates at 1°C and elucidate the impact on the microbial communities at low temperatures through the application of variable pressure scanning electron microscopy (VPSEM), confocal laser scanning microscopy (CLSM) and next generation sequencing. Investigating the microbial community during long exposure to 1°C will provide necessary information to understand the potential and design constraints of nitrifying MBBR systems in northern and cold climate regions.

5.4. Materials and methods

5.4.1. MBBR pilot

An MBBR pilot plant was installed after the last lagoon of a four pond-in-series treatment system at Masson Angers, Quebec, Canada. The pilot plant was comprised of four 223 L MBBR reactors with each MBBR reactor housing AnoxKaldnes K5 (protected surface area 800 m^2/m^3) biofilm support carriers. The MBBR reactors were configured with two parallel trains each with two reactors in series (Fig 5.1). A submersible pump was installed in the lagoons final effluent channel and run continuously to an elevated transfer tank in the pilot. The transfer tank had an HRT of less than 10 minutes and samples were periodically checked to ensure no biological activity was occurring. From the transfer tank, each train was gravity fed through air actuated valves and flowmeters (KROHNE, Can, ON) automated with a programmable logic controller (PLC). At sampling, the flow rates were manually tested to validate flow readings from the PLC. A regenerative blower provided process air to an aeration grid located in each MBBR reactor.

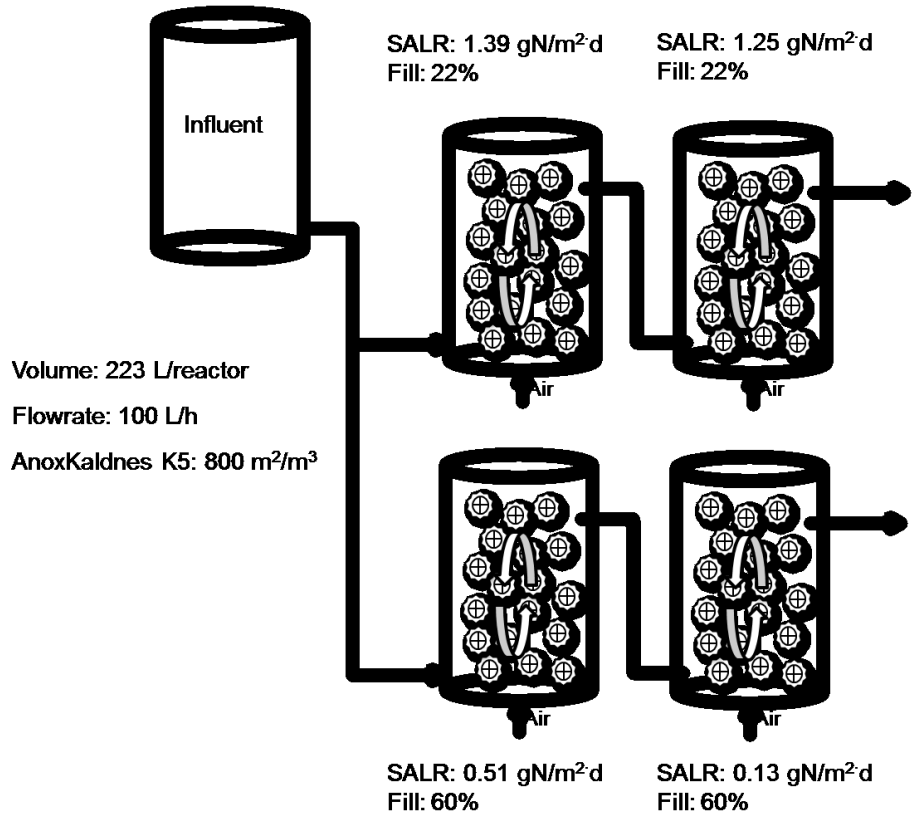

Figure 5.1 Pilot MBBR reactor configuration with SALRs during 1°C steady state operation

The carriers were initially seeded from an integrated fixed film activated sludge (IFAS) full-scale, partially nitrifying wastewater treatment plant. After four months of acclimatization, the nitrifying MBBR reactors achieved steady state operation at 20°C. During this steady state operation a full biofilm characterization was performed at the optimal surface area loading rate (SALR) of 2.36 $gN/m^2 \cdot d$ and a hydraulic retention time (HRT) of 1.5 h, pH of 6.98 ± 0.02 and dissolved oxygen (DO) concentration of 3.4 ± 0.1 mg/L. After nine months of operation, the temperature dropped gradually from 20°C to 1°C (September to January) and the HRT of the four MBBR reactors of the MBBR pilot system was increased to 2.2 h. Once the wastewater reached 1°C, operation was

maintained for a period of two months at a temperature of 1.0 ± 0.2°C. It is during this two month period of steady state operation that the 1°C kinetic and microbial data sets were acquired.

During winter operation, the HRT of each reactor was maintained at 2.2 h with relatively constant influent wastewater constituents (Table 4.1). Notably, the five day carbonaceous biological oxygen demand (BOD_5)/TKN ratio was 0.8 ± 0.3 and there was sufficient total alkalinity to achieve total nitrification without requiring pH control. In general the influent wastewater characteristics were in the optimal range for nitrification with the exception of the temperature decreasing to 1°C, a typical wastewater temperature for effluent from passive treatment systems in northern climate regions (Figueroa and Silverstein, 1992; Lee et al., 2004). All wastewater chemical analysis was performed in accordance to standard methods (APHA, 2005).

During winter operation, the four MBBR reactors were maintained at a constant HRT (2.2 h/reactor). The volume of carriers ranged from 49 L (22% fill) to 134 L (60% fill) allowing for various loading rates to be analyzed. The SALRs in the four MBBR reactors were 0.13, 0.51, 1.25 and 1.39 $gN/m^2 \cdot d$. A conventional SALR at 20°C is 1.0 $gN/m^2 \cdot d$, thus the reactors ranged from under loaded to overloaded. Each loading rate was maintained at steady state for a minimum of four weeks at 1°C at a constant DO concentration of 7.3 ± 0.4 mg/L and pH of 6.99 ± 0.04. Additional material with respect to the pilot, reactor setup and methodology is available in the supplemental information.

5.4.2. Biofilm thickness

A Vega II-XMU SEM (Tescan USA Inc., Cranberry, PA) variable pressure scanning electron microscopy (VPSEM) was used to measure in-situ biofilm thickness (Delatolla et al., 2009). At each loading rate, five images of four replicate carriers (20 total images) were acquired within 4 hours of harvesting, at a pressure of 40 Pa and ×60 magnification. The acquired images were processed with Atlas imaging processing software (Tescan USA Inc., Cranberry, PA). This imaging protocol resulted in 90 thickness measurements per loading rate.

5.4.3. Cell viability

Five replicate carriers were harvested during steady state operation at each of the five loading rates investigated in this study. The cell viability staining was performed using the FilmTracer LIVE/DEAD Biofilm viability kit (Life Technologies, US, CA). The viability kit is comprised of two stains. The first stain, SYTO9, is a green nucleic acid stain that is highly membrane-permeant and stains all cells. The second stain is propidium idodide (PI), a cell membrane-impermeable stain. PI is only capable of staining cells with compromised cell membranes, which are considered non-viable. A working solution containing both SYTO9 and PI were added to an undisturbed MBBR carrier for 30 min and protected from the light. After the 30 min staining period the working solution was gently rinsed twice with sterile water.

Calcofluor White Stain (Sigma-aldrich, US, MO) was used to stain the EPS in the biofilm matrix to determine where the viable/nonviable cells were located relative to the imaged biofilm area. Two drops of the Calcofluor stain were added to the undisturbed MBBR carriers and allowed to penetrate for 1 min. After the 1 min staining period the

dye was gently rinsed twice with sterile water. Immediately after the Calcofluor rinsing, the undisturbed MBBR carriers were observed using CLSM. A 510/AxioImager confocal laser scanning microscope (Zeiss, US, VA) with a ×63 water objective was used to acquire five stacks of five images (25 total images) per sample at a maximum depth per stack of 30 μm.

Cell viability analytical quantification of the acquired microscopic images was performed using Nikon NI Vision Assistant (National Instruments, LabVIew, 8.0). First the biofilm area was outlined and exported by tracing the Calcofluor stain. Second the image colour threshold function was used to calibrate the area of a single cell identified on the CLSM image. Once calibrated, the image was analyzed for viable and nonviable cells (Delatolla et al., 2009b).

5.4.4. Next generation DNA sequencing

Approximately 25 mg of wet biofilm was abraded from 5 replicate MBBR carriers into a 1.5 mL sterile eppendorf tube. DNA was extracted using FastDNA Spin Kit (MP Biomedicals, US, CA) and stored at -20°C until it was used for library construction.

Library construction used a two-step polymerase chain (PCR) targeting the V6 hyper-variable region of the 16S rRNA gene previously described in Young et al. (2016a). Briefly, the first PCR step amplified the V6 region and added 4-6 nucleotide known barcodes and the illumina sequencing adaptors. The second PCR step amplified the PCR1 product and simultaneously added the Illumina flow cell adaptor. Following the second PCR amplification, the amplicons were inspected on a 2% agarose gel and purified with Montage PCR96 cleanup kit (EMD Milipore, Billerica, MA). The purified amplicons

were quantified using Quant-iT dsDNA HS Assay Kit (Life Technologies, Burlington, Canada) and 50 ng of DNA from each sample was pooled together. The pooled sample was sent to The Center for Applied Genomics (TCAG, Toronto, Canada) to be sequenced on a Hiseq2500.

5.4.5. DNA sequencing analysis

The 2x100 base paired-end reads were assembled using the Fast Length Adjustment of Short reads (FLASH) software (Magoc and Salzberg, 2011) then filtered using the fastq_quality_filter command from the Fastx toolkit with a minimum quality score of 20 over 90% of the sequences. Reads that passed the quality filter were demultiplexed and the barcodes were trimmed using Novobarcode (Goecks et al., 2010). The Quantitative Insights into Microbial Ecology (QIIME) software, verson 1.8 (Caporaso et al., 2010), was used to compute operational taxonomical unit (OTU) clustering with closed reference strategy at 97% sequence similarity. Qiime aligned the OTUs against the Greengenes database 13.8 utilizing UCLUST algorithm. Then, the relative abundance of the bacterial taxa present in the biofilm was determined following the removal of singleton OTUs. Lastly, the OTUs were gene profiling using the PiCrust bioinformatics tool (Langille et al., 2013).

QIIME was used to determine the species richness and diversity. Species richness within the sampling groups was determined through alpha diversity and specifically the Chao1 index. Species diversity between the sampling groups was determined through weighted and unweighted Uni-Frac distant beta diversity. Finally, differences in bacterial taxa was determined through summarized taxa and LEfSe for relative abundances and

gene pathways respectively (Blankenberg et al., 2010; Giardine et al., 2005; Goecks et al., 2010).

5.4.6. Statistical analysis

Statistical significance across cell viability and microbial relative abundances was determined using the Kruskal-Wallis sum-ranked test analysis of variance with a p-value less than 0.05 signifying significance. Statistical significance for the gene pathway analysis used linear discriminate analysis (LDA) with an LDA-score of 2 identifying significantly differentially abundant pathways.

5.5. Results and discussion

5.5.1. Nitrification kinetics

The optimal ammonia removal rate at 20°C was measured at an SALR of 2.36 $gN/m^2 \cdot d$ with a corresponding surface area removal rate (SARR) of 2.0 ± 0.06 $gN/m^2 \cdot d$ (Table 5.1). Using this optimal loading as a benchmark, four SALRs were analyzed at a temperature of 1°C: 0.13, 0.51, 1.25 and 1.39 $gN/m^2 \cdot d$. The transition from 17°C to 5°C between days 40 to 100 (Fig 5.2a), demonstrated a distinction in the effluent ammonia concentrations and hence in turn the ammonia removal rates of the differently loaded MBBR reactors (Fig 5.2b). During this transition, from 17°C to 5°C, there was an observed spiked increase in nitrite at SALRs of 0.51 and 1.25 $gN/m^2 \cdot d$. In these reactors, the nitrite concentration spiked to maximum of 0.6 $mgNO_2$-N/L between days 45 and 60 (Fig 5.2c), which corresponded to a period of rapid temperature decrease from 17.3 to 8.6°C. Although the nitrite increased relative to the background nitrite concentrations during this period of rapid temperature change, it should be noted that the maximum observed nitrite concentration of 0.6 $mgNO_2$-N/L remains a low concentration of nitrite

accumulation. At temperatures below 15.0°C NOBs theoretically have a higher growth rate than AOBs (Heijnen et al., 1998; Paredes et al., 2007; Ge et al., 2015), however, the modest nitrite spike indicates NOBs are subject to slight inhibition through rapid temperature decline. After the inhibition period and the NOBs acclimatized to the low temperatures, the effluent nitrite was maintained at 0.1 mgNO_2-N/L for all loading rates between days 60 and 100.

Table 5.1 Kinetics and effluent ammonia concentrations

SALR ($gN/m^2 \cdot d$)	Temperature (°C)	Removal Rate (mgN/L)	Effluent Ammonia (mgN/L)
2.36 ± 0.05	20.6 ± 0.5	2.0 ± 0.06	3.9 ± 0.4
0.13 ± 0.05	1.0 ± 0.1	0.09 ± 0.01	2.1 ± 0.7
0.51 ± 0.02	1.0 ± 0.1	0.32 ± 0.03	5.8 ± 1.2
1.25 ± 0.01	1.0 ± 0.1	0.35 ± 0.05	12.4 ± 1.2
1.39 ± 0.05	1.0 ± 0.1	0.22 ± 0.03	20.3 ± 0.2

The transition from 5°C to 1°C between days 100 to 140 further reduced the rate of ammonia removal and increased the effluent ammonia concentrations during operation at 1°C for a period of 60 d. During operation at 1°C, the pilot reactors loaded at 0.13 and 0.51 $gN/m^2 \cdot d$ consistently maintained effluent ammonia concentrations below 4 and 10 mgN/L respectively (Fig 5.2b). Additionally, the nitrification process proceeded to completion in these reactors, with the effluents corresponding to less than 0.2 mgNO_2-N/L. Thus at conservative (0.13 $gN/m^2 \cdot d$) and conventional (0.51 $gN/m^2 \cdot d$) loading rates, post carbon removal nitrifying MBBR systems are herein shown to be a viable ammonia removal technology for operation at 1°C that are capable of producing a high quality effluent. In the overloaded reactor loaded at 1.25 $gN/m^2 \cdot d$, the effluent ammonia

concentration was maintained below 15 mgN/L. Although this effluent ammonia concentration is higher, the removal rate is statistically equal to the conventionally loaded reactor at 0.51 $gN/m^2 \cdot d$ (Table 5.2). Statistically equal removal rates for the conventional and overloaded reactor indicates that the kinetics of nitrification has reached zero order with respect to ammonia concentrations and that the maximum removal rate of 0.35 $gN/m^2 \cdot d$ was achieved. Hence, a removal rate of 0.35 $gN/m^2 \cdot d$ was anticipated for the highest loaded reactor. However, the highest loaded reactor, 1.39 $gN/m^2 \cdot d$, demonstrated a significantly lower removal rate of 0.22 ± 0.03 $gN/m^2 \cdot d$. The bulk free ammonia in the reactor loaded at 1.39 $gN/m^2 \cdot d$ was 0.022 mgN/L (Anthonisen et al., 1976). Although, this free ammonia concentration is significantly below the inhibition threshold of 4-22 mgN/L reported at 20°C, it is important to note that nitrification inhibition testing to date has not been published at low temperatures such as 1°C (Anthonisen et al., 1976; Van Hulle et al., 2010). As such, the low temperature conditions of 1°C may possibly exacerbate the inhibition of AOBs, reduce the ammonia removal rate and subsequently increase the effluent ammonia concentrations of the system.

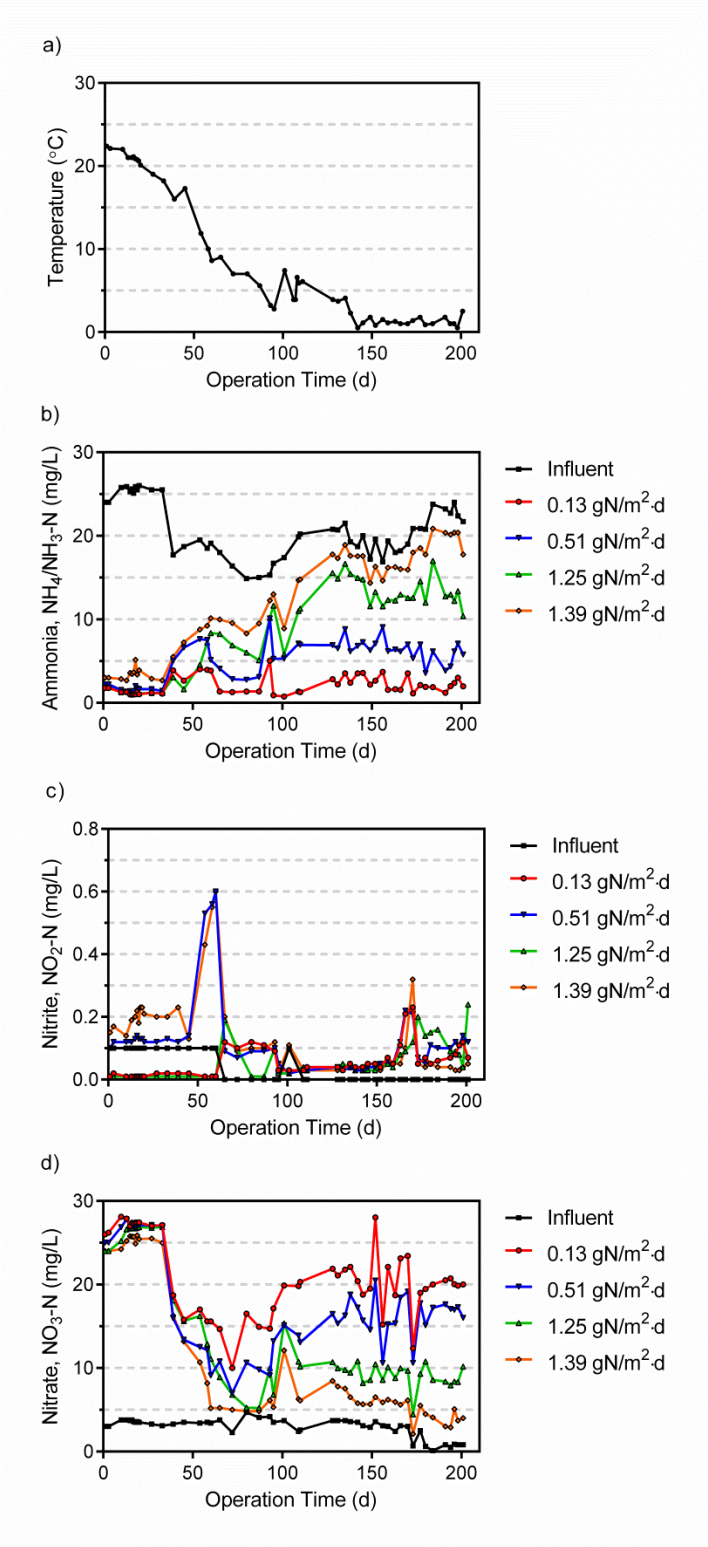

Figure 5.2 Post carbon removal MBBR nitrification at various SALRs across time of operation, a) temperature, b) ammonia concentration, c) nitrite concentration, d) nitrate concentration

In this study, three distinct Arrhenius correction coefficient models were applied to the relative ammonia removal rates of the 0.51 and 1.25 $gN/m^2 \cdot d$ loaded reactors across decreasing temperatures and steady operation at 1°C (Fig 5.3a). The 0.13 $gN/m^2 \cdot d$ loaded reactor was under loaded and operated below the maximum achievable removal rate and the 1.39 $gN/m^2 \cdot d$ loaded reactor demonstrated signs of inhibition, hence the Arrhenius correction coefficient models were not used to model these data, with the data sets being omitted from Fig 5.3a. An Arrhenius coefficient of 1.09 was applied to the transition from 12°C to 7.4°C to model the ammonia removal rate transition from moderate temperature operation to low temperature operation (R^2=0.89) (Fig 5.3a). The measured removal rates at temperature of 5°C and below were shown to no longer correlate to the predicted removal rates using an Arrhenius coefficient of 1.09. However during the transition from 5°C to 1°C, these rates were well predicted by the Delatolla et al. (2010) transition model (θ = 1.125 at the initial 1°C time point) (Delatolla et al., 2010). As such, Equations 5.1 and 5.2 were used to model the immediate effects of transitioning from low temperature ammonia removal rates (5°C) to very low temperature ammonia removal rates (1°C) (Fig 5.3a). The Delatolla et al. transition model also demonstrated the ability to predict the ammonia removal rates during the first 10 days of operation at 1°C (R^2=0.77); a period of low measured removal rates that are likely due to an acclimatization period of the AOB biomass in the 0.51 and 1.25 $gN/m^2 \cdot d$ loaded reactors. The ammonia removal rates steadily improved after the 10 days of operation at 1°C until the 49th day of operation at 1°C, where steady state removal was achieved. The steady state removal rates were modelled using an Arrhenius coefficient of 1.086 (CV=15%)

and were shown to remain steady at 22.8% of the ammonia removal rate measured at 20°C.

The highest loaded reactor (1.39 $gN/m^2 \cdot d$), which is likely free phase ammonia inhibited demonstrates a slight continual decline in performance with time of exposure at 1°C as opposed to the 0.51 and 1.25 $gN/m^2 \cdot d$ loaded reactors that show an acclimatization to this very low temperature (Fig. 5.3b). The 1.39 $gN/m^2 \cdot d$ loaded reactor achieves an average removal rate relative to 20°C of 12.2%, which corresponds to an Arrhenius coefficient value of 1.117. It is important to note that even the lower performing MBBR reactor operated at high loading was able to outperform the previously established Arrhenius coefficient value of 1.4 that was reported for suspended growth systems in the temperature range from 2 to 7°C (Oleszkiewicz and Berquist, 1988). This indicates that the MBBR technology is robust with respect to inhibition during low temperature operation, and that the effect of temperature shock, predicted bulk liquid free phase ammonia concentrations and time of exposure must be accounted for in the design of low temperature MBBR systems.

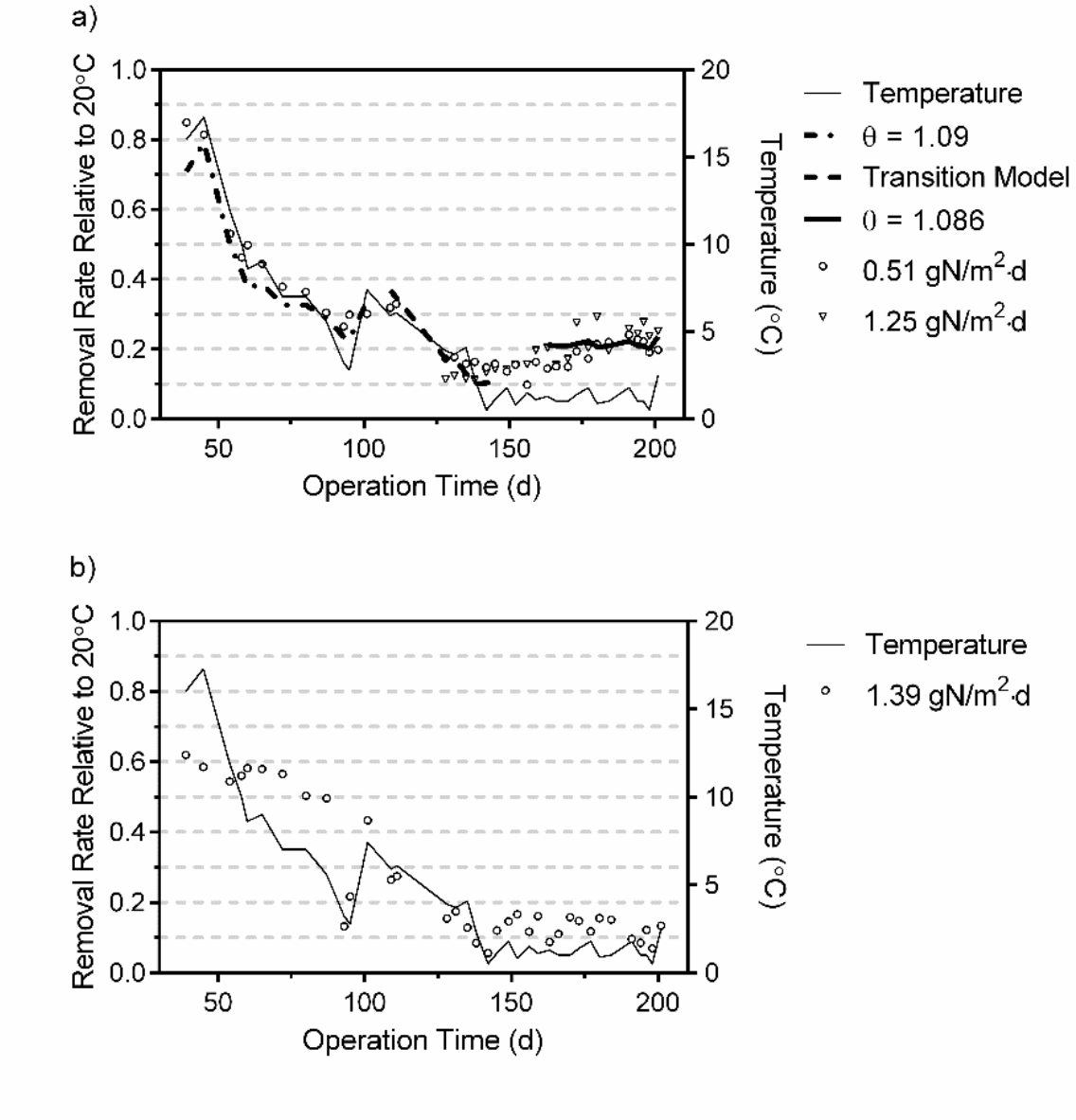

Figure 5.3 Removal rates relative to 20°C across time of operation, a) Arrhenius correction coefficient models applied to low temperature operation at SALR of 0.51 and 1.25 gN/m^2·d, b) low temperature operation at SALR of 1.39 gN/m^2·d

5.5.2. Cell viability

CLSM was used in combination with a biofilm cell viability kit and cell imaging software to identify and count viable and non-viable cells. The live fraction of total cells was determined by dividing the viable cells by the total number of cells (viable + non-viable) (Fig 5.4). Grouping the live fractions at 1°C and using Mann-Whitney U test the cell viability demonstrates a significant change with respect to temperature ($p=0.0005$), where the cells exhibit an increase in viability at 1°C as compared to 20°C. Overall, all loading rates at 1°C were operating at a live fraction of total cells of 82.9 ± 2.7%. This indicates the nitrifying biofilm allows for cells to survive in long exposures to wastewater temperatures of 1°C. This increase in cell viability at 1°C is consistent with previously observed responses to cold-shock, where cells have been shown to decrease the cellular metabolic rates during cold temperature shock while maintaining protein synthesis corresponding to an increase in the percent viability (Phadtare, 2004).

Analyzing the cell viability at 1°C shows that the loading rate does not significantly affect the live fraction of total cells (Fig 5.4). Although there is a statistically greater live fraction of total cells at an SALR of 0.51 $gN/m^2 \cdot d$ as compared to 0.13 $gN/m^2 \cdot d$ ($p=0.04$), there is not a statistically significant difference in live fraction of total cells between the loading rates for all other comparisons. Additionally, at an SALR of 1.39 $gN/m^2 \cdot d$, which corresponds to the suspected inhibitory free phase ammonia concentration at 1°C, the biomass did not show a significant decrease in live fraction of total cells. This suggests that lower ammonia removal kinetics is not caused by the biomass being less viable; instead the activity of the AOBs within the biofilm matrix are simply slowed during the 1.39 $gN/m^2 \cdot d$ loading operation.

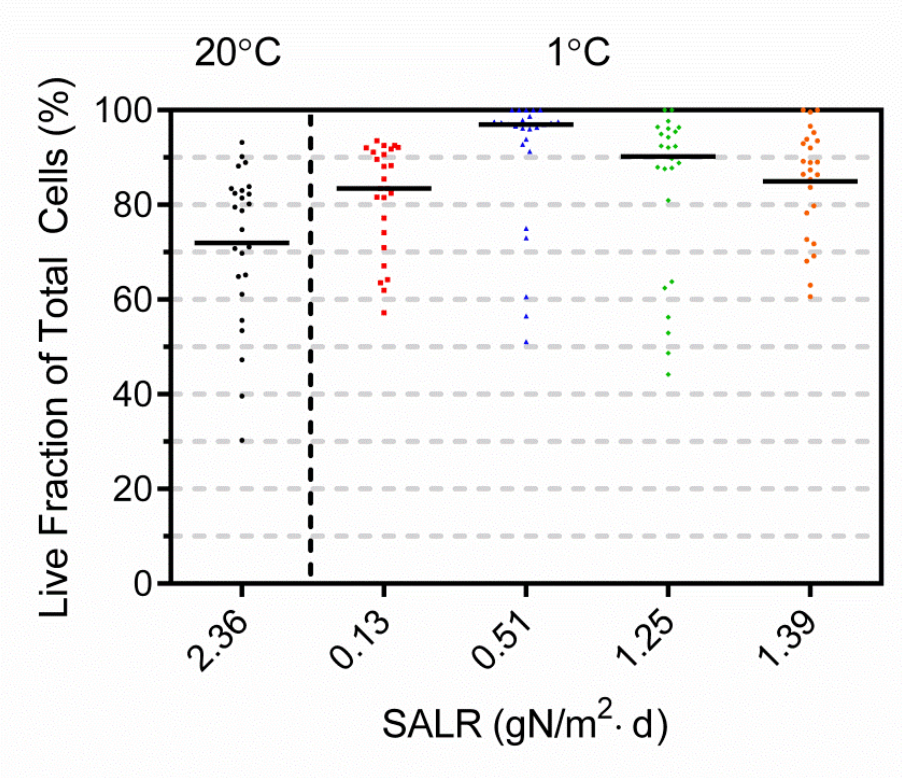

Figure 5.4 Live fraction of total cells across SALRs at 20°C and 1°C with the median value superimposed

5.5.3. Microbial community diversity

High throughput Illumina sequencing generated 22,653,360 reads with a mean of 943,890 ± 302,126 high quality reads per sample. For alpha and beta diversity the samples were normalized to 411,546 high quality reads corresponding to the sample with the least number of reads.

Alpha diversity measures the diversity of the microbial community within each loading rate. For this analysis, the Chao1 estimator of species predicts the total number of unique species at each loading rate (Fig 5.5). Overall, the post carbon removal nitrifying biofilm at 20°C has a greater estimated number of species than at 1°C. The greater estimated number of species observed at 20°C is likely due to the 20°C environment

being more suitable for a broad range of bacteria; hence allowing for a more diverse community within the biofilm.

At 1°C, the lowest loading rate of 0.13 $gN/m^2 \cdot d$ has a significantly more diverse microbial population as compared to loading rates of 0.51, 1.25 and 1.39 $gN/m^2 \cdot d$. It is likely under loading a post carbon removal nitrifying MBBR and operation in ammonia substrate limited condition allows for the proliferation of peripheral bacteria. As the loading rate increases and the post carbon removal nitrifying MBBR reaches its maximum kinetic rate, the peripheral organisms are outcompeted and the number of species in the biofilm stabilizes. The stabilized biofilm is highly diverse with greater than 2,000 species per sample indicating the long exposure to wastewater temperatures of 1°C remained a suitable environment for the bacterial consortia.

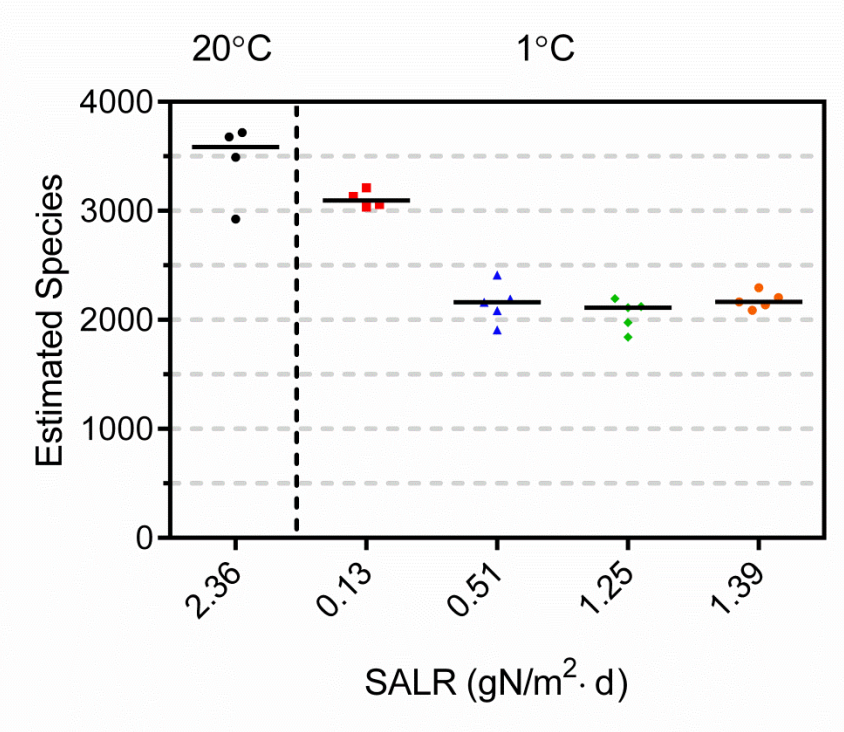

Figure 5.5 Alpha diversity of microbial communities across SALRs at 20°C and 1°C with the median value superimposed

Principal coordinate analysis (PCoA) was performed for the unweighted and weighted UniFrac distances to determine if the entire prokaryotic community exhibits significant population shifts with respect to temperature and loading rate. This UniFrac distance computes the dissimilarly of the microbial communities while incorporating phylogenetic distances. Specifically the unweighted PCoA analyzes the presence or absence of species in each community and the weighted PCoA normalizes against the relative abundance of species in each community.

The microbial community at 20°C is significantly different than the microbial community at 1°C for both the unweighted and weighted analysis (Fig 5.6a, 5.6b). It is clear there is a microbial community shift with temperature in a post carbon removal nitrifying MBBR. The microbial shift is most likely due to the environment at 20°C allowing for more microbial species to populate the biofilm. At an SALR of 0.13 $gN/m^2 \cdot d$ (lowest loaded reactor), the unweighted and weighted PCoA shows significant separation compared to all other loading rates (Fig 5.6c, 5.6d). This separation is expected as the SALR of 0.13 $gN/m^2 \cdot d$ has a significantly more diverse community as compared to the other loading rates. Although the separation does not identify the difference in community structure, it is clear an under loaded nitrifying MBBR has a significantly different microbial community than an optimal or overloaded nitrifying MBBR.

The reactor with an SALR of 0.51 $gN/m^2 \cdot d$ has a significantly different microbial community as compared to the under loaded and overloaded reactors with respect to the unweighted beta diversity (Fig 5.6c). The weighted beta diversity, however, exhibits less separation between the SALR of 0.51 $gN/m^2 \cdot d$ and the overloaded reactors. This

indicates the microbial communities of the 0.51 gN/m^2·d loaded reactor have different species of bacteria compared to the 1.25 and 1.39 gN/m^2·d loaded reactors, but the highest abundant organisms at all of these three loading conditions are similar (Fig 5.6d).

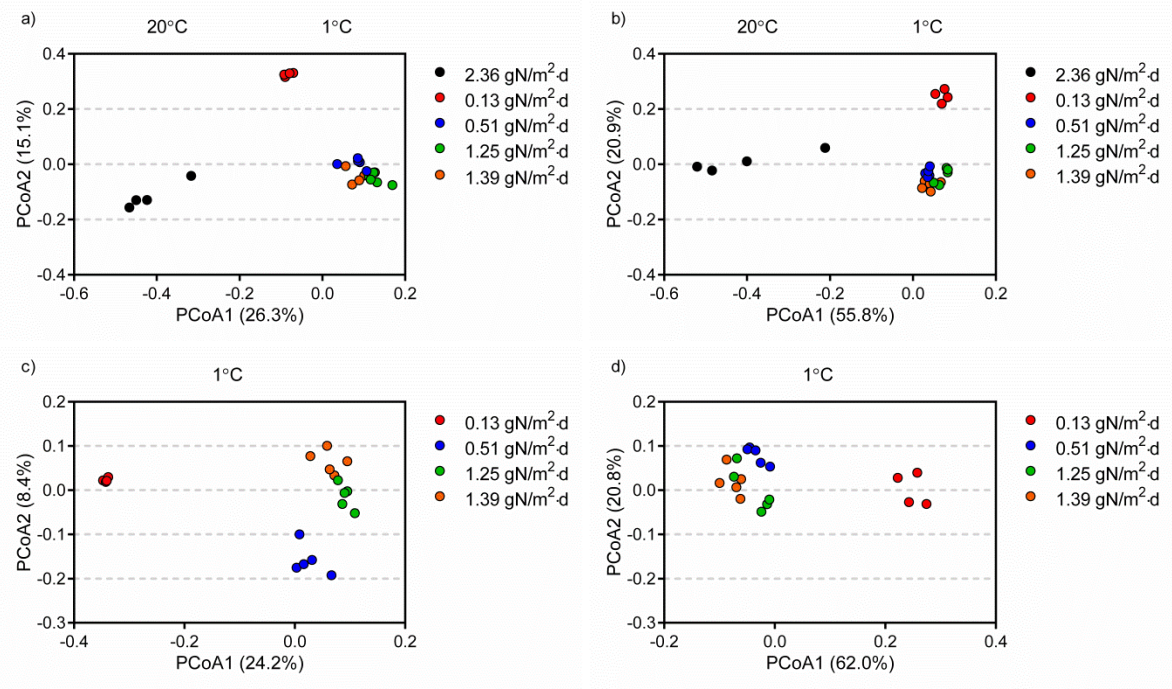

Figure 5.6 PCoA UniFrac distances at various SALRs, a) unweighted analysis of 20°C and 1°C, b) weighted analysis of 20°C and 1°C, c) unweighted analysis of 1°C and d) weighted analysis of 1°C

5.5.4. Relative abundance of AOBs and NOBs

At each operational temperature and loading rate the primary AOBs are in the family *Nitrosomonadacea*, which includes the genera *Nitrosomonas*, *Nitrosospira* and *Nitrosovibrio*. Due to sequence similarity, reliable identification at the genus level could not be achieved, with *Nitrosomonas* being observed to be the dominant AOB in municipal wastewater at 20°C in past studies (Shore et al., 2012; Almstrand et al., 2013; Wang et al., 2015). The family *Chromatiaceae*, which includes the genus *Nitrosococcus*,

was detected also at both 20 and 1°C in this study, however this family comprised less than 1x10-3% relative abundance at both temperatures; which conforms with previous studies (Daims and Nielsen, 2001; Gieskeke et al., 2001). Hence, *Nitrosoccus* and was observed to be outcompeted by the family *Nitrosomonadaceae* in the post carbon removal nitrifying biofilm system at all operational temperatures and loading rates.

The total relative abundance of AOBs was determined in this study by grouping the relative abundances of all known AOBs at 20°C and at the various loading rates at 1°C (Fig 5.7). At an SALR of 0.13 $gN/m^2 \cdot d$, the relative abundance of AOBs is significantly lower than all other loading rates. From a kinetic and effluent ammonia perspective this reactor is under loaded and hence simply leads to less proliferation of AOBs to fully oxidize the low rate of ammonia being fed to the system.

The AOB relative abundance was statistically equal at 20°C and SALRs of 0.51, 1.25 and 1.39 $gN/m^2 \cdot d$ at 1°C. The relative abundance at all loading conditions that achieved maximum removal rates (0.51 and 1.25 $gN/m^2 \cdot d$) was approximately 7.0 ± 1.8%. The AOB relative abundance at a loading rate of 1.39 $gN/m^2 \cdot d$, although exhibiting a reduced removal rate, was equal to loading rates 0.51 and 1.25 $gN/m^2 \cdot d$. Thus the AOBs at reduced performance operation were shown to remain present at similar percent abundances in the biofilm.

At each operational temperature and loading rate the primary NOB is in the family *Nitrospiraceae* with *Nitrospira* as the primary genus. *Nitrobacter* was detected, but of negligible relative abundance indicating *Nitrospira* is the primary NOB of the post carbon removal nitrifying reactors at 20 and 1°C. Grouping all of the known NOBs, the relative abundance of NOBs were consistently greater than the AOBs by a factor of 1.3 to

2 for all loading rates. This ratio is comparable to gene sequencing performed on nitrifying biofilms in other studies at 30°C (Winkler et al., 2012). In addition it was observed that the percent abundance of NOBs decreased significantly from 20 to 1°C. This decrease in percent abundance may explain why a modest nitrite spike temporarily occurred during rapid temperature shifts and may support previous work that demonstrates that NOB populations are susceptible to temperature shock effects (Alawi et al., 2009; Delatolla et al. 2010). However, at each temperature and loading rate the NOBs completely oxidized nitrite to nitrate. Hence this study indicates that the observed NOB populations, once acclimatized, are capable of achieving rates of nitrite oxidation that equal or exceed rates of ammonia oxidation, thus strengthening the finding of sustainable long term nitrification at 1°C using the MBBR technology.

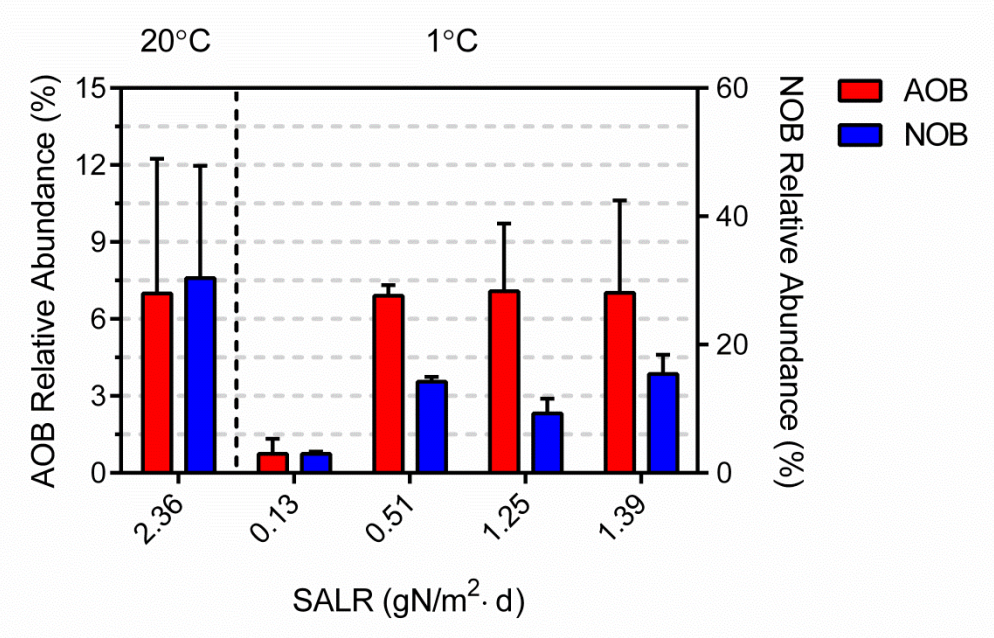

Figure 5.7 Relative abundance of AOB and NOBs with standard deviation (n=5) across SALRs at 20°C and 1°C

The viable ammonia oxidizing bacteria removal rate (VAOBRR) per viable cell was estimated (Equation 5.3) to normalize the ammonia removal rate for the number of viable AOB cells per reactor (Young et al., 2016a).

$$\mathrm{VAOBRR} = \frac{\mathrm{Q} \cdot (\mathrm{C_{in}} - \mathrm{C_{out}})}{\mathrm{V_c} \cdot \mathrm{a} \cdot \mathrm{B_T} \cdot \%\mathrm{Viable} \cdot \%\mathrm{AOB}} \qquad \text{Equation 5.3}$$

Where Q is the flowrate (m3/d), Cin (g/m3) is the influent ammonia concentration, Cout (g/m3) is the effluent ammonia concentration, Vc is the volume of carriers (m3), a is the surface area to volume ration (m2/m3), BT is the biofilm thickness (m), %Viable is the viable cells per biofilm area (%), %AOB is the relative abundance of AOBs (%). The viable nitrite oxidizing bacteria removal rate (VNOBRR) was calculated (Equation 5.4) using %NOB as the relative abundance of NOBs (%). These calculations assume the cell viability is homogenous across all cells in the biofilm. Ammonia concentrations for Cin and Cout are used to estimate VNOBRR due to a lack of nitrite in the influent or effluent from the reactors (complete conversion of ammonia to nitrate).

$$\mathrm{VNOBRR} = \frac{\mathrm{Q} \cdot (\mathrm{C_{in}} - \mathrm{C_{out}})}{\mathrm{V_c} \cdot \mathrm{a} \cdot \mathrm{B_T} \cdot \%\mathrm{Viable} \cdot \%\mathrm{NOB}} \qquad \text{Equation 5.4}$$

The VAOBRR and VNOBRR are significantly higher at 20°C as compared to 1°C operation (Table 5.2). The VAOBRR in the well performing reactors at 1°C is approximately 6% of the maximum VAOBRR at 20°C and the VNOBRR is approximately 13% of the maximum VNOBRR at 20°C. This decrease in specific cellular removal rate is expected to decrease with temperature. The overall performance of the post carbon removal nitrifying MBBR systems are enhanced at 1°C by an increase in the viable embedded biomass (Fig 5.4) as well as thicker biofilm (Table 5.2). This

effectively increases the number of viable cells present during low temperature operation, which in turn partially compensates for the significant decrease in cellular performance. Specifically, the maximum ammonia removal rate for a post carbon removal nitrifying MBBR at 1°C is 22.8% of the maximum ammonia removal rate at 20°C (Fig 5.3a).

The VAOBRR in the 1.39 $gN/m^2 \cdot d$ loaded reactor is approximately 67% of the VAOBRR of the 0.13, 0.51 and 1.25 $gN/m^2 \cdot d$ loaded reactors. A possible cause of this significant decrease in normalized cellular kinetics is free phase ammonia inhibition. The free ammonia concentration at a pH of 6.99 and temperature of 1°C is 0.022 mgN/L (Abeling and Seyfried, 1992; Furukawa et al., 2009). Although this concentration is significantly less than the reported inhibition level for AOBs at 20°C (Anthonisen et al., 1976; Van Hulle et al., 2010), this research suggests that the effect of free phase ammonia on nitrification kinetics may be exacerbated at 1°C.

Similarly, the VNOBRR of the high loaded reactor (1.39 $gN/m^2 \cdot d$) show an approximate 70% reduction compared to the 0.13, 0.51 and 1.25 $gN/m^2 \cdot d$ loaded reactors. The decrease in VNOBRR of the inhibited reactor does not however indicate inhibition of the NOBs since the oxidation of ammonia is limited and there is an overall lack of nitrite accumulation in the reactor. In the event of free phase ammonia inhibition, these findings suggest that the NOBs are less sensitive to free phase ammonia concentrations at 1°C.

Table 5.2 Average VAOBRR and VNOBRR across temperature and loading rate

SALR ($gN/m^2 \cdot d$)	Biofilm Thickness (μm)	VAOBRR ($gN/m^3 \cdot d$)	VNOBRR ($gN/m^3 \cdot d$)
2.36 ± 0.05	93 ± 20	960 ± 30	3.9 ± 0.4
0.13 ± 0.05	374 ± 24	40 ± 10	2.1 ± 0.7
0.51 ± 0.02	300 ± 17	190 ± 20	5.8 ± 1.2
1.25 ± 0.01	263 ± 15	220 ± 20	12.4 ± 1.2
1.39 ± 0.05	326 ± 24	90 ± 30	20.3 ± 0.2

5.5.5. Gene pathways

The bioinformatic software, PiCrust, predicts the metagenomics functional content from 16S gene sequencing (Langille et al., 2013). PiCrust predicts the KEGG pathways which are subsequently analyzed for differential abundance with LEfSe (Segata et al., 2011). LEfSe analysis allows for binary comparison between two sample groups.

In the context of post carbon removal nitrifying MBBR at 1°C, the identified inhibition point at a loading rate of 1.39 $gN/m^2 \cdot d$ is most important for successful long term operation. Comparing the predicted gene pathways between the 0.51 $gN/m^2 \cdot d$ loaded reactor and the high loaded 1.39 $gN/m^2 \cdot d$ reactor shows that the elevated loading rate enriches the microbial community with various stress response pathways (Fig 5.8a). The enrichment of stress response pathways and altered metabolic processes for survival indicates that the microbial community is in a state of stress and may be inhibited.

To confirm the stress response gene pathway, the 0.51 $gN/m^2 \cdot d$ loaded reactor was compared to the 1.25 $gN/m^2 \cdot d$ loaded reactor. The 1.25 $gN/m^2 \cdot d$ loaded reactor was operating at a free ammonia concentration of 0.017 mgN/L, just below the inhibition

point (Fig 5.8b). This comparison identified few differentially abundant pathways, with the identified pathways being indicative of normal cell function. Hence, post carbon removal MBBR nitrification is feasible at 1°C and stable at the microbial level with an enhanced sensitivity to free phase ammonia concentrations.

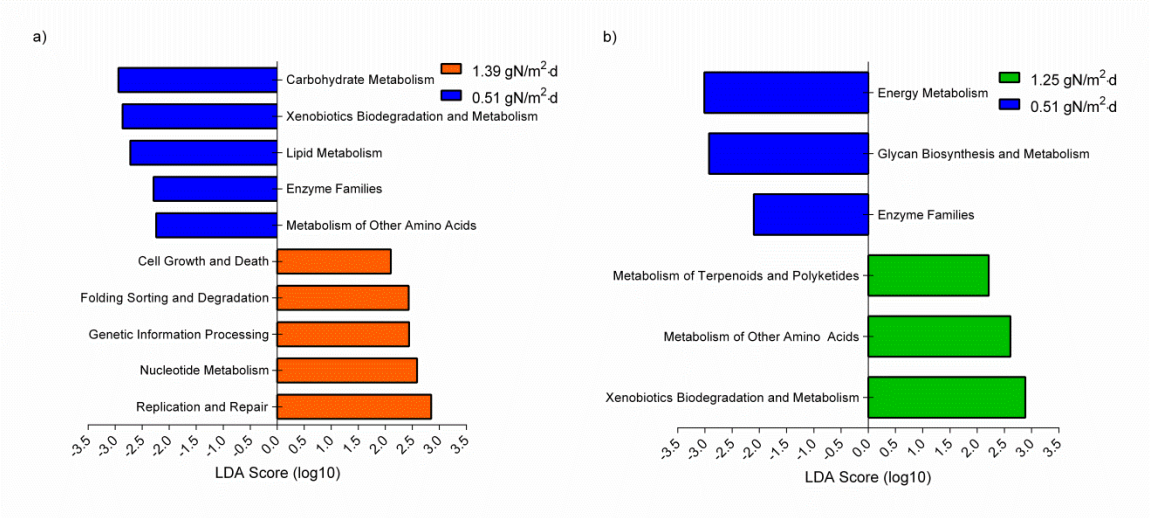

Figure 5.8 Differentially abundant predicted metagenomics pathways, a) 1.39 gN/m^2·d and 0.51 gN/m^2·d, b) 1.25 gN/m^2·d and 0.51 gN/m^2·d

5.6. Conclusion

This study investigated long term performance of post carbon removal MBBR nitrification through the transition from 20°C to 1°C and during long term operation at 1°C. The results show that a nitrifying MBBR system undergoes modest nitrite spikes during rapid temperature changes, which was alleviated after a 10 day acclimatization period. Operation at 1°C achieves nitrification rates that are 22.8% of the maximum ammonia removal rate at 20°C and that may be best approximated by an Arrhenius temperature correction coefficient of 1.086 after steady operation at 1°C. At the highest loading rate, corresponding to a bulk free phase ammonia concentration of 0.022 mgN/L,

the rate of ammonia removal was shown to significantly decrease at 1°C. As such, operation at high loading during low temperature conditions of 1°C may exacerbate the inhibition of AOBs, reduce the ammonia removal rate and subsequently increase the effluent ammonia concentrations of the system. The biomass in all pilot scale MBBR reactors was highly viable and diverse with greater than 2,000 species per sample; with a significant community shift being observed as the reactors transitioned from 20°C to 1°C operation. Although the overall community shifted, the primary AOBs were *Nitrosomonadaceae* and the primary NOB was *Nitrospira* in all reactors at all temperatures. Overall, the study shows that the performance of the post carbon removal nitrifying MBBR systems are enhanced at 1°C by an increase in the viable embedded biomass as well as thicker biofilm. This effectively increases the number of viable cells present during low temperature operation, which in turn partially compensates for the significant decrease in the rate of ammonia removal per nitrifying cell at 1°C.

5.7. Acknowledgements

The authors acknowledge and express thanks to the Natural Science and Engineering Council of Canada and Veolia Water Technologies for their financial support. The authors also thank the city of Gatineau for their support and permission to operate the MBBR pilot at the Masson Angers municipal lagoon treatment facility.

Chapter 6: Biofilm and biomass response of post carbon removal nitrifying MBBR in high loading and extreme low loaded condition

Bradley Young[a], Robert Delatolla[a*], Kevin Kennedy[a], Edith Laflamme[b], Alain Stintzi[c]

[a] Department of Civil Engineering, Faculty of Engineering, University of Ottawa, Ottawa, Canada

[b] Veolia Water Technologies Canada. Montreal, Quebec, Canada

[c] Ottawa Institute of Systems Biology, Department of Biochemistry, Microbiology and Immunology, Faculty of Medicine, University of Ottawa, Ottawa, Canada

6.1. Statement of manuscript status and author contributions

The manuscript “Biofilm and biomass response of post carbon removal nitrifying MBBR in high loading and extreme low loaded condition” is in preparation

Young, B. Operated and maintained the pilot MBBR, performed all constituent, microscopy, library creation and bioinformatics processing. Young, B. wrote and revised the manuscript.

Delatolla, R. was the primary project supervisor, conceived and designed the project, provided direction and feedback on the experiments. Delatolla, R. wrote and revised the manuscript.

Kennedy, K. was a project supervisor, helped conceive and design the project, provided direction and feedback on the experiments.

Laflamme, E. was an industrial collaborator and project supervisor. Laflamme, E. helped conceive and design the project, provided direction and feedback on the experiments.

Stintzi, A. was a project supervisor, provided feedback on the experiments. Stintzi, A. wrote and revised the manuscript.

6.2 Abstract

This study investigates the long term performance of MBBR nitrifying biofilm post carbon removal and secondary settling at high loading and extreme low loaded conditions. At high loading conditions the nitrifying MBBR achieved a maximum SARR of 2.13 $gN/m^2 \cdot d$ with complete conversion to ammonia to nitrate. High loading corresponded to biofilm thicknesses ranging between 54 to 92 μm and optimal biofilm densities between 66 to 103 kg/m^3. The results also show the MBBR technology is capable of maintaining a stable biofilm under extreme low loaded conditions for passive or mechanical plants that nitrify intermittently. The biomass exhibited a higher live fraction of total cells in the high loaded reactors (73 to 100%) as compared to the reactors operated in extreme low loaded condition (26 to 82%). For both the high loaded and extreme low loaded condition, the microbial communities significantly changed with time of operation. The nitrifying community, however, remained steady with *Nitrosomonas* as the primary AOB and *Nitrospira* as the primary NOB. During extreme low loaded conditions, the relative abundance of AOBs decreased and *Nitrospira* increased corresponding to an NOB/AOB ratio of 5.2 to 12.1. Although the next generation sequencing technologies currently do not have a high enough resolution to differentiate at the species level, this study postulates the comammox bacteria may be important to the nitrogen cycle in wastewaters. Additionally, the prevalence of commamox in the biofilm matrix may help prevent nitrifier washout and assist acclimatization during periods of extreme low loading.

6.3 Introduction

Nitrification, the biological oxidation of ammonia to nitrate, is a conventional process used for wastewater treatment. Historically this process has been described as being performed by two distinct groups of autotrophic bacteria in a symbiotic relationship. The first group of bacteria, ammonia oxidizing bacteria (AOB), catalyze the oxidation of ammonia to nitrite. The second group of bacteria, nitrite oxidizing bacteria (NOB), catalyze the oxidation of nitrite to nitrate. Both AOBs and NOBs are inherently slow growing autotrophs and are susceptible to various inhibitory compounds (Fumasoli et al., 2015; Gonzalez-Silva et al., 2016; Lay et al., 2010). Additionally, it is well documented that organic matter is a preferential electron donor (heterotrophic growth) and as such biological BOD removal outcompetes the slower growing nitrifying organisms (autotrophic growth). This competition creates challenges in achieving reliable nitrification in conventional treatment systems.

The process of nitrification can be achieved in suspended or biofilm growth systems. Recently, biofilm systems have been of interest due to their reduced land demand, decreased susceptibility to temperature fluctuations and low energy consumption. The moving bed biofilm reactor (MBBR), which houses biofilm support carriers in constant submersion and suspension, is widely considered one of the most flexible and effective biofilm wastewater treatment technologies (Hem et al., 1994). This technology has been trialed at the lab, pilot and full scale at various locations during the wastewater treatment process to achieve nitrification (Houweling et al., 2007). Previous MBBR studies have investigated integrated biofilm systems into conventional wastewater treatment plants or add-on units between the first and second aerated lagoon in multi-pond facilities

(Delatolla et al., 2010; Sriwiriyarat et al., 2008). These studies were able to nitrify, however, nitrification rates were limited due to high BOD concentrations entering the MBBR systems (Melin et al., 2005). Additional studies with respect to BOD effects on nitrification kinetics conclude that the ideal conditions for nitrification are BOD_5/TKN ratios less than 1 and a bulk liquid BOD_5 concentration less than 20 mg/L (Figueroa and Silverstein, 1992).

The majority of research has been conducted with respect to integrating the MBBR technology prior to secondary settling (Bassin et al., 2012; Jiménez et al., 2012; Lay et al., 2010; McQuarrie and Boltz, 2011). Prior to secondary settling, the high solids concentration has been shown to increase abrasion forces on the biofilm surface (Rusten et al., 2016) and subsequently increase the biofilm detachment rate. Decreasing the abrasion forces through operation after secondary settling could aid maintenance on the carriers. Additionally, it is possible the lack of particulates in a post-secondary nitrifying MBBR can increase the mass transfer of oxygen and nutrients into the biofilm thereby achieving significantly higher removal rates than is currently presented in the literature (Rusten et al., 2016).

One of the challenges with post-secondary nitrification is the variability of wastewater effluents in passive systems in northern and cold climate countries, particularly in aerated lagoons. Although not specifically designed for nitrification, aerated lagoons are capable of nitrifying intermittently. During this nitrification period, an add-on biofilm technology will be starved for substrate having currently unknown impacts on the biofilm morphology and causing stress on the AOB/NOB communities. Hence, the biofilms resistance to extreme low loading and washout remains unknown.

Previous studies using low throughput molecular techniques have identified *Nitrosomonas* as the dominant AOB in design substrate loading, with *Nitrosospira* more prevalent in substrate limiting conditions and *Nitrospira* as the dominant NOB (Bai et al., 2012; Lydmark et al., 2007). More recent studies using next generation sequencing techniques have also identified *Nitrosomonas* to be the dominant AOB, however, have identified species within the genus *Nitrospira* which are capable of complete ammonia oxidation to nitrate (comammox) (Daims et al., 2015; Van Kessel et al., 2015). It is theorized that comammox bacteria are most prevalent in environments with low nitrogen substrates and high dissolved oxygen concentrations (Gonzalez-Martines et al., 2016). Hence, operating an add-on MBBR unit post secondary settling with the increased mass transfer of oxygen and nutrients could promote the growth of AOB, NOB and comammox bacteria to achieve higher rates of nitrification and stabilize the biofilm during extreme low loading conditions.

This study aims to determine the maximum removal rates for post-secondary and post carbon removal MBBR nitrification and determine the impact of prolonged extreme low loaded conditions. This study investigates the impacts of high loading and extreme low load on the biofilm morphology, cell viability and full characterization of the microbial communities embedded in the biofilm with the use of next generation sequencing.

6.4 Material and methods

6.4.1 MBBR pilot

An MBBR pilot was installed at the Masson-Angers four pond aerated lagoon treatment plant (Gatineau, Quebec, Canada). The pilot was configured with two parallel

treatment trains, each with two reactors in series (Fig 6.1). The first two reactors in series, A reactors, were fed with treated wastewater from the last lagoon to simulate a post BOD removal and secondary settling add-on unit. The non-nitrogenous effluent constituents from the last lagoon were relatively stable soluble chemical oxygen demand (SCOD) of 31.6 ± 1.8 mg/L, pH of 7.2 ± 0.1 and alkalinity of 153 ± 1.9 mg$CaCO_3$/L. The second reactors in series, B reactors, were fed with the effluent of the A train reactors. Hence, the B train reactors were operated in extreme low loading conditions simulating wastewater treatment systems that intermittently nitrify prior to post carbon removal and secondary settling nitrifying add-on units.

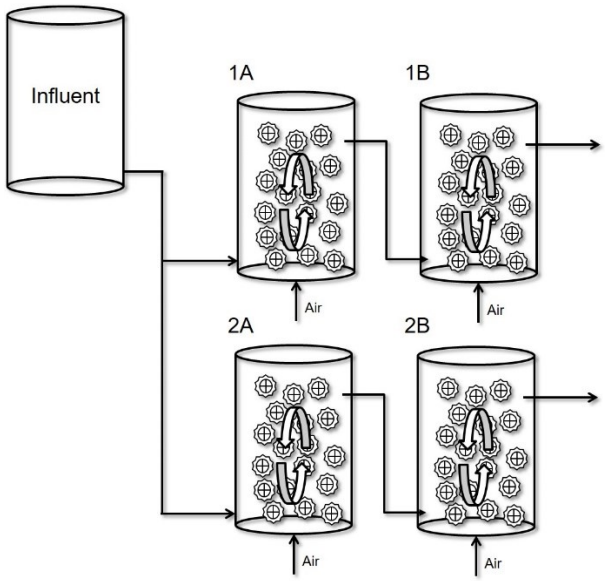

Figure 6.1 Reactor configuration and experimental set-up

All four reactors had a reactor volume of 223 L and were filled with AnoxKaldnes K5 carriers. These carriers have a bulk specific surface area of 800 m^2/m^3, a diameter of 25 mm and a depth of 4 mm. The carriers were initially seeded from a full scale IFAS reactor and underwent a start-up phase for two months to acclimatize for post carbon

removal and secondary settling operation. After the start-up phase, operation was maintained for a total of 126 days at a hydraulic retention time (HRT) of 1.5 h with two steady state runs defined by ± 10% effluent ammonia. During run 1, the influent to the A reactors was fed with natural lagoon effluent, corresponding to 19.8 ± 0.4 mgNH_4-N/L. During run 2, to achieve higher rates without adjusting the HRT, the influent ammonia was augmented to 25.4 ± 0.3 mgNH_4-N/L with concentrated ammonium sulfate. Ammonia augmentation was performed with a peristaltic pump directly into an equalization tank prior to feeding into the MBBR reactors. In both runs, the B reactors were fed 100% effluent from the A reactors. The airflow rates into the MBBR reactors were adjusted to ensure adequate mixing of the carriers. This airflow rate corresponded to dissolved oxygen (DO) concentrations between 4 to 6 mg/L in each reactor.

Table 6.1 Operational conditions for each reactor during each experimental run

Reactor	Influent Ammonia (mgNH_4-N/L)	Influent TSS (mg/L)	Loading Rate (g$N/m^2 \cdot d$)
1A (Run 1)	19.8 ± 0.4	2.2 ± 1.2	1.82 ± 0.04
1A (Run 2)	25.4 ± 0.3	2.2 ± 0.7	2.32 ± 0.03
2A (Run 1)	19.8 ± 0.4	2.2 ± 1.2	1.33 ± 0.03
2A (Run 2)	25.4 ± 0.3	2.2 ± 0.7	1.71 ± 0.02
1B (Run 1)	1.2 ± 0.1	3.4 ± 3.0	0.11 ± 0.01
1B (Run 2)	3.9 ± 0.3	4.9 ± 3.8	0.36 ± 0.03
2B (Run 1)	0.9 ± 0.1	1.9 ± 1.6	0.06 ± 0.01
2B (Run 2)	1.6 ± 0.1	3.0 ± 2.2	0.11 ± 0.01

6.4.2 Cell viability

Five replicate carriers were harvested from all four reactors during run 1 and run 2. The interior supports were cut to expose the biofilm for staining. The exposed biofilm was stained with a working solution (SYTO9 and propidium iodide) of live and dead viability cell staining (Life Technologies, USA). After 30 minutes of staining, the biofilm extracellular polymeric substance (EPS) was stained with calcofluor white (Sigma-Aldrich, USA) for 1 minute. Immediately after staining, the images were analyzed with a Zeiss LSM510/Axio imager M.1 confocal microscope (Carl Zeiss, Canada) with a 63x water immersion objective. A minimum of 20 images were acquired across the entire biofilm support media at various biofilm depths per reactor per run. Cell viability analytical quantification was performed using NI Vision Assistant 7.1 software (LabView 8.0, National Instruments, Canada) (Delatolla et al., 2009b).

6.4.3 Biofilm thickness and mass

Four replicate carriers were harvested from all four reactors during run 1 and run 2. Within four hours of harvesting, the carriers were imaged on a Tescan Vega II-XMU variable pressure scanning electron microscope (VPSEM) at a pressure of 40 Pa and ×60 magnification (Tescan USA Inc., USA). To minimize the potential effects of biofilm dehydration the maximum exposure duration for a carrier was 15 minutes. During this exposure time, five images across the entire carrier were captured corresponding to 20 total images per condition. The acquired images were analyzed for thickness on an Axio Vision LE software (Carl Zeiss, Canada) resulting in a total of 90 thickness measurements per condition (Delatolla et al., 2009b).

Five replicate carriers were harvested all four reactors during run 1 and run 2. Within 4 hours of harvesting the carriers were placed in a drying oven at 105°C overnight. After the drying period, the carriers were allowed to cool in a desiccator for twenty minutes and their weight was recorded (W1). The dried carriers were then thoroughly cleaned with warm water and a stiff bristled brush. The clean carriers were then placed in a drying oven at 105°C overnight. The clean and dried carriers were allowed to cool in a desiccator for twenty minutes and their weight was recorded (W2). The mass of biofilm is then the difference between W1 and W2 (Delatolla et al., 2008).

6.4.4 Next generation DNA sequencing and analysis

Five replicate carriers were harvested from all four reactors during run 1 and run 2. Within 2 hours of harvesting, 25 mg of wet biofilm was extracted into 1.5 mL sterile ependorf tubes. DNA was extracted using FastDNA Spin Kit (MP Biomedicals, US). The extracted DNA was stored at -20°C until all the samples were ready for library construction. Library construction was performed with a two-step polymerase chain reaction (PCR) targeting the V6 hyper-variable region of the 16S rRNA gene as described by Young et al. (2016a). The final library was sent to The Centre for Applied Genomics (TCAG) and sequenced on an Illumina HiSeq 2500.

The Illumina HiSeq 2500 generated 2x100 base paired-end reads which were assembled using the Fast Length Adjustment of Short reads (FLASH) software (Magoč and Salzberg, 2011). The assembled reads were quality filtered using the Fastx toolkit with a minimum quality score of 20 over 90% of the sequences. The high quality reads were demultiplexed and the barcodes were trimmed using Novobarcode (Goecks et al., 2010). The trimmed reads were assigned operational taxonomical units (OTUs) against

the Greengenes database 13.8 with a closed reference strategy at 97% sequence similarity. The OTU table was then filtered for singletons and doubletons and ready for downstream analysis. The Quantitative Insights into Microbial Ecology (QIIME) software was used to determine diversity and summarized taxa. Species diversity between the groups was determined with weighted and unweighted UniFrac distant beta diversity (Blankenberg et al., 2010; Goecks et al., 2010). All samples were sequenced on the same sequencing run to reduce variance from sequencing bias.

6.5 Results and discussion

6.5.1 Nitrification

Post carbon removal MBBR nitrification was monitored via the testing of the influent and effluent concentrations for ammonia, nitrite and nitrate (Fig 6.2a-c). The A reactors (first reactors in series), had the highest ammonia loading rates throughout the study. The first run was fed with lagoon effluent, ranging from 18.4 to 20.7 mgNH_4-N/L, which corresponded to SALRs of 1.33 (2A) and 1.82 (1A) g$N/m^3 \cdot d$. At these SALRs, the effluent ammonia concentrations were maintained below 2 mgNH_4-N/L (Fig 6.2a). This corresponds to surface area removal rates (SARRs) of 1.27 and 1.70 g$N/m^2 \cdot d$ respectively. Additionally, the conversion of ammonia to nitrate was complete with less than 0.25 mgNO_2^--N/L (Fig 6.2b) and less than 10% mass balance error.

After steady operational data was acquired, the influent ammonia was augmented to 25 mgNH_4-N/L over a period of 17 days. After 26 days of operation at 25 mgNH_4-N/L, contamination in the ammonium sulfate caused significant inhibition of the nitrifying

biomass. A new batch of ammonium sulfate was acquired and augmentation was resumed.

Run 2 was operated at SALRs of 1.71 (2A) and 2.32 (1A) $gN/m^2 \cdot d$. Operation at 1.71 $gN/m^2 \cdot d$ (2A) produced statistically equivalent performance with respect to ammonia conversion to nitrate at the same loading rate during run 1 (1A) (Fig 6.2a). Hence, the ammonia removal rate is consistent over time and the nitrifying biofilm was able to recover from short term inhibition. The highest loaded reactor, 2.32 $gN/m^2 \cdot d$ (1A), showed a decrease in ammonia removal efficiency with an average effluent ammonia concentration of 3.8 ± 0.3 $mgNH_4$-N/L. This reactor also corresponded to the highest effluent nitrite concentrations 0.22 ± 0.01 $mgNO_2^-$-N/L. It is important to note, this nitrite concentration is still below inhibitory thresholds for AOBs and NOBs as well as toxicity thresholds for aquatic life (Anthonisen et al., 1976; Van Hulle et al., 2010).

Using the removal rates of the A reactors, the maximum attainable removal rate achieved in the post carbon removal nitrifying MBBR system was 2.13 $gN/m^2 \cdot d$. This removal rate is significantly higher than the conventional design rates of 1.0 $gN/m^2 \cdot d$ and significantly higher than the previously determined maximum rate pre secondary settling (Rusten et al., 2006). In pre secondary settling applications, the TSS is often greater than 100 mg/L which results in abrasion forces on the biofilms and the adherence of particulates onto the biofilm surface. By operating post secondary settling, with an average 2.2 mg/L of TSS entering the reactor, there were less interactions of solids at the biofilm surface. As such it is likely there was a more efficient mass transfer of oxygen and nutrients into the biofilm and potentially a more active biomass.

The B train reactors (second reactors in series) is representative of a system that nitrifies intermittently. In this case, the nitrifying MBBR is subject to substrate stress and is at risk of nitrifier washout. During the extreme low loading periods in this study the SARRs were limited by effluent low influent ammonia concentrations and effluent ammonia below 1 mgNH_4-N/L. Overall, the average removal efficiency was 57% with effluent ammonia concentrations of 0.76 mgNH_4-N/L. In essence, the extreme low loaded reactors maintained a nitrifying biomass and acted as a polishing unit. In all reactors the effluent nitrite was near the detection limit of 0.01 mgNO_2^--N/L and there was less than 10% mass balance error.

With operation after secondary settling, the effluent TSS must be below a certain threshold or incorporate a tertiary solids removal step. In this study, the average effluent TSS yield from the A reactors was 0.16 ± 0.05 gTSS/gN removed. At this TSS yield, an MBBR removing 25 mgNH_4-N/L produces 4.0 ± 2.0 mgTSS/L. In the B reactors, there was no significant increase in TSS, which was expected due to the low influent ammonia into the reactor. The lack of TSS production does indicate the nitrifying biomass was not actively sloughing and washing out of the system. Hence the major indicator of effluent TSS production in a post carbon removal and secondary settling MBBR is the concentration of ammonia oxidized. The need for a post MBBR settling unit will be specific to each applications discharge permits and upstream solids removal efficiency.

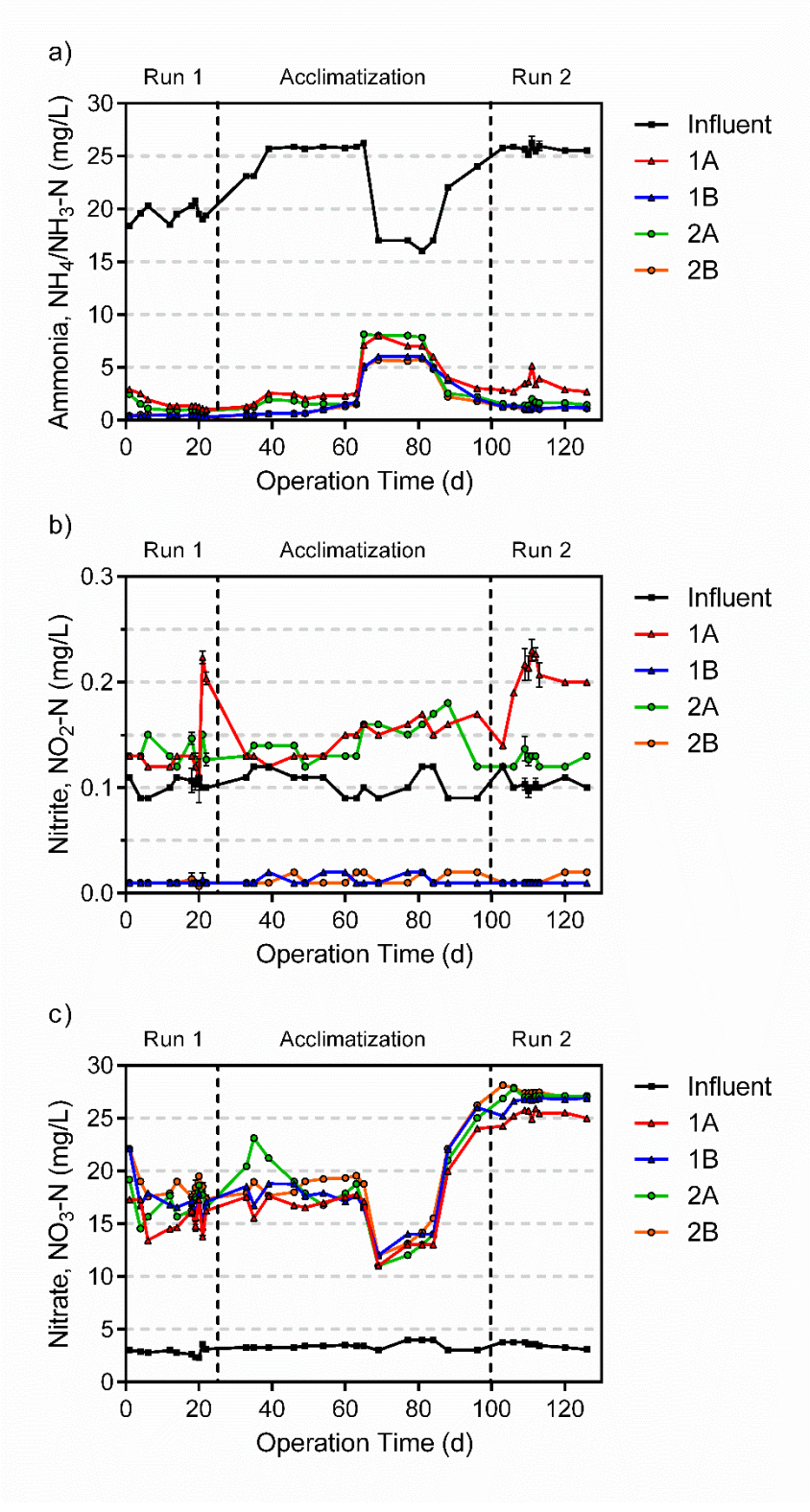

Figure 6.2 Post carbon removal MBBR nitrification over the time of operation expressed with constituents a) ammonia, b) nitrite, c) nitrate

6.5.2 Biofilm characterization

During steady state operation of run 1 and run 2 the biofilm was characterized for thickness and mass. The biofilm thickness and mass in the A reactors (first reactors in series in trains 1 and 2) ranged from 54 to 92 μm and 7.7 to 10.6 mg/carrier respectively (Fig 6.3). Conversely, the biofilm thickness and mass in the B reactors (second reactors in series) ranged from 25 to 33 μm and 2.2 to 4.3 mg/carrier respectively (Fig 6.3). For both trains, the A and B reactors thicknesses and mass corresponded to biofilm densities of 55 to 103 kg/m^3, which is in the predicted range for nitrifying biofilms (Laspidou and Rittmann, 2004). Additionally, these biofilm densities are near the optimal density of 75 kg/ m^3 for substrate uptake that was identified in biofilm systems by previous studies (Tanyola and Beyenal, 1997).

The biofilm thickness for the A train did not significantly change with loading rate or time of operation. The similar loading rates of 1.82 (1A run 1) and 1.71 gN/m^2·d (2A run 2) as well as the highest loading rate of 2.32 gN/m^2·d (1A run 2) and lowest loading rate 1.33 gN/m^2·d (2A run 1) were not significantly different with respect to thickness. The biofilm mass for the A reactors did change based on reactor and time of operation, however, increased in thickness from run 1 to run 2 in train 1 while decreasing in thickness in train 2. Thus, operating a post carbon removal nitrifying MBBR at conventional to maximum loading rates does not clearly impact the biofilm characteristics or demonstrate a link to ammonia removal efficiency.

The carriers in the B reactors (second reactors in series) started with the same seeded carriers on the first day of operation as the A train reactors (first reactors in series). After 20 days of operation (run 1), the biofilm thickness of the B reactors lost approximately

50% of the biofilm thickness and mass as compared to the A reactors. After 100 days of operation in low ammonia loaded operation the biofilm thickness of the B reactors decreased by an additional 16.8% while the biofilm mass decreased by an additional 36.1%. Although both the biofilm thickness and mass decreased, there wasn't an observed TSS spike in the reactor effluent. Assuming the detachment rate was steady over the 100 day extreme low load period, the observed loss of biofilm would account for a TSS production of 0.10 mg/L·d. This TSS production from biofilm loss is below the detection limit for standard methods and indicates the biofilm remains stable during prolonged extreme low loading periods.

Qualitative assessments of the biofilm morphology indicated the A reactors showed more rough biofilms, whereas the B train reactors showed more smooth biofilms (Fig 6.4). This morphology was represented in the variance in the biofilm thickness measurements (Fig 6.3). Additionally, the variance in thickness measurements did increase in the A train from the lowest SALR of 1.33(2A run 1) to the highest SALR of 2.32 $gN/m^2 \cdot d$ (1A run 2). Previous authors have described an optimal morphology for nitrifying biofilms as rough, thin and evenly distributed which promotes efficient mass transfer of oxygen and ammonia into the biofilm (Li et al., 2015). Although there isn't a quantifiable measurement for optimal variance in biofilm thickness, the results of this study show the biofilm morphology in post carbon removal and secondary settling MBBR systems is relatively stable up to the maximum SARR of 2.13 $gN/m^2 \cdot d$. For a period of over 120 days, the biofilm did not undergo significant sloughing and the ammonia removal rates were consistent.

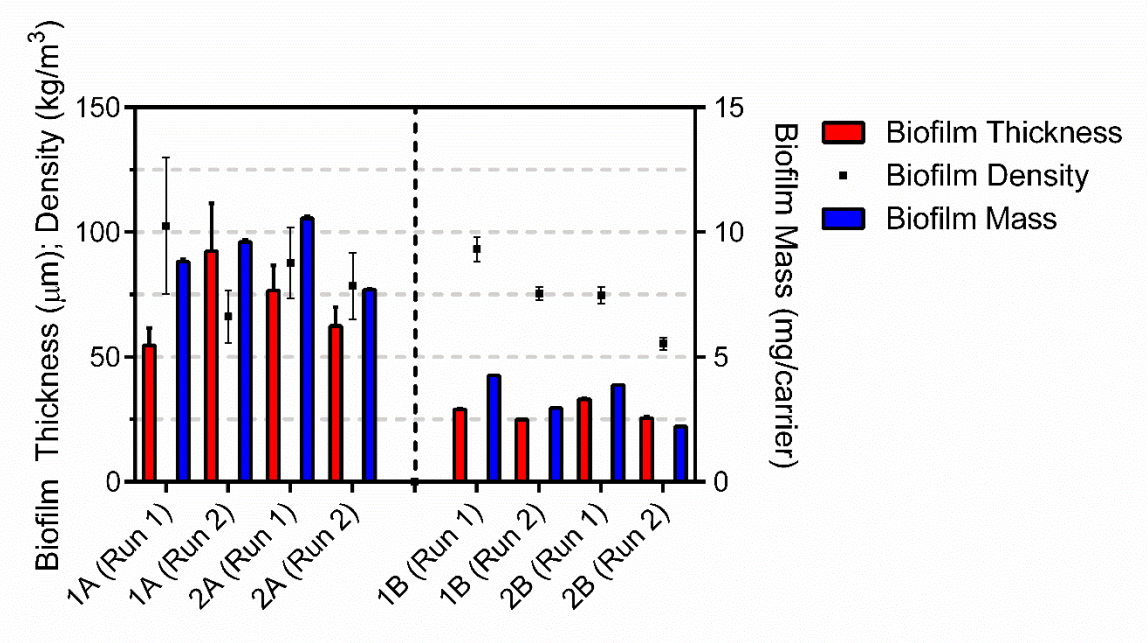

Figure 6.3 Biofilm thickness with standard deviation (n=90), biofilm density with standard deviation (n=5) and biofilm mass with standard deviation (n=5) for each reactor during steady state operation in the experimental runs

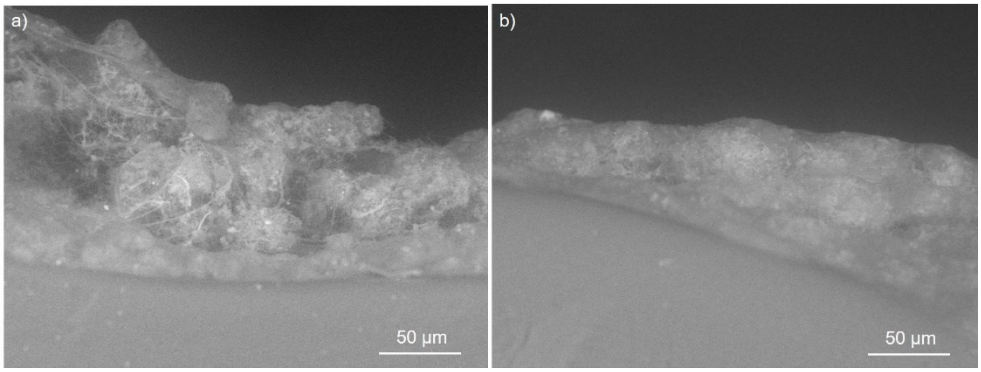

Figure 6.4 Representative VPSEM images at ×500 magnification for qualitative assessment of biofilm morphology in a) A reactors and b) B reactors

6.5.3 Cell viability

The biofilm was stable from a thickness and mass perspective, however, the biomass embedded in the biofilm is ultimately responsible for the reactor performance. Overall the median cell viability ranged from 73 to 100% in the A reactors and from 26 to 82% in

the B train (Fig 6.5). The cell viability was likely affected by available ammonia and the specific embedded microbial communities.

In the A reactors, the viabile cells as a fraction of total cells did not show significant changes with loading rate (Fig 6.5a). This finding is consistent with previous studies investigating the viability of nitrifying biofilms (Chae et al., 2012). The viability of the biofilm with respect to total cells, however, did show a significant decrease with time of operation from run 1 to run 2 ($p < 0.0001$) (Fig 6.5a). The decrease in percentage of total cells that are viable over time was likely due to the maturation of the biofilm on the carriers (Hoang et al., 2014a). The biofilm in run 1 was newly formed and acclimatized for post carbon removal nitrification. As the biofilm matured, the average viable cell coverage per biofilm area increased (Fig 6.5b). This indicates that although the embedded biomass shows a higher fraction of non-viable cells relative to the total number of cells across operation time, the overall density of embedded cells increased per biofilm area and subsequently the quantity of embedded viable cells in the biofilm increased with time. This maturation process also demonstrated a greater variance in live cell coverage for both fraction of total cells and per biofilm area. This variance could be attributed to the roughness of the biofilm and subsequent impact on the localized mass transfer of nutrients (Herrling et al., 2015). Hence, the microbial viability was dependent on biofilm maturation, however in all cases, nitrification was unaffected.

The B reactors also demonstrated a reduction in cell viability as a fraction of total cells with time of operation, with this effect being exacerbated in the extreme low loaded conditions. Specifically, reactor 1B demonstrated a 45% reduction in cell viability as a fraction of total cells from run 1 to run 2 after 100 days of operation. This reduction,

contrary to the A train reactors, did not correspond to an increase in live cell coverage per biofilm area with respect to time of operation. The steady live cell coverage per biofilm area in extreme low loaded condition indicated the biomass were in preservation rather than proliferation. Additionally, it has been shown the mass transfer of nutrients in smooth biofilms is less efficient but more uniform (Li et al., 2015). Qualitatively the B reactor biofilm were smooth (Fig 6.4) thus decreasing the variability of cell density at various locations in the biofilm. Overall, operation for over 120 days in extreme low loaded conditions in a post carbon removal nitrifying MBBR maintained biofilm on the carriers and a viable biomass to nitrify when influent ammonia concentrations increase.

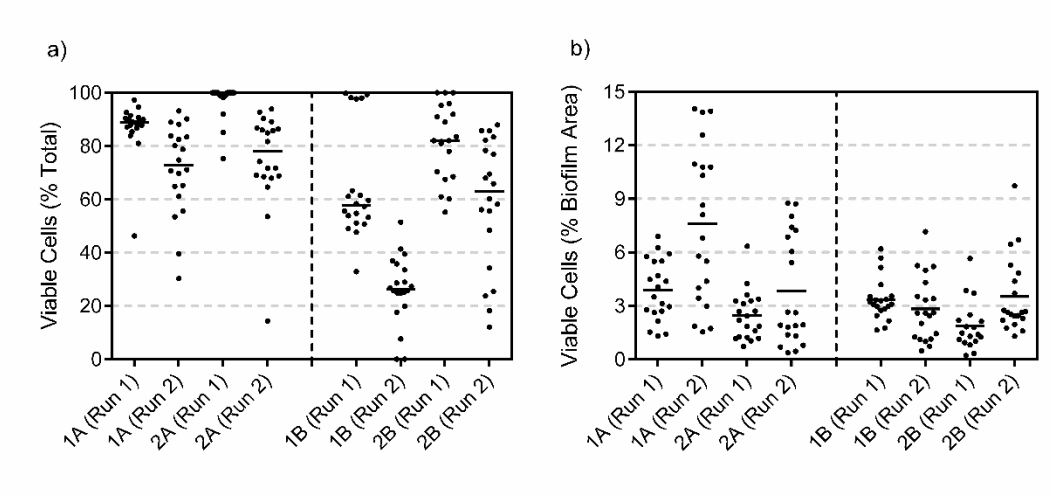

Figure 6.5 Cell viability for each reactor during steady state operation in the experimental runs where each data point represents the live fraction of total cells of a random piece of biofilm (n=20) a) viability as a fraction of total cells, b) viability as a fraction of biofilm area

6.5.4 Microbial community diversity

The microbial community was investigated with next generation 16S-rDNA based Illumina sequencing to fully understand the impacts of long term post carbon removal nitrifying MBBR operation. For this study, a total of 25,605,064 high quality reads were

generated with an average of 775,911 ± 334,028 high quality reads per sample. Principal coordinate analysis (PCoA) was performed on all the samples to determine if the microbial community shifts with respect to the reactors and time of operation. For this analysis, PCoA is used on the unweighted (no relative abundance) and weighted (with relative abundance) UniFrac distances to assess the microbial population shifts.

The microbial communities in the post carbon removal nitrifying MBBR did not clearly separate based on loading rate (Fig 6.6a, b). The repeated loading rates (1A Run 1 and 2A Run 2), which exhibited similar removal rates and biofilm morphology (Fig 6.2 and 6.3), were comprised of significantly different microbial communities. This was also observed in the B train reactors, where all four time points operated in low ammonia conditions were not all clustered together. Instead, the microbial communities for all the reactors separated based on time of operation. Specifically, the microbial communities in Run 1 and Run 2 clustered together irrespective of loading rate (Fig 6.6c,d).

Previous studies identified loading rate as a primary driver of microbial diversity in lab scale reactors fed with consistent synthetic wastewater (Young et al., 2016a). In real systems, however, the microbial community is subject to significantly greater variability in the wastewater feed and underwent the biofilm maturation process. The combined effect of wastewater variability and biofilm maturation in this study was the primary driver in community shifts for both the unweighted and weighted PCoA. Although this analysis does not isolate the organisms responsible for the microbial community shift, it does indicate the microbiota in the nitrifying biofilm was complex and constantly changing. These changes were occurring without significantly affecting the nitrification process.

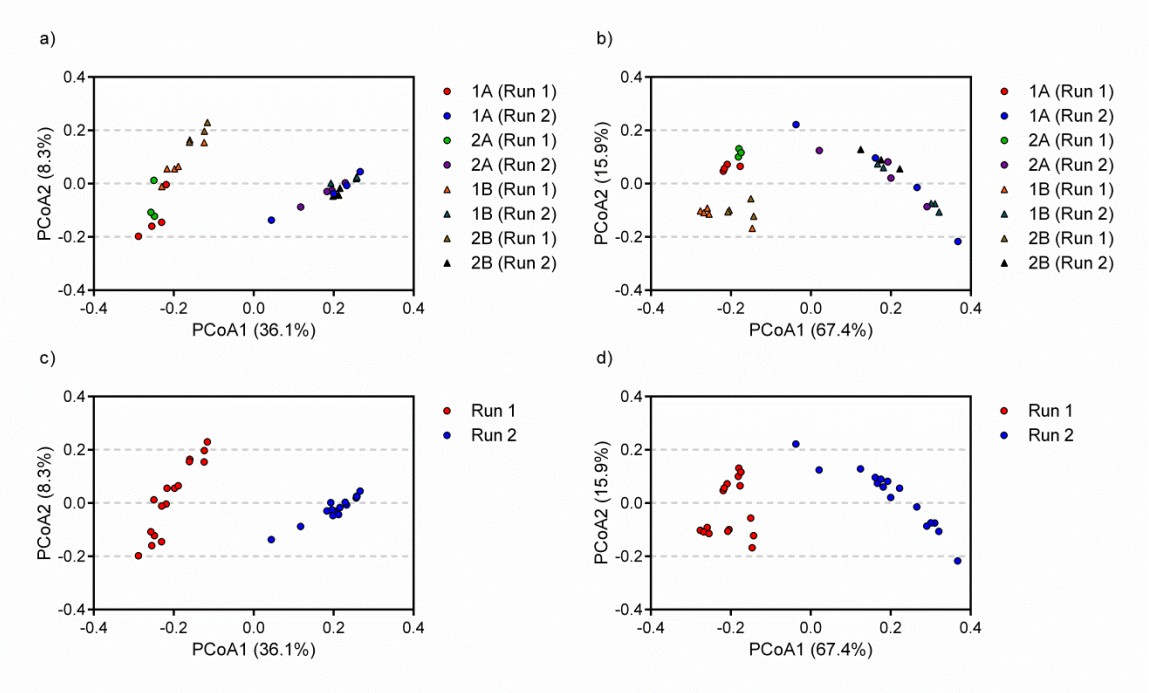

Figure 6.6 PCoA for the entire microbial population in a) unweighted all samples, b) weighted all samples, c) unweighted isolating Run 1 and Run 2, d) weighted isolating Run 1 and Run 2

Analyzing the taxonomical changes in the microbial communities showed all samples contained the same 52 unique *phyla* with the same 10 *phyla* representing at least 1% relative abundance (Fig 6.7). As expected from the PCoA, the microbial diversity was significantly changed with respect to time of operation. In both the A and B reactors, run 1 was primarily comprised of *Bacteroidetes*, *Nitrospirae*, *Proteobacteria* and *Planctomycetes*. Throughout the 80 days of operation from run 1 to run 2, the *Planctomycetes*, *Bacteroidetes* and *Acidobacteria phyla* were significantly decreased in relative abundance which corresponded to an enrichment in *Fusobacteria* and *Firmicutes.* Specifically, *Fusobacteria* on average increased from 1.0 ± 1.2% during run 1 to 10.5 ± 4.6% during run 2 ($p < 0.01$).

Fusobacteria are obligate anaerobic gram-negative bacilli, hence the bacteria belonging to this *phylum* require dissolved oxygen depletion within the biofilm. This penetration depth was exceeded for the A train reactors and near the critical point in the B train reactors for both Run 1 and Run 2 (Fig 6.3). It is important to note, the seeded biofilm underwent an initial sloughing period during the start-up phase. This sloughing period was followed by biofilm regrowth, stabilization and steady state nitrification prior to run 1. With the lack of sequences aligning to anaerobic bacteria in run 1, it is likely the anaerobic bacteria had not been established within the biofilm. After 100 additional days of operation, the obligate anaerobic bacteria were able to establish and survive within the biofilm matrix. These bacteria are not critical to the nitrification process, however, their presence indicates a dynamic process with changes in microbial composition within the biofilm matrix in response to varying conditions. Change in microbial composition likely helps stabilize and maintain the biofilm matrix (Flynn et al., 2016).

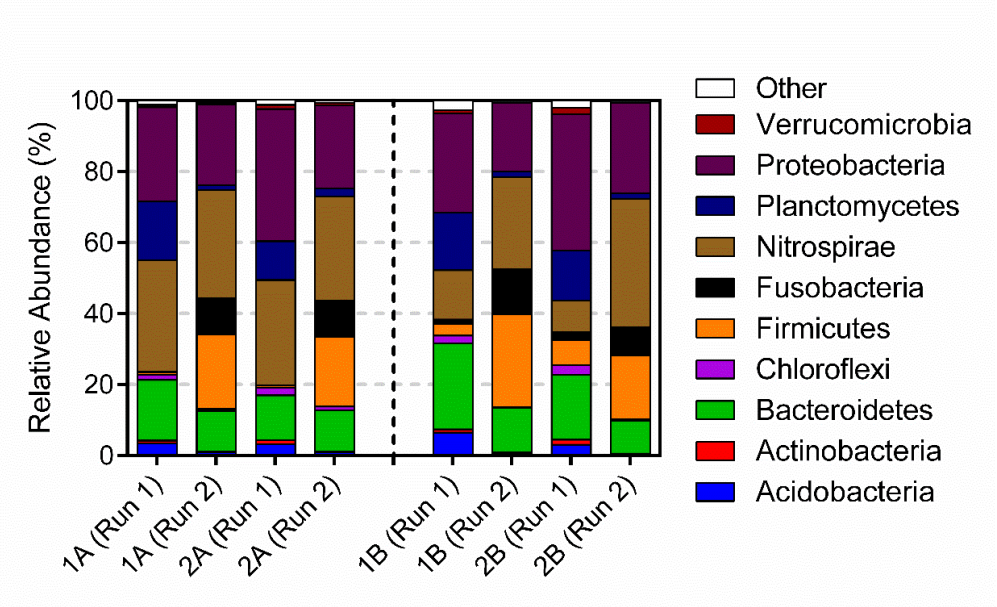

Figure 6.7 Relative abundance at the phylum level for each reactor during steady state operation in the experimental runs (n=5)

6.5.5 AOB and NOB communities

In all reactors for both run 1 and run 2 the primary AOBs were within the family *Nitrosomonadacea*, with *Nitrosomonas* as the primary genera responsible for ammonia oxidization. The genera *Nitrosococcus and Nitrosovibirio* were detected, however these genera were of negligible relative abundance. In this study *Nitrosospira*, a suspected wastewater AOB in nitrifying systems, was not detected. In all reactors and sampling points the primary NOBs were in the genera *Nitrospira.* The genera *Nitrobacter* was detected, however was of negligible relative abundance.

Grouping the known AOB taxa showed there isn't a significant difference in AOB relative abundance in the A reactors across loading rate or time of operation with an average relative abundance ranging from 5.8 to 11.0% (Fig 6.8). The A reactors, were consistently in a high loaded condition and as such it is probable the AOB communities reached their maximum relative abundance. Similar to the AOB profile, grouping the NOBs did not show a significant difference in relative abundance in the A reactors with relative abundance ranging from 29.5 to 31.4%. This resulted in NOB/AOB ratio in the A reactors ranged from 2.8 to 5.4.

The B reactors which were in an extreme low loaded condition corresponded to an average AOB relative abundance between 1.1 to 5.3%, which is significantly lower than the A reactors ($p < 0.001$). Conversely, the B reactors demonstrated an increase in NOBs from Run 1 to Run 2 with average relative abundances ranging from 9.1 to 36.3% ($p < 0.001$). The increase in NOB relative abundance resulted in NOB/AOB ratios from 5.2 to 12.1. This increase in NOB/AOB ratio during AOB stress is contrary to previous research

in suspended growth systems. In suspended growth systems it is common during AOB stress to have significant NOB washout and nitrite buildup (Graham et al., 2007).

Previous granule studies with complete nitrification (lack of nitrite accumulation) have shown average NOB/AOB ratios of 3 to 4 with a theoretical nitrite oxidizing capacity three times higher than ammonia oxidizing capacity (Mozumder et al., 2014; Winkler et al., 2012). This finding was postulated to be due to a nitrite oxidation/nitrate reduction loop (nitrite loop) within the granule structure. In this study however, the post carbon removal MBBR system is absent carbon for a nitrite loop to occur.

Daims et al. (2015) presented the first empirical evidence that species within the genus *Nitrospira*, the most prevalent NOB in this study, are capable comammox bacteria. The first study investigating comammox bacteria in wastewater treatment plants could not determine the prevalence of comammox in activated sludge plants, however, postulate the bacteria preferentially occur in low substrate and high dissolved oxygen environments (Gonzalez-Martines et al., 2016). In our study, both the A and B reactors were composed of a higher relative abundance of *Nitrospira* than AOBs. The ratio of *Nitrospira* to AOB relative abundance increased during operation in extreme low loaded condition indicating nitrification was possibly supplemented by comammox bacteria. Hence it is possible in this study there was a mix of conventional NOBs and comammox bacteria. Although the next generation sequencing technologies currently do not have a high enough resolution to differentiate at the species level, this study suggests the comammox bacteria may be important to the nitrogen cycle in wastewaters. Additionally, the prevalence of commamox in the biofilm matrix may help prevent nitrifier washout and assist acclimatization during periods of extreme low loading.

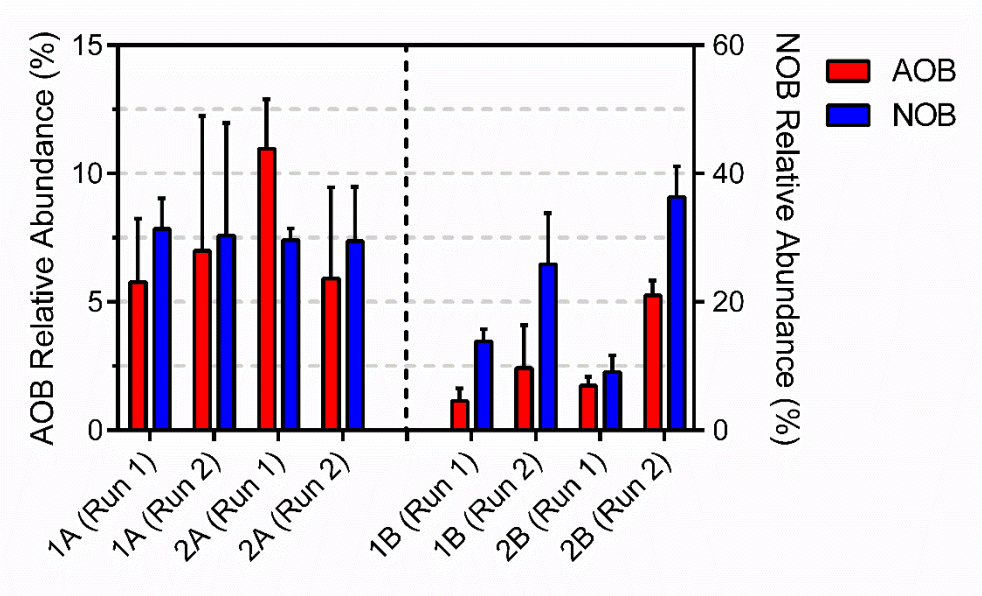

Figure 6.8 AOB and NOB relative abundances with standard deviation (n=5) for each reactor during steady state operation in the experimental runs. Note there is a significant scale difference between the left and right hand y-axis.

6.6 Conclusion

This study investigated installing a nitrifying MBBR post settling and carbon removal in high loading and extreme low loading conditions. At high loading a maximum SARR of 2.13 $gN/m^2 \cdot d$ was achieved. The high rate of removal was attributed to low TSS in the influent which thereby decreased particle attachment to the biofilm surface and increased the rate of mass transfer of oxygen and nutrients into the biofilm. The biofilm maintained a stable thickness and the biomass remained highly viable throughout the 130 day operational period. This demonstrated the long term efficiency and performance of treatment. In extreme low loaded condition, the results show the MBBR acted as a polishing unit. The biofilm thickness and cell viability reduced over the 130 day operational period, however, the system remained stable. In all conditions, the AOB and NOB communities were present with peripheral organisms stabilizing the biofilm matrix.

6.7 Acknowledgments

The authors thank the Natural Science and Engineering Council of Canada and Veolia Water Technologies for their financial support. The authors also thank the city of Gatineau for their support and permission to operate the pilot plant at the Masson Angers municipal lagoon treatment facility.

Chapter 7: Discussion and Conclusion

7.1 Discussion and conclusions

This study has performed an in-depth characterization of the MBBR technology applied as a nitrifying add-on unit to receive the final effluent of wastewater treatment plants. In passive wastewater treatment systems, particularly in the northern climate regions, the final effluent may potentially vary seasonally. Seasonal changes include variation in ammonia concentrations, with the possibility of low concentrations during the summer months, as well as temperatures reaching 1°C in the winter months. Thus, the installation of an add-on unit faces challenges with respect to maintaining a stable biomass to achieve target effluent ammonia concentrations throughout the year.

7.1.1 Ammonia removal

In this study the application of the MBBR technology was located at the effluent of the last lagoon in series. At this location, design challenges include reduction of kinetic rates with respect to temperature and potential extreme low loaded conditions from intermittent nitrification in the lagoons during the summer months. Particularly, the challenges include maintaining the kinetic rates by maintaining a stable biofilm preventing nitrifier washout during seasonal changes. These challenges were addressed throughout the two year pilot operation where this work effectively created the first design curve for the limited kinetic rates at 1°C (Chapter 4) as well as demonstrated the robustness of the biofilm and biomass during the summer and transitory conditions (Chapters 5 and 6). Additionally, all of the acquired data for reactor 2A was collated to assess the long term sustainability of the MBBR technology from start-up through the

end of the second year of operation. This reactor is highlighted in this discussion as it was the first reactor in series and was operated most closely to design standards.

From the data acquired in reactor 2A (Figure 7.1), it is clear the MBBR technology achieved high quality effluents near or below 5 mgN/L for nearly two years of consecutive operation even with variable loading rates and HRTs as outlined in the previous chapters. The elevated ammonia concentrations during feed contamination (days 156 to 172) and the cold temperature data (days 250 to 400) were discussed in previous chapters. The following year (days 400 to 607) was used to validate a design load of 500 $gN/m^3 \cdot d$ during the summer months as well as the maximum attainable removal rate at 1°C. On the 581st day of operation, the oxygen valve to the reactor malfunctioned and the reactor was anoxic for nearly a week prior to acquiring the necessary parts to fix the valve. As a result, the effluent ammonia temporarily increased, however, within two weeks the system was operating at full capacity. Immediately following the low DO event the temperature rapidly dropped reaching 1°C on the 645th day of operation. Operation at 1°C remained stable for 18 days and achieved a maximum removal rate of 220 $gN/m^3 \cdot d$, thus confirming the maximum rate in Chapter 4. Unfortunately, the feed line to the pilot froze and even with multiple attempts to thaw the line as well as installing a new line, the pilot was unable to be restarted. As such, we weren't able to complete a secondary 1°C pilot study, however, were able to confirm the process was repeatable with respect to the transition into cold temperatures up to the maximum attainable removal rate.

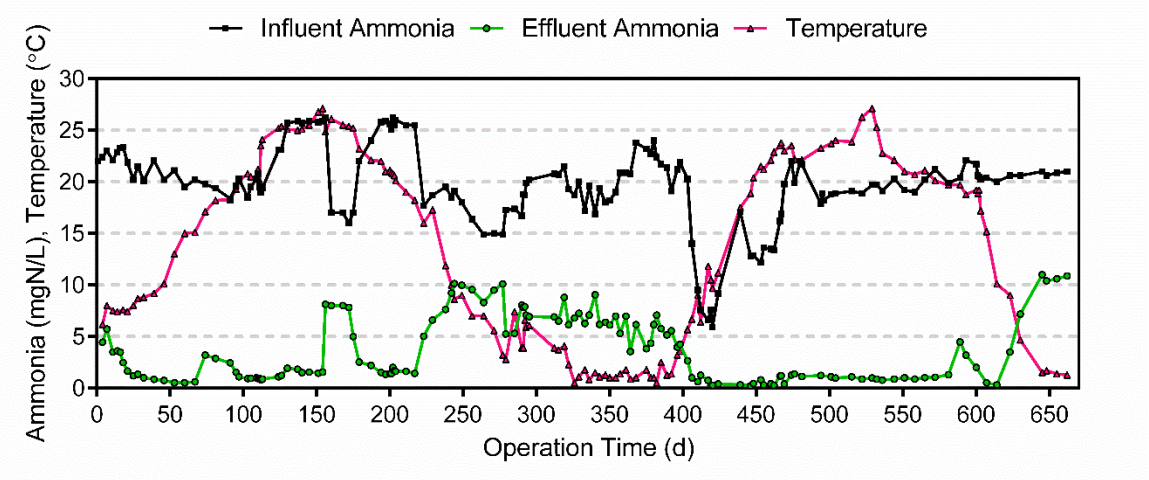

Figure 7.1 Timeline of pilot operation from start-up to demobilization of reactor 2A

7.1.2 Biofilm and biomass

In addition to the effluent ammonia, the biofilm thicknesses and ammonia relative abundances further demonstrated the MBBR technology is robust and is capable of adapting to the varying conditions experienced in the northern climate regions. At the end of the start-up phase (Chapter 2), the biofilm stabilized at 200 µm at 10°C. The remainder of the pilots operation demonstrated the biofilm thickness decreased in the warm temperatures (near 20°C) to a minimum of 62.4 µm up to a maximum of 300 µm at 1°C. From an operational perspective, the selected MBBR carriers must have suitable pore spaces to accommodate the thickest biofilm to avoid clogging and subsequent decreased performance (Chapter 2). Additionally, between day 455 and day 494 of operation, the system wasted 59% of the attached biofilm from the reactor. During this time period, the maximum observed TSS concentration was 22.3 mg/L. Although below 25 mg/L, to guarantee compliance with effluent guidelines many lagoons will require a solids separation step after the MBBR unit during this time period.

The biomass response with respect to the microbial ecology demonstrated the community is constantly shifting temporally, however, in all cases (start-up, transition, cold temperatures, varying loads and HRTs) the AOBs and NOBs have a symbiotic relationship with the peripheral organisms. Collating all the AOB relative abundances throughout the experimental trial shows after the initial start-up period (days 0 to 30), the relative abundance of AOBs remains fairly constant at 7.6 ± 1.9% irrespective of temperature and loading rate.

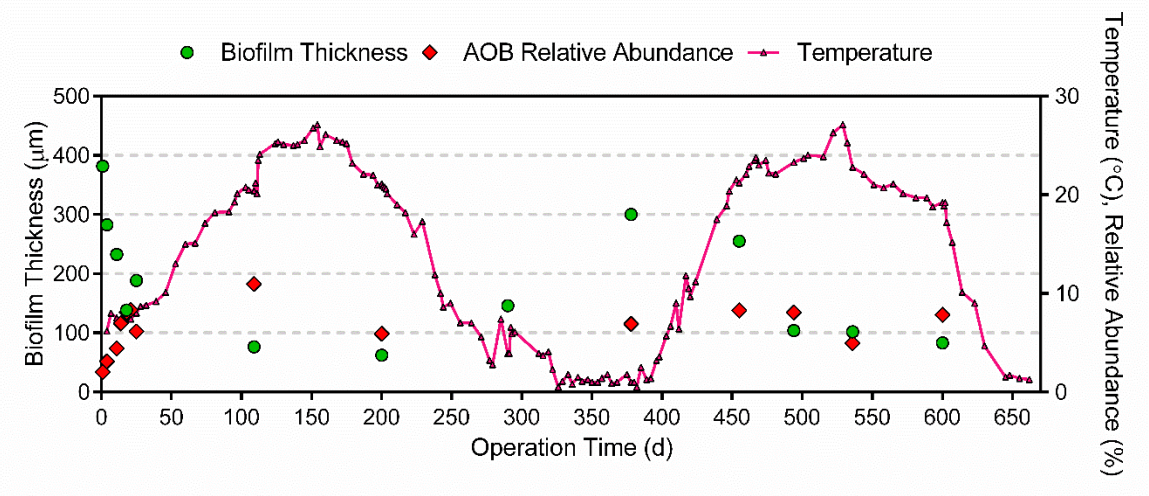

Figure 7.2 Timeline of biofilm thickness and AOB relative abundance from start-up to decommissioning for reactor 2A

7.1.3 Design of MBBR for post carbon removal nitrification

With all the data at the constituent, biofilm morphology and microbial levels, this work effectively demonstrates the ability for the MBBR technology to provide constant year round nitrification in the norther climate regions. The data acquired in this study, can be used to effectively size the MBBR technology for full scale installations. Using a conservative loading rate of 100 $gN/m^3 \cdot d$ (Fig 4.1) and the final effluent flow data for the Masson Angers, QC lagoon treatment facility, an add-on MBBR will require 1950 m^3 of

AnoxKaldnes K5 carriers. As such, the add-on MBBR at a filling ratio of 40% will have a bulk liquid volume of 4800 m^3 and an HRT of 7.8 h. With this bulk liquid volume and typical length to width to depth ratio of 1:1:1.75 the add-on MBBR design would be 14 m in length, 14 m in width (196 m^2 land area) and 24.5 m in depth including 1 m of freeboard. This design, although simplistic, allows us to visualize the MBBR installation at Masson Angers lagoon treatment facility (Fig 7.3).

Figure 7.3 Simplistic design representation of a post carbon removal nitrifying MBBR at the Masson Angers lagoon treatment wastewater treatment plant

7.2 Future directions

The findings in this thesis open several avenues for future research on post-carbon removal MBBR nitrification. While it is now clear the MBBR can achieve high quality effluents at 1°C in municipal treatment systems, there are outstanding questions on the

impact of these extreme cold temperatures with respect to overloading and toxicity effects within the system. Although the research was able to postulate the system is susceptible to decreased performance when overloaded, the mechanism of inhibition is still unclear. For future upgrades and understanding of the system, a constructed controlled inhibition study could further elucidate the impacts of temperature on nitrifying MBBR systems.

This study effectively demonstrated the biofilm and biomass is capable of adapting to potential low loading rates in the summer months and transition to cold temperature and design loading rates in the winter months. This operation is simplistic, however, may not be the most efficient. Investigating the feasibility of bypassing the MBBR in the summer months (if ammonia removal is not required) and restarting the system when necessary could increase the efficiency of the MBBR technology. This approach could also be taken in a non-nitrifying lagoon by operating more than one MBBR in series to reduce energy costs during the summer months where less surface area is required to achieve target ammonia effluents.

References

Abeling, U., Seyfried, C.F., 1992. Anaerobic-aerobic treatment of high strength ammonium wastewater – nitrogen removal via nitrite. Water Science Technology 26(5-6), 1007-1015.

Abeysinghe, D.H., Viraj de Silva, D.G., Stahl, D.A., Rittmann, B.E., 2002. The effectiveness of bioaugmentation in nitrifying systems stressed by a washout condition and cold temperature. Water Environment Research 74(2), 187-199.

Abujamel, T., Cadnum, J.L., Sunkesula, V.C., Kundrapu, S., Jump, R.L., Stintzi, A.C., Donskey, C.J., 2013. Defining the vulnerable period for re-establishment of *Clostridium difficile* colonization after treatment of *C. difficile* infection with oral vancomycin or metronidazole. PloS One 8(10), e76269.

Alawi, M., Off, S., Kaya, M., Spieck, E., 2009. Temperature influences the population structure of nitrite-oxidizing bacteria in activated sludge. Environmental Microbiology Reports 1(3), 184-190.

Alleman, J.E., 1984. Elevated nitrite occurrence in biological wastewater treatment systems. Water Science and Technology 17, 409-419.

Almomani, F.A., Delatolla, R., Örmeci, B., 2014. Field study of moving bed biofilm reactor technology for post-treatment of wastewater lagoon effluent at 1°C. Environmental Technology 35(13), 1596-1604.

Almstrand, R., Holger, D., Persson, F., Sorensson, F., Hermansson, M., 2013. New methods for analysis of spatial distribution and coaggregation of microbial populations in complex biofilms. Applied Environmental Microbiology 79(19), 5978-5987.

Ahimou, F., Semmens, M.J., Haugstad, G., Novak, P.J., 2007. Effect of protein, polysaccharide, and oxygen concentration profiles on biofilm cohesiveness. Applied Environmental Microbiology 73(9), 2905-2910.

Anthonisen, A.C., Srinath, E.G., Loehr, R.C., Prakasam, T.B.S., 1976. Inhibition of nitrification and nitrous acid compounds. Journal of Water Pollution Control Federation 48, 835–852.

Aonofriesei, F., Petrosanu, M., 2007. Activated sludge bulking episodes and domi- nant filamentous bacteria at wastewater treatment plant constanta sud (Romania). Proceedings of the Romanian Academy 2, 83-87.

APHA A, WEF (Eds)., 1998. Standard methods for the examination of water and wastewater. 19 ed. A.P.H.A.A.W.W.A.W.E. Federation, Washington DC, USA.

Bae, H., Chung, Y.C., Yang, H., Lee, C., Aryapratama, R., Yoo, Y.J., Lee, S., 2015. Assessment of bacterial community structure in nitrifying biofilm under inorganic

carbon-sufficient and -limited conditions. Journal of Environmental Science and Health Part A Toxic/Hazardous Substances and Environmental Engineering 50(2), 201-212.

Bai, Y., Sun, Q., Wen, D., Tang, X., 2012. Abundance of ammonia-oxidizing bacteria and archaea in industrial and domestic wastewater treatment systems. FEMS Microbiology Ecology 80, 323–330.

Bassin, J.P., Kleerebezem, R., Rosado, a S., van Loosdrecht, M.C.M., Dezotti, M., 2012. Effect of different operational conditions on biofilm development, nitrification, and nitrifying microbial population in moving-bed biofilm reactors. Environmental Science and Technology 46, 1546–1555.

Beccari, M., Marani, D., Ramadori, R., 1979. A critical analysis of nitrification alternatives. Water Research 13, 185-192.

Blackburne, R., Vadivelu, V.M., Yuan, Z., Keller, J., 2007. Kinetic characterisation of an enriched *Nitrospira* culture with comparison to *Nitrobacter*. Water Research 41, 3033-3042.

Blankenberg, D., Von Kuster, G., Coraor, N., Ananda, G., Lazarus, R., Mangan, M., Nekrutenko, A., Taylor, J., 2010. Galaxy: a web-based genome analysis tool for experimentalists. Current Protocols in Molecular Biology 19.10.1-19.10.21.

Bryan, C., Marchal, M., Battaglia-Brunet, F., Kugler, V., Lemaitre-Guillier, C., Liévremont, D., Bertin, P., Arséne-Ploetze, F.L., 2009. Carbon and arsenic metabolism in *Thiomonas* strains: differences revealed diverse adaptation processes. BMC Microbiology 9(127), doi: 10.1186/1471-2180-9-127.

Bryers, J.D., 2000. Biofilms. Second ed. John Wiley, New York.

Canada Gazette, July 18 2012. Wastewater systems effluent regulations. Part II, vol. 146, No. 15.

Caporaso, J.G., Kuczynski, J., Stombaugh, J., Bittinger, K., Bushman, F.D., Costello, E.K., Fierer, N., Gonzalez Peña, A., Goodrich, J.K., Gordon, J.I., Huttley, G.A., Kelley, S.T., Knights, D., Koenig, J.E., Ley, R.E., Lozupone, C.A., McDonald, D., Muegge, B.D., Pirrung, M., Reeder, J., Sevinsky, J.R., Turnbaugh, P.J., Walters, W.A., Widmann, J., Yatzunenko, T., Zaneveld, J., Knight, R., 2010. QIIME allows analysis of high-throughput community sequencing data. Nature Methods 7(5), 335–336.

CCME., 2010. Canadian water quality guidelines for protection of aquatic life.

Chae, K.J., Kim, S.M., Oh, S.E., Ren, X., Lee, J., Kim, I.S., 2012. Spatial distribution and viability of nitrifying, denitrifying and ANAMMOX bacteria in biofilms of sponge media retrieved from a full-scale biological nutrient removal plant. Bioprocess and Biosystems Engineering 35, 1157–1165.

Costerton, J.W., Stewart, P.S., Greenberg, E.P., 1999. Bacterial biofilms: a common cause of persistent infections. Science 284, 1318-1322.

Cottrell, M.T., Kirchman, D.L., 2000. Natural assemblages of marine proteobacteria and members of the *Cytophaga-Flavobacter* cluster consuming low and high molecular-weight dissolved organic matter. Applied Environmental Microbiology 66(4), 1692-1697.

Daims, H., Brühl, A., Amann, R., Schleifer, K.H., Wagner, M., 1999. The domain-specific probe EUB338 is insufficient for the detection of all bacteria: development and evaluation of a more comprehensive probe set. Systematic and Applied Microbiology 22, 434-444.

Daims, H., Lebedeva, E.V., Pjevac, P., Han, P., Herbold, C., Albertsen, M., Jehmlich, N., Palatinszky, M., Vierheilig, J., Bulaev, A., Kirkegaard, R.H., von Bergen, M., Rattei, T., Bendinger, B., Nielsen, P.H., Wagner, M., 2015. Complete nitrification by *Nitrospira* bacteria. Nature 528, 504-509.

Daims, H., Lücker, S., Wagner, M., 2006. Daime, a novel image analysis program for microbial ecology and biofilm research. Environmental Microbiology 8, 200–213.

Daims, H., Nielsen, J.L., 2001. In situ characterization of *Nitrospira*-like nitrite-oxidizing bacteria active in wastewater treatment plants. American Society of Microbiology 67(11), 5273-5284.

Delatolla, R., Berk, D., Tufenkji, N., 2008. Rapid and reliable quantification of biofilm weight and nitrogen content of biofilm attached to polystyrene beads. Water Research 42, 3082-3088.

Delatolla, R., Tufenkji, R., Comeau, Y., Gadbois, A., Lamarre, D., Berk, D., 2009a. Kinetic analysis of attached growth nitrification in cold climates. Water Science and Technology 60(5), 1173-1184.

Delatolla, R., Tufenkji, N., Comeau, Y., Gadbois, A., Berk, D., 2009b. In situ characterization of nitrifying biofilm : minimizing biomass loss and preserving perspective. Water Research 43(6), 1775-1787.

Delatolla, R., Tufenkji, N., Comeau, Y., Gadbois, A., Lamarre, D., Berk, D., 2010. Investigation of laboratory-scale and pilot-scale attached growth ammonia removal kinetics at cold temperatures and low influent carbon. Water Quality Research Journal of Canada 45(4), 427-436.

Delatolla, R., Tufenkji N., Comeau, Y., Gadbois, A., Lamarre, D., Berk, D., 2012. Effects of long exposure to low temperatures on nitrifying biofilm and biomass in wastewater treatment. Water Environment Research 84(4), 328-338.

Di Guilio, R.T., Hinton, D.E., 2008. The toxicology of fishes. CRC Press, New York.

Di Trapani, D., Christensson, M., Torregrossa, M., Viviani, G., Ødegaard, H., 2013. Performance of a hybrid activated sludge/biofilm process for wastewater treatment in a cold climate region: Influence of operationg conditions. Biochemical Engineering Journal 77, 214-219.

Dubois, M., Gilles, K.A., Hamilton, J.K., Rebers, P.A., Smith, F., 1956. Colorimetric method for determination of sugars and related substances. St. Paul, MN: Division of Biochemistry, University of Minnesota.

Dugan, P., Stoner, D., Pickrum, H., 2006. The genus *Zoogloea*. Prokaryotes 7, 960-970.

EEC., 1991. Council directive concerning urban waste-water treatment. OJEC 134(40).

Figueroa, L.A., Silverstein, J., 1992. The effect of particulate organic matter on biofilm nitrification. Water Environment Research 64, 728-733.

Flemming, H-C., Neu, T.R., Wozniak, D.J., 2007. The EPS matrix: the "house of biofilm cells". Journal of Bacteriology 189(22), 7945-7947.

Flemming, H-C., Szewzyk, U., Griebe, T., 2000. Biofilms Investigative Methods & Applications. Technnomic, Pennsylvania.

Flemming, H-C., Wingender, J., 2010. The biofilm matrix. Nature Reviews Microbiology 8(9), 623-633.

Flynn, K., Dowell, G., Johnson, T.M., Koestler, B.J., Waters, C.M., Cooper, V.S., 2016. Evolution and ecological diversity in biofilms of *Pseudomonas aeruginosa* by altered cyclic diguanylate signaling. Journal of Bacteriology 198(19), 2608-2618.

Frolund, B., Griebe, T., Nielsen, P.H., 1995. Enzymatic-Activity in the activated-sludge floc matrix. Applied Microbiology and Biotechnology 43, 755-761.

Fumasoli, A., Morgenroth, E., Udert, K.M., 2015. Modeling the low pH limit of *Nitrosomonas eutropha* in high-strength nitrogen wastewaters. Water Research 83, 161–170.

Furukawa, K., Inatomi, Y., Qiao, S., Quan, L., Yamamoto, T., Isaka, K., Sumino, T., 2009. Innovative treatment system for digester liquor using anammox process. Bioresource Technology 100(22), 5437-5443.

Gao, J., Fan, X., Wu, G., Li, T., Pan, K., 2015. Chanages of abundance and diversity of ammonia-oxidizing archaea (AOA) and bacteria (AOB) in three nitrifying bioreactors with different ammonia concentrations. Desalination and Water Treatment 57, 21463-21475.

Garrett, T.R., Bhakoo, M., Zhang, Z., 2008. Bacterial adhesion and biofilms on surfaces. Progress in Natural Science 18, 1049-1056.

Ge, S., Wang, S., Yang, X., Qiu, S., Li, B., Peng, Y., 2015. Detection of nitrifiers and evaluation of partial nitrification for wastewater treatment: A review. Chemosphere 140, 85-98.

Gerardi, M.H., 2002. Nitrification and Denitrification in the Activated Sludge Process. John Wiley & Sons Inc, New York.

Giardine, B., Riemer, C., Hardison, R.C., Burhans, R., Shah, P., Zhang, Y., Blankenberg, D., Albert, I., Taylor, J., Miller, W., Kent, J., Nekrutenko, A., 2005. Galaxy : A platform for interactive large-scale genome analysis. Genome Research 15, 1451–1455.

Gieseke, A., Bjerrum, L., Wagner, M., Amann, R., 2003. Structure and activity of multiple nitrifying bacterial populations co-existing in a biofilm. Environmental Microbiology 5, 355-369.

Gieseke, A., Nielsen, J.L., Amann, R., Nielsen, P.H., de Beer, D., 2005. In situ substrate conversion and assimilation by nitrifying bacteria in a model biofilm. Environmental Microbiology 7(9), 1392-404.

Gieskeke, A., Purkhold, U., Wagner, M., Amamm, R., Schramm, A., 2001. Community structure and activity dynamics of nitrifying bacteria in a phosphate-removing biofilm. Clininical Microbiology Reviews 67, 1351-1362.

Gilbert, E.M., Agrawal, S., Schwartz, T., Horn, H., Lackner, S., 2015. Comparing different reactor configurations for partial Nitritation/Anammox at low temperatures. Water Research 81, 92-100.

Goecks, J., Nekrutenko, A., Taylor, J., The Galaxy Team., 2010. Galaxy : a comprehensive approach for supporting accessible, reproducible, and transparent computational research in the life sciences. Genome Biology 11, R86.

Gönenç, E.J., Harremöes, P., 1985. Nitrification in rotating disk systems-I: criteria for transition from oxygen to ammonia rate limitation. Water Research 19(9), 1119-1127.

Gonzalez-Martinez, A., Rodriguez-Sanchez, A., van Loosdrecht, M.C.M., Gonzalez-Lopez, J.. Vahala, R., 2016. Detection of comammox bacteria in full-scale wastewater treatment bioreactors using *tag*-454-pyrosequencing. Environmental Science Pollution Research DOI 10.1007/s11356-016-7914-4.

Gonzalez-Silva, B.M., Jonassen, K.R., Bakke, I., Østgaard, K., Vadstein, O., 2016. Nitrification at different salinities: biofilm community composition and physiological plasticity. Water Research 95, 48–58.

Graham, D.W., Knapp, C.W., Van Vleck, E.S., Bloor, K., Lane, T.B., Graham, C.E., 2007. Experimental demonstration of chaotic instability in biological nitrification. ISME Journal 1, 385–393.

Hallin, S., Lydmark, P., Kokalj, S., Hermansson, M., Sorensson, F., Jarvis, A., Lindgre, P.E., 2005. Community survey of ammonia-oxidizing bacteria in full-scale activated sludge proceses with different solids retention time. Journal of Applied Microbiology 99, 629-640.

Hall-Stoodley, L., Stoodley, P., 2002. Developmental regulation of microbial biofilms. Current Opinion in Biotechnology 13, 228-233.

Hall-Stoodley, L., Costerton, J.W., Stoodley, P., 2004. Bacterial biofilms: from the natural environment to infectious diseases. Nature Reviews Microbiology 2, 95-108.

Head, M.A., Oleszkiewicz, J.A., 2004. Bioaugmentation for nitrification at cold temperatures. Water Research 38(3), 523-530.

Heijnen, J.J., Hellinga, C., Mulder, J.W., Schellen, A.A.J.C., Van Loosdrecht, M.C.M., 1998. The Sharon process: an innovative method for nitrogen removal from ammonium-rich waste water. Water Science and Technology 37(9), 135-142.

Hem, L., Rusten, B., Ødegaard, H., 1994. Nitrification in a moving bed biofilm reactor. Water Research 28, 1425–1433.

Herrling, M.P., Guthausen, G., Wagner, M., Lackner, S., Horn, H., 2014. Determining the flow regime in a biofilm carrier by means of magnetic resonance imaging. Biotechnology and Bioengineering 122(5), 1023-1032.

Hibiya, K., Tsuneda, S., Hirata, A., 2000. Formation and characteristics of nitrifying biofilm on a membrane modified with positively-charged polymer chains. Colloids and Surfaces B: Biointerfaces 18(2), 105-112.

Hoang, V., Delatolla, R., Abujamel, T., Mottawea, W., Gadbois, A., Laflamme, E., Stintzi, A., 2014a. Nitrifying moving bed biofilm reactor (MBBR) biofilm and biomass response to long term exposure to 1°C. Water Research 49, 215-224.

Hoang, V., Delatolla, R., Laflamme, E., Gadbois, A., 2014b. An Investigation of Moving Bed Biofilm Reactor Nitrification during Long-Term Exposure to Cold Temperatures. Water Environment Research 86, 36–42.

Houweling, D., Monette, F., Millette, L., Comeau, Y., 2007. Modelling nitrification of a lagoon effluent in moving-bed biofilm reactors. Water Quality Research Journal of Canada 42(4), 284-294.

Hupeden, J., Wegen, S., Off, S., Lucker, S., Bedarf, Y., Daims, H., Kuhn, C., Spieck, E., 2016. Relative abundance of *Nitrotoga spp*. in a biofilter of a cold-freshwater aquaculture plant appears to be stimulated by slightly acidic pH. Applied and Environmental Microbiology 82(6), 1838-1845.

Hurse, T.J., Connor, M.A., 1999. Nitrogen removal from wastewater treatment lagoons. Water Science Technology 39, 191-198.

Huws, S.A., McBain, A.J., Gilbert, P., 2005. Protozoan grazing and its impact upon population dynamics in biofilm communities. Journal of Applied Microbiology 98(1), 238-244.

Ivanovic, I., Leiknes, T.O., 2012. Particle separation in moving bed biofilm reactor: applications and opportunities. Separation Science and Technology 47(5), 647-653.

Ivanovic, I., Leiknes, T., Ødegaard, H., 2006. Influence of loading rates on production and characteristics of retentate from a biofilm membrane bioreactor (BF-MBR). Desalination 199(1-3), 490-492.

Jang, A., Bishop, P.L., Okabe, S., Lee, S.G., Kim, I.S., 2003. Effect of dissolved oxygen concentration on the biofilm and in situ analysis by fluorescence in situ hybridization (FISH) and microelectrodes. Water Science and Technology 47, 49-57.

Jiménez, E., Giménez, J.B., Seco, A., Ferrer, J., Serralta, J., 2012. Effect of pH, substrate and free nitrous acid concentrations on ammonium oxidation rate. Bioresource Technology 124, 478–484.

Kaewpipat, K., Grady, C., 2002. Population dynamics in laboratory-scale activated sludge reactors. Water Science and Technology 46(1-2), 19-27.

Karizmeh, M., Delatolla, R., Narbaitz, R., 2014. Investigation of settleability of biologically produced solids and biofilm morphology in moving bed biofilm reactors (MBBRs). Bioprocess and Biosystems Engineering 37(9), 1839-1848.

Kertesz, M., Kawaski, A., 2010. Handbook of hydrocarbon and lipid microbiology. K. N. Timmis ed. Springer Verlag, Berlin.

Kindaichi, T., Ito, T., Okabe, S., 2004. Ecophysiological interaction between nitrifying bacteria and heterotrophic bacteria in autotrophic nitrifying biofilms as determined by microautoradiography-fluorescence in situ hybridization. Applied and Environmental Microbiology 70(3), 1641-1650.

Kindaichi, T., Kawano, Y., Ito, T., Satoh, H., Okabe, S., 2006. Population dynamics and in situ kinetics of nitrifying bacteria in autotrophic nitrifying biofilms as determined by real-tie quantitative PCR. Biotechnology and Bioengineering 94(6), 1111-1121.

Konneke, M., Schubert, D.M., Brown, P.C., Hugler, M., Standfest, S., Schwander, T., Schada von Borzyskowski, L., Erb, T.J., Stahl, D.A., Berg, I.A., 2014. Ammonia-oxidizing archaea use the most energy-efficient aerobic pathway for CO_2 fixation. PNAS 111(22), 8239-8244.

Kors, L.J., Moorman, J.H.N., Wind, A.P.M., van der Hoek, J.P., 1998. Nitrification and low temperature in a raw water reservoir and rapid sand filters. Water Science and Technology 37, 169-176.

Krhutkovi, O., Novak, L., Pachmanova, L., Benakova, A., Wanner, J., Kos, M., 2006. Insitu bioaugmentation of nitrification in the regeneration zone: practical application and experiences at full-scale plants. Water Science and Technology 53(12), 39-46.

Kulichevskaya, I.S., Suzina, N.E., Liesack, W., Dedysh, S.N., 2010. *Bryobacter aggregatus* gen. nov., sp. Nov., a peat-inhibiting, aerobic chemo-organotroph from subdivision 3 of the Acidobacteria. International Journal of Systematic and Evolutionary Microbiology 60(Pt 2), 301-306.

Kwon, S., Kim, T., Yu, G.H., Jung, J., Park, H., 2010. Bacterial community composition and diversity of a full-scale integrated fixed-film activated sludge system as investigated by pyrosequencing. Journal of Microbiology and Biotechnology 20(12), 1717-1723.

Langille, M.G.I., Zaneveld, J., Caporaso, J.G., McDonald, D., Knights, D., Reyes, J., Clemente, J.C., Burkepile, D.E., Vega Thurber, R.L., Knight, R., Beiko, R.G., Huttenhower, C., 2013. Predictive functional profiling of microbial communities using 16S rRNA marker gene sequences. Nature Biotechnology 31, 814-821.

Laspidou, C.S., Rittmann, B.E., 2004. Evaluating trends in biofilm density using the UMCCA model. Water Research 38, 3362–72.

Lay, W.C.L., Liu, Y., Fane, A.G., 2010. Impacts of salinity on the performance of high retention membrane bioreactors for water reclamation: A review. Water Research 44, 21–40.

Layton, A.C., Dionisi, H., Kuo, H.W., Robinson, K.G., Garrett, V.M., Meyers, A., Sayler, G.S., 2005. Emergence of competitive dominant ammonia-oxidizing bacterial populations in a full-scale industrial wastewater treatment plant. Applied and Environmental Microbiology 71, 1105-1108.

Lee, L.Y., Ong, S.L., Ng, W.J., 2004. Biofilm morphology and nitrification activities: recovery of nitrifying biofilm particles covered with heterotrophic outgrowth. Bioresource Technology 95(2), 209-214.

Lee, S-H., Ka, J-O., Cho, J-C., 2008. Members of the phylum *Acidobacteria* are dominant and metabolically active in rhizosphere soil. FEMS Microbiology Letters 285, 263-269.

Leu, S.Y., Stenstrom, M.K., 2010. Bioaugmentation to improve nitrification in activated sludge treatment. Water Environment Research 82(6), 524-535.

Leyva-Díaz, J.C., Martín-Pascual, J., Gonzalez-Lopez, J., Hontoria, E., Poyatos, J.M., 2013. Effects of scale-up on a hybrid moving bed biofilm reactor - membrane bioreactor for treating urban wastewater. Chemical Engineering Science 104, 808-816.

Li, C., Wagner, M., Lackner, S., Horn, H., 2016. Assessing the influence of biofilm surface roughness on mass transfer by combining optical coherence tomography and two-dimensional modeling. Biotechnology and Bioengineering 113(5), 989-1000.

Lydmark, P., Almstrand, R., Samuelsson, K., Mattsson, A., Sörensson, F., Lindgren, P.E., Hermansson, M., 2007. Effects of environmental conditions on the nitrifying population dynamics in a pilot wastewater treatment plant. Environmental Microbiology 9, 2220–2233.

Maas, C.L., Parker, W.J., Legge, R.L., 2008. Detachment of solids and nitrifiers in integrated, fixed-film activated sludge systems. Water Environment Research 80(12), 2202-2208.

Madsen, J.S., Burmølle, M., Hansen, L.H., Sørensen, S.J., 2012. The interconnection between biofilm formation and horizontal gene transfer. FEMS Immunology and Medical Microbiology 65, 183–195.

Manser, R., Gujer, W., Siegrist, H., 2005. Consequences of mass transfer effects on the kinetics of nitrifiers. Water Research 39(19), 4633-4642.

Magoč, T., Salzberg, S., 2011. L. FLASH: fast length adjustment of short reads to improve genome assemblies. Bioinformatics 27(21), 2957–2963.

Martins, A.M., Paqilla, K., Heijnen, JJ., van Loosdrecht, M., 2004. Filamentous bulking sludge--a critical review. Water Research 38(4), 793-817.

Martín-Pascual, J., Lopez-Lopez, C., Cerda, A., Gonzalez-Lopez, J., Hontoria, E., Poyatos, J.M., 2012. Comparative kinetic study of carrier type in a moving bed system applied to organic matter removal in urban wastewater treatment. Water Air and Soil Pollution 223(4), 1699-1712.

McQuarrie, J.P., Boltz, J.P., 2011. Moving Bed Biofilm Reactor Technology: Process Applications, Design, and Performance. Water Environment Research 83, 560-575.

Melin, E., Leiknes, T., Helness, H., Rasmussen, V., Ødegaard, H., 2005. Effect of organic loading rate on a wastewater treatment process combining moving bed biofilm and membrane reactors. Water Science and Technology 51, 421-430.

Metcalf and Eddy., 2003. Wastewater engineering: Treatment and reuse. Fourth ed. McGraw-Hill, New York.

Monod, J., 1949. The growth of bacterial cultures. Annual Reviews Microbiology 3, 371-394.

Montanaro, L., Poggi, A., Visai, L., Ravaioli, S., Campoccia, D., Speziale, P., Arciola, C. R., 2011. Extracellular DNA in biofilms. International Journal of Artificial Organs 34, 824–831.

Monteiro, M., Séneca, J., Magalhães, C., 2014. The history of aerobic ammonia oxidizers: from the first discoveries to today. Journal of Microbiology 52(7), 537–47.

Mozumder, M.S.I., Picioreanu, C., van Loosdrecht, M.C.M., Volcke, E.I.P., 2014. Effect of heterotrophic growth on autotrophic nitrogen removal in a granular sludge reactor. Environmental Technology 35, 1027-1037.

Murdoch, P.S., Baron, J.S., Miller, T.L., 2000. Potential effects of climate change on surface-water quality in North America. Journal of the American Water Resources Association 36(2), 347-366.

Nadell, C.D., Xavier, J.B., Foster, K.R., 2009. The sociology of biofilms. FEMS Microbiology Reviews 33(1), 206-24.

Nogueira, R., Melo, L.S.F., Purkhold, U., Wuertz, S., Wagner, M., 2002. Nitrifying and heterotrophic population dynamics in biofilm reactors: effects of hydraulic retention time and the presence of organic carbon. Water Research 36(2), 469-481.

Ødegaard, H., 2006. Innovation in wastewater treatment: the moving bed biofilm process. Water Science and Technology 53, 17-33.

Ødegaard, H., Gisvold, B., Strickland, J., 2000. The influence of carrier size and shape in the moving bed biofilm process. Water Science and Technology 41(4-5), 383-391.

Ødegaard, H., Rusten, B., Westrum, T., 1994. A new moving bed biofilm reactor-applications and results. Water Science and Technology 29(10-11), 157-165.

Okabe, S., Satoh, H., Watanabe, Y., 1999. In situ analysis of nitrifying biofilms as determined by in situ hybridization and the use of microelectrodes. Applied and Environmental Microbiology 65(7), 3182-3191.

Oleszkiewicz, J.A., Barnard, J.L., 2006. Nutrient removal technology in North America and the European Union: a review. Water Quality Research Journal of Canada 41(4), 449-462.

Oleszkiewicz, J., Berquist, S., 1988. Low temperature nitrogen removal in sequencing batch reactors. Water Research 22(9), 1163-1171.

Otawa, K., Asano, R., Ohba, Y., Sasaki, T., Kawamura, E., Koyama, F., Nakamura, S., Nakai, Y., 2006. Molecular analysis of ammonia-oxidizing bacteria community in intermittent aeration sequencing batch reactors used for animal wastewater treatment. Environmental Microbiology 8(11), 1985-1996.

Paredes, D., Kuschk, P., Mbwette, T.S.A., Strange, F., Muler, R.A., Koser, H., 2007. New aspects of microbial nitrogen transformations in the context of wastewater treatment – a review. Engineering in Life Science 7(1), 13-25.

Park, I., Zhao, R., West, J.A., Yabuuchi, A., Huo, H., Ince, T.A., Lerou, P.H., Lensch, M.W., Daley, G.Q., 2008. Reprogramming of human somatic cells to pluripotency with defined factors. Nature 451(7175), 141-146.

Paulson, J., Stine, O., Bravo, H., Pop, M., 2013. Differential abundance analysis for microbial marker-gene surveys. Nature Methods 10(12), 1200-1202.

Phadtare, S., 2004. Recent developments in bacterial cold-shock response. Current Issues Molecular Biology 6, 125-136.

Podmirseg, S.M., Schoen, M.A., Murthy, S., Insam, H., Wett, B., 2010. Quantitative and qualitative effects of bioaugmentation on ammonia oxidisers at a two-step WWTP. Water Science and Technology 61, 1003-1009.

Randall, C.W., Buth, D., 1984. Nitrite build-up in activated sludge resulting from temperature effects. Journal Water Pollution Control Federation 56, 1039-1044.

Rittman, B.E., Whiteman, R., 1994. Bioaugmentation: a coming of age. Water Quality International 1, 12-16.

Rowan, A.K., Snape, J.R., Fearnside, D., Barer, M.R., Curtis, T.P., Head, I.M., 2003. Composition and diversity of ammonia-oxidising bacterial communities in wastewater treatment reactors of different design treating identical wastewater. FEMS Microbiology Ecology 43, 195-206.

Rusten, B., Eikebrokk, B., Ulgenes, Y., Lygren, E., 2006. Design and operations of the Kaldnes moving bed biofilm reactors. Aquaculture Engineering 34, 322–331.

Rusten, B., Hem, L.J., Ødegaard, H., 1994. Nitrification in a moving bed biofilm reactor. Water Research 28(6), 1425-1433.

Rusten, B., Hem, L.J., Ødegaard, H., 1995. Nitrification of municipal wastewater in moving-bed biofilm reactors. Water Environment Research 67(1), 75-86.

Rusten, B., Razafimanantsoa, V.A., Andriamiarinjaka, M.A., Otis, C.L., Sahu, A.K., Bilstad, T., 2016. Impact of fine mesh sieve primary treatment on nitrogen removal in moving bed biofilm reactors. Water Science and Technology 73, 337-344.

Salvetti, R., Azzellino, A., Canziani, R., Bonomo, L., 2006. Effects of temperature on tertiary nitrification in moving-bed biofilm reactors. Water Research 40, 2981-2993.

Schramm, A., Larsen, L.H., Revsbech, N.P., Ramsing, N.B., Amann, R., Schleifer, K.H., 1996. Structure and function of a nitrifying biofilm as determined by in situ hybridization and the use of microelectrodes. Applied and Environmental Microbiology 62(12), 4641-4647.

Segata, N., Izard, J., Waldron, L., Gevers, D., Miropolsky, L., Garrett, W.S., Huttenhower, C., 2011. Metagenomic biomarker discovery and explanation. Genome Biology 12, R60.

Shammas, N.K., 1986. Interactions of temperature, pH, and biomass on the nitrification process. Journal Water Pollution Control Federation 58, 52-59.

Sharma, B., Ahlert, R.C., 1977. Nitrification and nitrogen removal. Water Research 11, 879–925.

Shore, J.L., M'Coy, W.S., Gunsch, C.K., Deshusses, M.A., 2012. Application of a moving bed biofilm reactor for tertiary ammonia treatment in high temperature industrial wastewater. Bioresource Technology 112, 51-60.

Siripong, S., Rittmann, B.E., 2007. Diversity study of nitrifying bacteria in full-scale municipal wastewater treatment plants. Water Research 41, 1110-1120.

Spieck, E., Keuter, S., Wenzel, T., Bock, E., Ludwig, W., 2014. Characterization of a new marine nitrite oxidizing bacterium. *Nitrospina watsonii* sp. nov., a member of the newly proposed phylum *Nitrospinae*. Systematic and Applied Microbiology 37(3), 170-176.

Sriwiriyarat, T., Ungkurarate, W., Fongsatitkul, P., Chinwetkitvanich, S., 2008, Effects of dissolved oxygen on biological nitrogen removal in integrated fixed film activated sludge (IFAS) wastewater treatment process. Journal of Environmental Science and Health Part A Toxic/Hazardous Substances and Environmental Engineering 43(5), 518–527.

Sorensen, S.J., Bailey, M., Hansen, L.H., Kroer, N., Wuertz, S., 2005. Studying plasmid horizontal transfer in situ: a critical review. Nature Reviews Microbiology 3, 700-710.

Stenstrom, F., Jansen, I.C., 2016. Promotion of nitrifiers through side-stream bioaugmentation: a full-scale study. Water Science Technology 74(7), 1736-1743.

Stewart, P.S., 2003. Diffusion in Biofilms. Journal of Bacteriology 185, 1485-1491.

Stewart, P., Franklin, M., 2008. Physiological heterogeneity in biofilms. Nature Reviews Microbiology 6, 199-210.

Sumino, T., Nakamura, H., Mori, N., Kawaguchi, Y., 1992. Immobilization of nitrifying bacteria by polyethylene glycol prepolymer. Journal of Fermentation and Bioengineering 73(1), 37–42.

Sutherland, I.W., 2001. Biofilm exopolysaccharides: a strong and sticky framework. Microbiology 147, 3-9.

Taherzadeh, D., Picioreanu, C., Horn, H., 2012. Mass transfer enhancement in moving biofilm structures. Biophysical Journal 102(7), 1483-1492.

Tanyola, A., Beyenal, H., 1997. Prediction of average biofilm density and performance of a spherical bioparticle under substrate inhibition. Biotechnology and Bioengineering 56, 319–329.

Telgmann, U., Horn, H., Morgenroth, E., 2004. Influence of growth history on sloughing and erosion from biofilms. Water Research 38(17), 3671–3684.

Terada, A., Lackner, S., Kristensen, K., Smets, B.F., 2010. Inoculum effects on community composition and nitritation performance of autotrophic nitrifying biofilm

reactors with counter-diffusion geometery. Environmental Microbiology 12(10), 2858-2872.

Thomas, C.M., Nielsen, K.M., 2005. Mechanisms of, and barriers to, horizontal gene transfer between bacteria. Nature Reviews Microbiology 3, 711-721.

Tijhuis, L., Van Loosdrecht, M.C.C., Heijnen, J.J., 1994. Formation and growth of heterotrophic aerobic biofilms on small suspended particles in airlift reactors. Biotechnology and Bioengineering 44(5), 595-608.

Tsuneda, S., Park, S., Hayashi, H., Jung, J., Hirata, A., 2001. Enchancement of nitrifying biofilm formation using selected EPS produced by heterotrophic bacteria. Water Science and Technology 43(6), 197-204.

U.S. Environmental Protection Agency (USEPA)., 2014. State development for nitrogen and phosphorus pollution.

Van Dyke, S., Jones, S., Ong, S.K., 2003. Cold weather nitrogen removal deficiencies of aerated lagoons. Environmental Technology 24(6), 767-777.

Van Hulle, S.W.H., Helge, J.P., Vandeweyer, H.J.P., Meesschaert, B.D., Vanrolleghem, P.A., Dejans, P., Dumoulin, A., 2010. Engineering aspects and practical application of autotrophic nitrogen removal from nitrogen rich streams. Chemical Engineering Journal 162, 1-20.

Van Kessel, M.A.H.J., Speth, D.R., Albertsen, M., Nielsen, P.H., Opden Camp, H.J.M., Kartal, B., Jetten, M.S.M., Lucker, S., 2015. Complete nitrification by a single microorganism. Nature 528, 555-559.

Wang, R., Wen, X., Qian, Y., 2005. Effect of carrier concentration on the performance and microbial characteristics of a suspended carrier biofilm reactor. Process Biochemistry 40(9), 2992-3001.

Wagner, M., Rath, G., Koops, H.P., Flood, J., Amann, R., 1996. In situ analysis of nitrifying bacteria in sewage treatment plants. Water Science and Technology 34, 237-244.

Water Environment Federation (WEF)., 2010. Design of municipal wastewater treatment plants: WEF Manual of Practice, No. 8 ASCE Manuals and Reports on Engineering Practice No. 76, Fifth Ed. McGraw-Hill, New York.

Water Environment Federation (WEF), 2011. Biofilm Reactors WEF MoP35. McGraw-Hill Professional, New York.

Watnick, P., Kolter, R., 2000. Biofilm, city of microbes. Journal of Bacteriology 182(10), 2675–2679.

Wijffels, R.H., Englund, G., Hunik, J.H., Leenen, E.J.T.M., Bakketun, A., Gunther, A., Obon de Castro, J.M., Tramper, J., 1994. Effects of diffusion limitation on immobilized

nitrifying microorganisms at low temperatures. Biotechnology and Bioengineering 45, 1-9.

Winkler, M.K., Bassin, J.P., Kleerebezem, R., Sorokin, D.Y, Van Losdrecht, M.C., 2012. Unravelling the reasons for disproportion in the ratio of AOB and NOB in aerobic granular sludge. Applied Microbiology and Biotechnology 94(6), 1657-1666.

Wittebolle, L., Vervaeren, H., Verstraete, W., Boon, N., 2008. Quantifying community dynamics of nitrifiers in functionally stable reactors. Applied and Environmental Microbiology 74(1), 286-293.

Xue, X., Zhang, K., Cai, F., Dai, J., Wang, Y., Rahman, E., Fang, C., 2012. Altherery-throbacter xinjiangenesis sp. nov., isolated from desert sand, and emended description of the genus Althererythrobacter. International Journal of Systematic Evolutionary Microbiology 62(1), 28-32.

Young, B., Banihashemi, B., Forrest, D., Kennedy, K., Stintzi, A., Delatolla, R., 2016a. Meso and micro-scale response of post carbon removal nitrifying MBBR biofilm across carrier type and loading. Water Research 91, 235-243.

Young, B., Delatolla, R., Ren, B., Kennedy, K., Laflamme, E., Stintzi, A., 2016b. Pilot scale tertiary MBBR nitrification at 1°C: Characterization of ammonia removal rate, solids settleability and biofilm characteristics. Environmental Technology 37(16), 2124-2132.

Zhang, S., Wang, Y., He, W., Wu, M., Xing, M., Yang, J., Gao, N., Yin, D., 2013. Responses of biofilm characteristics to variations in temperature and NH_4-N loading in a moving bed biofilm reactor treating micro-polluted raw water. Bioresource Technology 131(March), 365-373.

Supplementary material

Supplemental figures

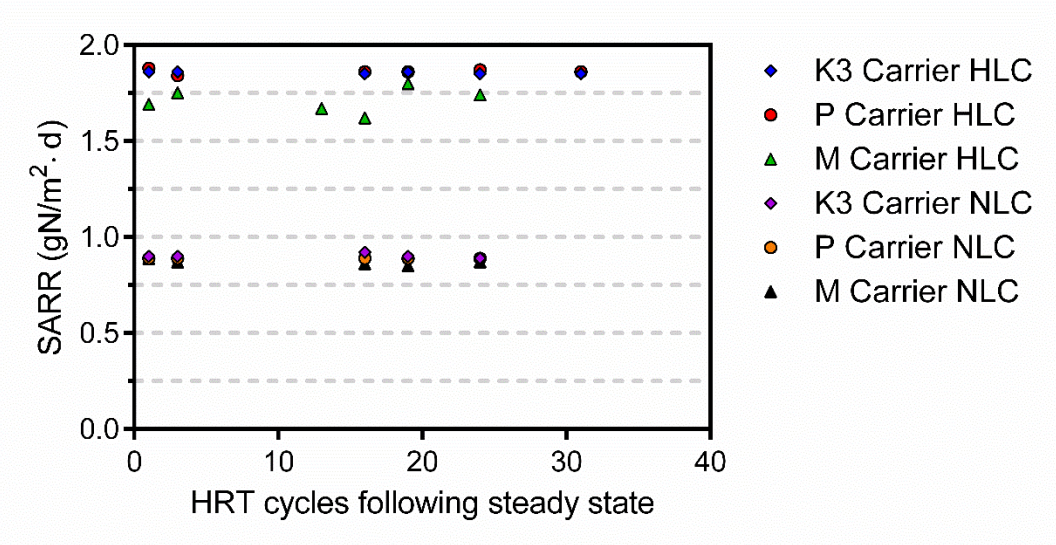

Figure S1 Nitrification kinetics of reactors with different carrier types measured across steady state operation where HLC SALR = 1.89 gN/m^2·d and NLC SALR = 0.9 gN/m^2·d

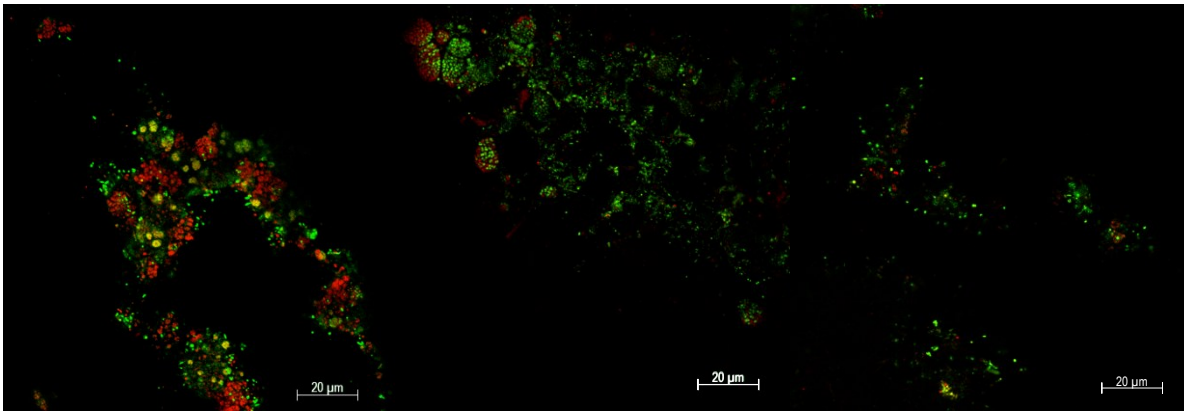

a) b) c)

Figure S2 Representative CLSM images acquired after three weeks of steady state operation at 6 µm depth (1 µm thick images showing live cells in green and dead cells in read); a) K3 carrier, b) P carrier, c) M carrier

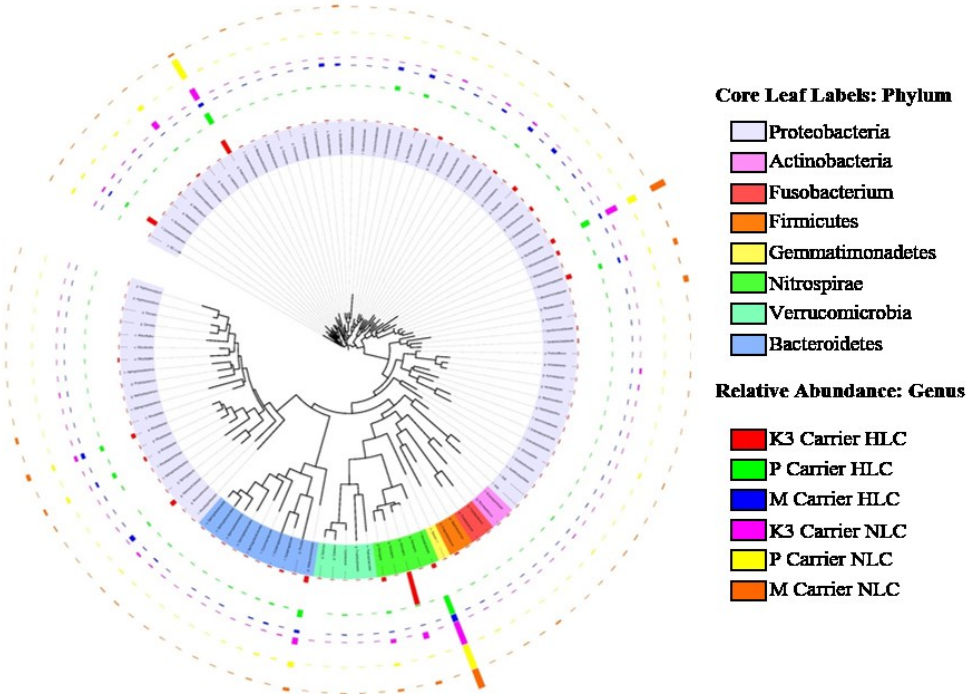

Figure S3 Core OTU phylogenetic tree with relative abundance where biofilm samples were acquired after three weeks of steady state operation

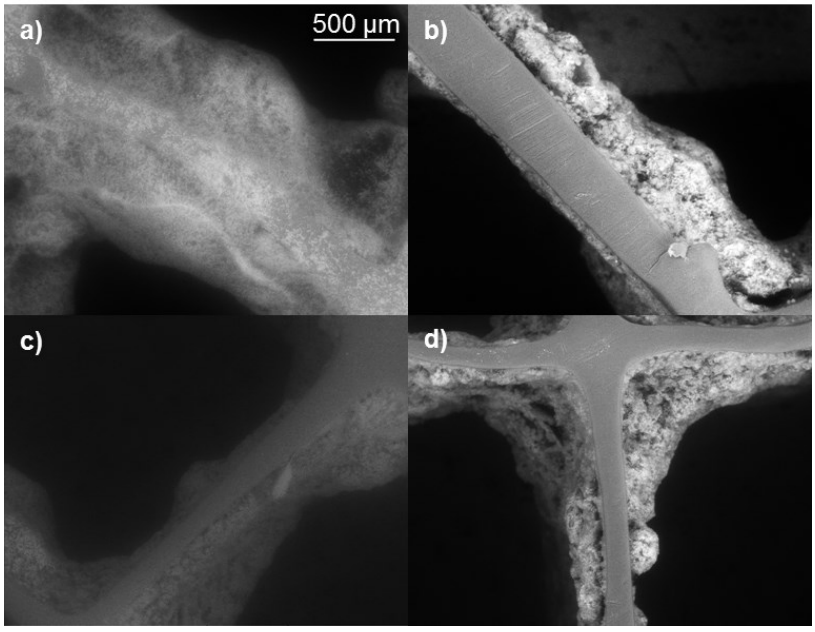

Figure S4 Representative VPSEM images of the carriers throughout the post carbon removal nitrifying MBBR start-up; a) IFAS biofilm, b) MBBR1 day 5, c) MBBR1 day 19, d) MBBR1 day 26

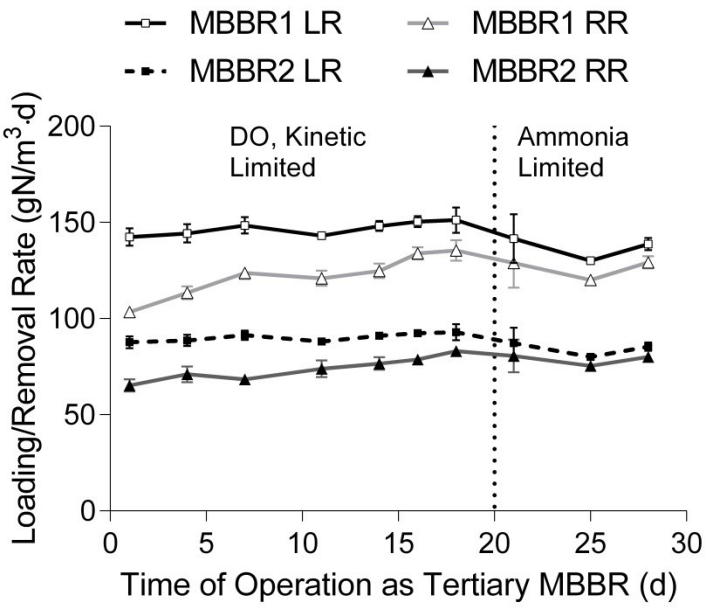

Figure S5 Kinetic rates during transition and stabilization of post carbon removal MBBR system

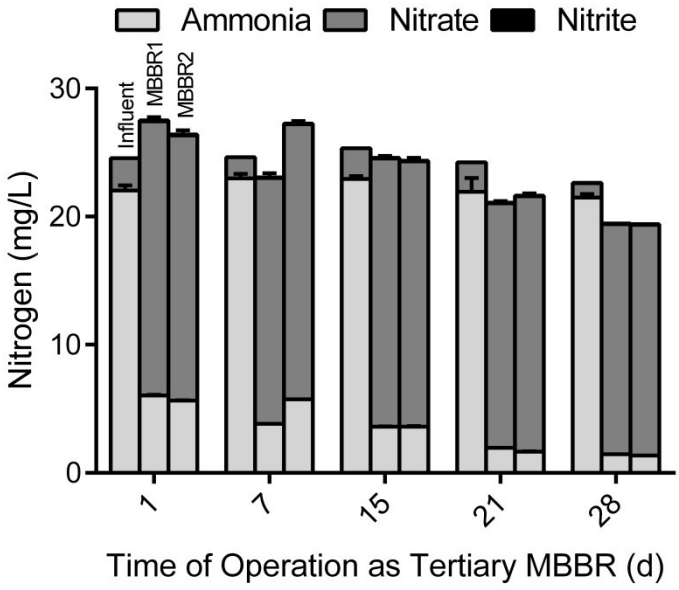

Figure S6 Nitrogen mass balance

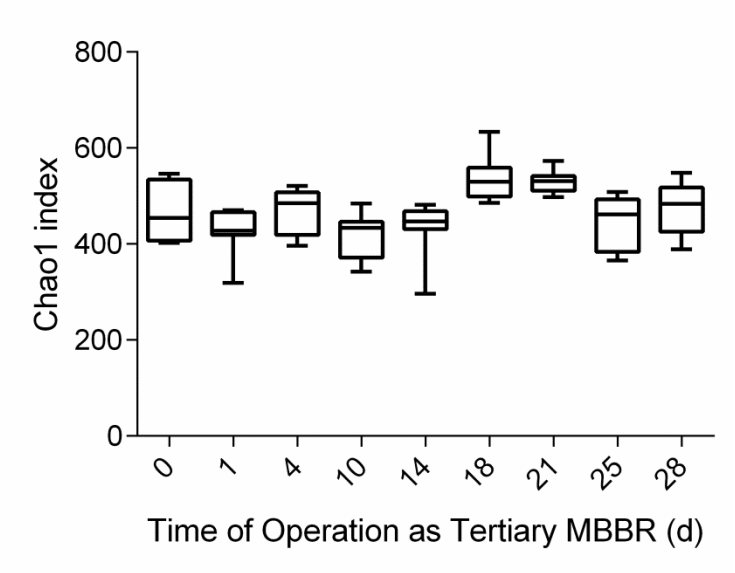

Figure S7 Alpha diversity for OTUs normalized for biofilm mass where the Chao1 index represents the non-parametric estimator of species. The Chao1 index signifies the diversity within each group. Kruskal-Wallis test showed no significant changes between the IFAS biofilm (time 0) and the MBBR groups. Days 18 and 21 are significantly more diverse (p<0.05) than days 1, 10 and 14

Supplemental tables

Table S1 Effluent wastewater characteristics measured across steady state operation (average ± standard deviation)

		HLC		
Carrier type	**TSS (mg/L)**	**NH_4^+ (mg-N/L)**	**NO_2^- (mg-N/L)**	**NO_3^- (mg-N/L)**
K3 Carrier	19 ± 7	0.75 ± 0.26	0.18 ± 0.05	50.18 ± 1.50
P Carrier	23 ± 4	0.75 ± 0.35	0.22 ± 0.06	49.77 ± 8.42
M Carrier	13 ± 5	4.70 ± 2.45	0.35 ± 0.07	50.10 ± 7.00
		NLC		
Carrier type	**TSS (mg/L)**	**NH_4^+ (mg-N/L)**	**NO_2^- (mg-N/L)**	**NO_3^- (mg-N/L)**
K3 Carrier	15 ± 6	0.30 ± 0.32	0.50 ± 0.60	25.05 ± 0.71
P Carrier	13 ± 3	0.65 ± 0.15	0.25 ± 0.32	26.10 ± 1.00
M Carrier	12 ± 3	1.02 ± 0.26	0.55 ± 0.48	23.90 ± 1.20

Table S2 Pilot MBBR reactor operational conditions

	MBBR1	**MBBR2**
Carrier	AnoxKaldnes K5	AnoxKaldnes K5
Volume (L)	223	223
Flowrate (L/h)	40	40
Loading Rate ($gN/m^3 \cdot d$)	144 ± 5	86 ± 5
HRT (h)	5.6	5.6

Table S3 Percent abundance of the most prominenent heterotrophic genera. Degree of significance was determined by perforing Kruskal-Wallis sum-ranked test followed by Dunn's post-hoc on MBBR biofilm relative to the IFAS biofilm (* p<0.05, ** p<0.01, *** p<0.001).

Genus	**Day 0 (%)**	**Day 4 (%)**	**Day 14 (%)**	**Day 21 (%)**	**Day 28 (%)**
Flavobacterium	7.5 ± 3.5	3.2 ± 0.2	1.4 ± 0.5	1.1 ± 0.1***	0.9 ± 0.2***
Novosphingobium	5.0 ± 2.7	3.2 ± 0.2	3.0 ± 1.6	2.6 ± 0.2*	2.3 ± 0.3**
Zoogloea	4.5 ± 3.3	7.0 ± 1.0	4.6 ± 1.5	2.9 ± 0.5	2.0 ± 0.5*
Thiomonas	3.9 ± 2.9	5.7 ± 0.5	5.0 ± 1.6	4.1 ± 0.6	3.8 ± 0.5
Fluviicola	2.2 ± 1.1	1.6 ± 0.2	2.1 ± 0.8	2.3 ± 0.2	2.8 ± 0.4
Dechloromonas	1.9 ± 1.4	2.7 ± 0.4	1.7 ± 0.6	1.3 ± 0.1	1.0 ± 0.1*